Characterisation and Role of SLFN5 in Castration Resistant Prostate Cancer

Rafael Sánchez Martínez

Submitted in fulfilment of the requirements for the Degree of Doctor of Philosophy in Cancer Studies

Institute of Cancer Sciences

College of Medical, Veterinary and Life Sciences

University of Glasgow

September 2020

Abstract

Castration resistant prostate cancer (CRPC) is a currently incurable form of prostate cancer. While varying in different countries, prostate cancer recurrence typically manifests clinically around 12-24 months after androgen deprivation therapy, signifying disease treatment resistance[1]. Tumour heterogeneity at the molecular level driving CRPC is a major challenge for developing effective treatment. In order to address this diversity, an unbiased SILAC-based proteomic study was performed using three different *in vivo* CRPC models. Three matched pairs of hormone naïve and respective isogenic castration resistant cell models (namely LNCaP/LNCaP AI, CWR22/22Rv1, VCAP/VCAPCR cells) were optimised to generate orthotopic xenografts (orthografts) in CD8 nude mice. Pair-wise analysis identified Schlafen 5 (SLFN5) protein to be highly expressed in all three CRPC orthografts.

SLFN5 belongs to the relatively understudied Schlafen family of genes and has not been implicated in prostate cancer. SLFN5 has been shown to have both pro- or anti- tumorigenic depending on the tissue type, and it has been described to be able to regulate cell growth and migration. In this thesis, I tested the hypothesis that SLFN5 is mechanistically required for the development and maintenance of CRPC, and further explored the molecular basis involved.

In vitro analysis revealed enhanced SLFN5 expression following suppression androgen receptor in LNCaP cells, and suppression of SLFN5 after addition of androgens to the castration resistant cells LNCaP AI and 22Rv1. I further investigated the clinical relevance of SLFN5 expression in a clinical cohort of prostate cancer including CRPC samples. SLFN5 immunoreactivity was predominantly nuclear and significantly upregulated in CRPC. SLFN5 expression positively correlated with high Gleason score, PSA recurrence and risk of premature. CRISPR/Cas9 technology was utilised to create *SLFN5* knockout LNCaP AI and 22Rv1 CRPC cell clones. LNCaP AI SLFN5 KO cells have reduced migratory and *in vitro* growth capabilities. Furthermore, the growth of the SLFN5 KO orthografts was significantly impaired in *in vivo* androgen deprived conditions.

Transcriptomic analysis of 22Rv1 KO tumours and 22Rv1 KO cells from androgen-depleted condition was carried out. 64 genes were significantly altered ($p < 0.05$) in both *in vitro* and *in vivo* conditions, among which 52 genes were downregulated, raising the possibility that these downregulated genes may be positively regulated by SLFN5 in CRPC. Of note, the transcripts of both components of the LAT1 amino acid transporter were severely reduced, *SLC7a5* and *SLC3a2*. In addition, proteomic analysis of 22Rv1 KO tumours in castrated mice revealed significant downregulation of 38 proteins, two of which are the aforementioned LAT1 components.

LAT1 expression in prostate cancer is transcriptionally regulated by MYC and ATF4. Transient silencing of ATF4 in 22Rv1 cells impaired the expression of several SLFN5 regulated genes, including *SLC7a5* and *SLC3a2*. Further analysis discovered that predicted ATF4 binding sequences existed with high confidence in the proximity of 15 out of the 26 analysed SLFN5 KO affected genes and that SLFN5 and ATF4 interacted closely in the nucleus of 22Rv1 cells.

LAT1 mediates cellular intake of essential amino acid (EAA) and functions as part of the amino acid sensing machinery to activate the mTOR pathway for anabolism and growth during carcinogenesis. Metabolomic analysis of androgen-depleted 22Rv1 SLFN5 KO cells identified severely reduced levels of six amino acids, including 4 EAA: leucine, isoleucine, methionine and lysine. Western blot analysis highlighted impaired growth machinery due to SLFN5 KO with reduced phosphorylation of mTOR targets (P70S6K, rpS6, 4EBP1) signifying suppressed mTOR activity. Furthermore, increased levels of the autophagy marker LC3-II were detected as well. These results signalled that the growth machinery of the 22Rv1 KO cells was impaired and could explain the reduced tumour growth observed in the metabolically straining context of *in vivo* castration. Importantly, forced expression of LAT1 in 22Rv1 SLFN5 KO cells rescued mTOR activation. Collectively, for the first time, data presented in this thesis reveal an important role of SLFN5 in CRPC by regulating LAT1 expression to control mTOR mediated signalling required for cancer growth.

Table of Contents

List of Tables

List of Figures

Acknowledgements

First, I want to thank my host institutions, the Beatson Institute for Cancer Research and the University of Glasgow. They provided a plethora of resources and invaluable people, and great support for my research work. I would also like to thank the European Commission and the Marie Skłodowska-Curie program for Early Stage Researchers for funding this opportunity.

On a personal level, I want to thank Dr. Hing Leung for giving me the great chance to join this prestigious project. I also greatly appreciate the invaluable scientific and overall life experience working with him has provided me. I would also like to extend my thanks to Dr. Mark Salji for providing the basis of my research. It is thanks to him and his discovery of SLFN5 that I was able to obtain the fruitful results that comprise this thesis.

I would like to acknowledge all my formidable laboratory colleagues. I don´t have enough thanks for Linda Rushworth´s patience and care. She is truly a wonderful person and helped me find my way around and feel comfortable in this work, as well as being a great friend and a good laugh. I would also like to thank Arnaud Blomme, who was basically mon grand frère in the lab. It was his scientific guidance that helped me get the best of this project and myself. I have yet to see a match for his love and dedication to science. I would also like to thank everyone else that I have worked with during my time in this lab, as everybody was a joy to work with and I will remember a lot of shared moments, specially at lunchtime. Laura Galbraith, Rachana Patel, Ee Hong, Andrew Hartley (and Beth!), Catriona Ford, Ernest Mui, Carolyn Loveridge and Imran Ahmad are all names I will remember fondly.

To my great friend Calum Johnston, I want to give my appreciation for all the silly good times we have had and all the food we have consumed together. He really helped me feel welcome from the first day and never stopped since them. Finally, I would like to thank Chara Ntala for being an excellent friend and colleague in this journey. I believe all the visits to the restaurants of Glasgow and all the tea sessions were fundamental for our sanity. I am truly happy to have shared my three years in Scotland with such great people.

Back in Spain I would like to thank my parents for their unwavering support. I would not have achieved what I have without their help and love, and I feel truly blessed to be their son. Thanks to my brother for helping me feel at home 2.000 kilometres away. Thanks to all my family, specially my grandmothers for I have felt their love every day. Thanks to my late grandfathers for being part of who I am. Thanks to all my friends for always being there every time I visited Murcia in my holydays, and for visiting me in Scotland. Thanks to my cat Kima for being so wholesome and taking good care of my family while I was gone. And finally, I would like to give my most special thanks to my love Celia for all the patience and support she has given me through these years and all the great moments we have shared, whether it be on Skye, Glasgow, Spain or Skype. With you, I would go where no man has gone before.

Author´s Declaration

I declare that, except where explicit reference is made to the contribution of others, that this thesis is the result of my own work and has not been submitted for any other degree at the University of Glasgow or any other institution.

Signature:

Printed name: Rafael Sánchez Martínez

Definitions and abbreviations

CRPC – Castration Resistant Prostate Cancer
DRE – Digital Rectal Examination
PSA – Prostate Specific Antigen
TRUS – Transrectal Ultrasound
mp-MRI - Multi-parametric Magnetic Resonance Imaging
PIRADS - Prostate Imaging Reporting and Data System
GnRH – Gonadotropin Release Hormone
LH - Luteinizing Hormone
LHRH – Luteinizing-Hormone Release Hormone
DHT – Dihydrotestosterone
AR – Androgen Receptor
NTD – Amino Terminal Domain (of AR)
DBD – DNA Binding Domain (of AR)
LBD – Ligand Binding Domain (of AR)
NLS – Nuclear Localisation Signal
ARE - Androgen Response Elements
NES – Nuclear Export Signal
ADT – Androgen Deprivation Therapy
DHEA – Dehydroepiandrosterone
EGF – Epidermal Growth Factor
IGF-1 – Insulin-like Growth Factor 1
GR – Glucocorticoid Receptor
PIP_3 - Phosphatidylinositol-3,4,5-triphosphate
PIP_2 - Phosphatidylinositol-4,5-biphosphate
LC-MS – Liquid Chromatography – Mass Spectrometry
IFN-α/β – Interferons alpha and beta
EMT – Epithelial-Mesenchymal Transition
ChIP – Chromatin Immunoprecipitation
mTOR – Mammalian Target of Rapamycin
mTORC1/2 – Mammalian Target of Rapamycin Complex 1 and 2
EAA – Essential Amino Acid
FBS – Foetal Bovine Serum
CSS - Charcoal Stripped Foetal Bovine Serum
ATCC - American Type Culture Collection
CRISPR - Clustered Regularly Interspaced Short Palindromic Repeats
NEPC – Neuro Endothelial Prostate Cancer
NHT – Neoadjuvant Hormonal Therapy
G6P – Glucose 6-phosphate
F16DP – Fructose 1,6 diphosphate
DAPI - 4′,6-diamidino-2-phenylindole

Chapter 1 - Introduction

1.1 Prostate Cancer and Androgen Receptor

Prostate cancer is the most common cancer in males. In the UK alone, around 48.500 cases are detected every year, affecting mainly (95% of the cases) males older than 55 years. Even though when compared to other types of cancers it presents a comparatively favourable survival rate of 78% for 10 or more years, the considerable amount of cases means more than 11.500 people die per year due to prostate cancer in the UK[2].

The main risk factors of prostate cancer development are age, ethnicity[3] and a family history of prostate cancer[4,5]. Environmental and dietary risk factors have been studied, but conclusions are mixed. It is also worthy to note that sometimes separating these factors from family factors can be difficult. The general consensus is that prostate cancer susceptibility is influenced mainly by several intertwined genetic factors, although mutations in some genes such as BRCA2, have been shown to increase the relative risk of prostate cancer up to 8 fold[6].

1.1.1 Diagnosis of prostate cancer

Several strategies exist to aid in the detection of prostate cancer. These are not exclusive to each other and are used in conjunction to classify the disease risk and determine an effective treatment.

As the prostate rests in close contact with the rectum, a digital rectal examination (DRE) can be performed by the clinician to detect physical abnormalities such as asymmetry, nodularity and abnormal texture to palpation[7]. This technique is considered uncomfortable, provides variable results due to inconsistent criteria, and can lead to over-investigation[8]. When its use is recommended in the literature, it is always with the support of other diagnostic tests such as the PSA test[9].

Prostate specific antigen[10] (PSA, gene name *KLK3*) is a protein produced in the prostate that can be detected in the blood. PSA levels in serum are representative of prostate activity and are used in the clinic to detect and

monitor progression of prostate cancer. The role of the PSA test screening in early detection is debated, as there exist contradictory clinical studies about its benefit to patient survival[11]. Henceforth, the PSA test is usually utilised in combination with other techniques such as DRE to assess the risk of the disease and as a monitoring tool for disease progression[12].

Imaging techniques are used in prostate cancer to aid with tissue sampling during biopsies, making them more precise and representative of the lesion grade. Imaging the prostate before the biopsy can reveal the biopsy to be unnecessary, avoiding the invasive procedure and its side effects[11]. Transrectal ultrasound (TRUS) is used to aid in the biopsy procedure. Multi-parametric magnetic resonance imaging (mp-MRI) can be used pre- or post-biopsy to assess the need for further biopsies. To evaluate and categorise mp-MRI findings, the standardised PIRADS (Prostate Imaging Reporting and Data System) criteria are used. Its latest version, PIRADS v2.1 emerges from expert consensus and data-based improvement over the initial PIRADS guidelines[13]. This system provides a strong frame for MRI based diagnostic and standardizes criteria. This allows for consistent diagnoses among different centres, helping pathology management and research. Positron emission tomography (PET) imaging is also used as a diagnostic tool, with particular success in the detection of small metastatic developments[14].

When the previously described diagnostic methods suggest the presence of prostate cancer, a biopsy is conducted to extract 10 to 12 representative tissue samples to evaluate the extent and progression of the pathology. If MRI prostate scan revealed a lesion of interest, targeted prostate biopsies can be considered, thus reducing the need for multiple sampling biopsies, minimising the risk of over-diagnosis of indolent disease. The histological samples are scored following an established criterion known as Gleason sum scoring. This scoring method evaluates the appearance of the cellular morphology and the loss of tissue architecture as measures of lesion progression. Gleason patterns are graded from 1 to 5, with higher scores representing more severe loss of tissue integrity and more aggressive disease. A combination of two scores, the predominant pattern plus the secondary pattern, is used to determine the sum score of the samples, with a total score of 7 or more being considered aggresive[15]. This scoring system allows a better risk stratification and therefore improved

assessment of the pathology than the previously used grading in which one score for the whole tissue was used[16]. More recently, the refined Gleason grade groups were introduced[17].

To this array of well stablished diagnostic techniques, new research aims to introduce novel strategies and biomarkers of the disease that help in detecting prostate cancer and monitoring its progress. Several panels of gene expression are being used as biomarkers for cancer aggressiveness, clinical progression and metastatic risk[18]. Preliminary studies are testing the use of PET imaging that targets amino acid transporters overexpressed in tumour tissue to help localise the tumoral lesions and serve as an indicative of their metabolic activity[19].

1.2 Normal Prostate Physiology

1.2.1 Androgens

Under normal conditions, androgens are necessary for the natural development and functions of the prostate[20]. Testosterone production is controlled by the hypothalamic-pituitary-gonadal axis. The hypothalamus secretes gonadotropin release hormone (GnRH), which activates the production of luteinizing hormone (LH) on the anterior pituitary gland. In response to LH, testosterone is produced mainly in the testicles and then distributed to the prostate and other androgen-sensitive tissues. There, the testosterone is converted into the more potent 5α-dihydrotestosterone (DHT) by the enzyme 5α-reductase. The DHT molecule binds the androgen receptor (AR), causing its homodimerization and translocation to the nucleus, where it will control the expression of many genes[21]. Testosterone also participates in a self-regulatory negative feedback loop by inhibiting production of GnRH by the hypothalamus and LH in the anterior pituitary gland[22] (Figure 1-1).

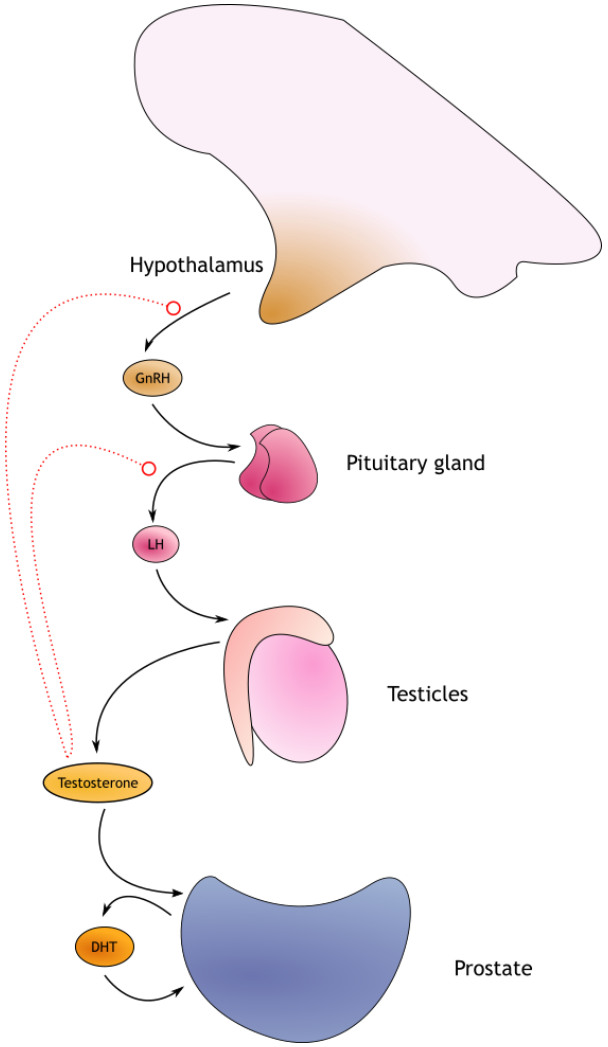

Figure 1-1 - Androgen production regulation

Figure shows the signaling hormones involved in promoting androgen synthesis in the testes and the negative feedback loop that allows testosterone to regulate its own expression.

AR activation and signaling are a necessity for the maintenance of the secretory epithelium of the prostate. AR signaling allows the epithelium to function and keep a steady rate of proliferation, replenishing the cells that die off during prostate homeostasis. Reduced levels of testosterone cause not only the degeneration of the secretory epithelium directly, but also affect vascularization and blood flow to the prostate tissue itself, which adds to the degenerative effects of insufficient testosterone levels. This is because DHT promotes the secretion of growth factors such as the vascular endothelial growth factor[23]. Due to this, androgen receptor signalling enabled by constant androgen availability in the prostate is crucial to maintain its integrity and activity.

1.2.2 Androgen Receptor

Androgen receptor (sometimes referred as NR3C4 or nuclear receptor subfamily 3, group C, member 4) belongs to the steroid and nuclear receptor superfamily, which includes other receptors such as the glucocorticoid, mineralocorticoid, progesterone and estrogen receptors.

Androgen receptor consists of three distinct domains: the amino terminal domain (NTD), the DNA binding domain (DBD) and the ligand binding domain (LBD)[24] (Figure 1-2). The DBD and LBD domain are separated by a hinge region that contains a nuclear localisation signal (NLS). In its non-active state, AR is found in the cytoplasm bound to heat shock proteins (HSP56, HSP70 and HSP90) and cytoskeletal proteins[25]. These associated proteins keep the AR in the cytoplasm and are believed to facilitate ligand binding.

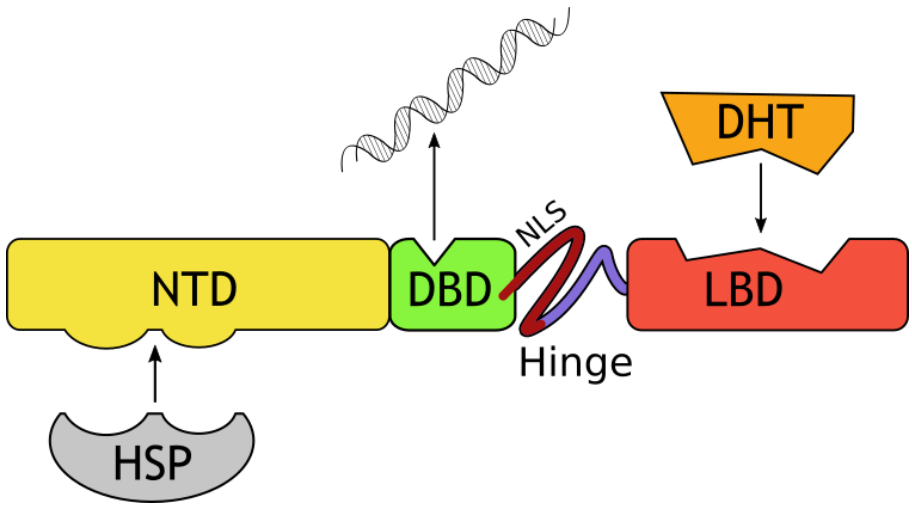

Figure 1-2 – Structure of Androgen Receptor
Figure shows the different domains of AR and simplified interactions.

The NTD constitutes the transcriptionally active part of AR, as it can activate transcription by itself in absence of the LBD[26]. The composition of the NTD also affects AR conformation, as it contains several tri-nucleotide repeats that encode poly-glutamine and poly-glycine sequences[27]. The length of these repeats affects AR function, with a smaller number of repeats suggested to be a clinically relevant risk marker for prostate cancer[28]. NTD also contains interaction sites for several coregulators of AR[29], and possesses two transcription activation units, namely TAU-1, capable of ligand-independent activation of

transcription, and TAU-5, which is instrumental in the recruitment of p160 coactivators[30].

The DBD's main function is binding to specific DNA sequences known as androgen response elements (ARE)[31] as well as to the enhancer regions. It is composed of two zinc-finger domains, the first of them mediating the interaction of the receptor with specific regions of the DNA, while the second zinc finger promotes the homodimerization of two AR proteins[32]. The amino acid sequence of this domain is highly similar to that of the other steroid hormone receptors that share family with AR, which causes some overlap in the regulatory networks of the different receptors[33].

The hinge region is a 50 amino acids long region of the protein sequence that lays between the DBD and the LBD and contains a part of the NLS, with the rest existing on the DBD[34]. When the ligand binds to AR, the conformational change will cause the NLS located in the hinge region to be exposed and Filamin-A, a cytoskeletal protein, will bind to the hinge region and translocate the AR protein to the nucleus[35].

The LBD is the region where androgens bind to activate AR signalling. This domain contains a nuclear export signal (NES) whose activity is neutralized by the ligand binding[36]. The exposed NES keeps the AR localised in the cytoplasm superseding the NLS until the ligand is bound. Ligand binding modifies the conformation of AR, which causes inactivation of the NES and reveals the NLS, allowing its recognition by Filamin-A and its subsequent transport to the nucleus.

1.2.3 AR activation and regulation

When testosterone or DHT binds to the LBD, AR undergoes structural changes that will expose the DBD and the NLS. This will cause coregulators to bind to the AR and transport it to the nucleus. In there, AR will form homodimers that will interact with the DNA and activate the AR regulatory functions[37]. Through this mechanism, AR is capable of mediating several processes, such as cell proliferation, differentiation, apoptosis, cell metabolism and production of prostate specific antigen (PSA) in response to androgens[38]. While the biological function of circulating PSA is not that well known, it has been characterized to

activate vascular endothelial growth factor C (VEGF-C) in seminal plasma to help with sperm liquefaction[39].

On top of ligand binding, phosphorylations of the receptor can also modulate its activity. Several serine residues have been described as capable of mediating AR activity by integrating several signals to mediate the AR response[40]. Ligands for other molecular receptors such as epidermal growth factor, insulin-like growth factor 1 and keratinocyte growth factor have been shown to be able to stimulate AR gene expression[41]. AR signal can also be boosted when low levels of androgens are available by direct phosphorylation by signalling kinases JNK, AKT, and MAP-kinases[42]. Androgen independent activation can also be achieved by phosphorylation via several kinases such as the human epidermal growth factor receptor 2 (HER2) and members of the G protein-coupled receptors (GPCRs) family[40], and protein kinase A (PKA)[43].

Once AR is activated and has translocated to the nucleus, it will bind to ARE. Then, co-regulators along with the transcription machinery are recruited to the site to interact with AR and drive genomic expression. The interaction kinetics of this transcriptional complex also play a role in regulating the intensity of the gene transcription. Depending on how long the complex remains stable, some genes are transcribed more actively than others, determining in the end the protein levels of such genes[44]. At the same time, the activated AR is also capable to repress transcription of selected genes. The AR can interact with epigenetic repressors such as histone deacetylases and lysine demethylases, and with bona fide transcription repressors such as E2F4[45].

Once AR-mediated transcription has finished and the ligand has detached, the AR can be redirected to the cytoplasm. In there, it will become ready to be activated again[46], or it can be ubiquitylated in a consensus site by the MDM2 E3 ubiquitin ligase, marking the AR for degradation by the proteasome[47].

1.3 Treatment of Prostate Cancer

There are several treatment strategies for prostate cancer. The use of an appropriate therapy depends on the risk classification of the tumour but the possibility of death by other causes must be taken into account. Several factors

like age and comorbidities increase the risk of the procedure being fatal to the patient and the choice therapeutic strategy should be adjusted to the specific circumstances of the patient and the disease[48].

1.3.1 Primary treatment

The improvement in the use of diagnostic techniques such as the PSA test has allowed for an earlier diagnosis and localisation of prostate cancer in the past decades. This results in the discovery of small, localized tumours that pose minimal risk to the diagnosed patients that previously went undetected. For these patients, the side effects of primary treatment might be worse than the natural course of the disease. In such cases, an active surveillance strategy is adopted. This approach involves the continuous use of PSA testing, DRE and repeated biopsies in order to assess the stage and progression of the disease with the intent of avoiding primary treatment when unnecessary. If the monitored cancer becomes potentially harmful, active treatment strategies are used. As immediate use of primary treatment has not been reported to have any advantage in the treatment of low-risk, manageable tumours, active surveillance is useful to avoid overtreatment and unnecessary risks[48,49].

A similar approach to active surveillance is watchful waiting. In this case, no active monitoring is performed in absence of symptoms. Watchful waiting constitutes a passive approach in comparison to active surveillance and the main objective is to avoid treatment to patients who will not particularly benefit from it, usually for individuals with several other co-morbidities[50].

Treatment of prostate cancer by surgical methods consist of performing a radical prostatectomy. This procedure is defined as the removal of the prostate gland along with the seminal vesicles and neighbouring tissue in order to avoid positive surgical margins. The objective of the surgical procedure is the complete eradication of the tumoural tissue. Recent advances have allowed surgery to be performed with the aid of a surgeon-operated robot. The robot-assisted laparoscopic prostatectomy allows for higher precision and reduces the chance of negative effects associated with the procedure, such as urinary problems and erectile dysfunction[12].

There are two main procedures in the radiotherapy treatment of prostate cancer. External beam radiotherapy is often appropriate to treat medium to high risk patients and is used as a long term control of the disease[51]. For lower risk patients, brachytherapy (internal radiotherapy) is more suitable. This technique consists on the implantation of radioactive sources inside the body of the patient with aims to irradiate the nearby tumour tissue[52]. Choice of radiotherapy to treat prostate cancer has to be made taking into account the array of possible side effects and general risk to the patient's life. Radiotherapy treatment is not exclusive with other treatment options like hormonal therapy.

1.3.2 Hormonal treatment and chemotherapy

As described previously, androgens and AR signalling are necessary for the growth and proliferation of prostate cancer. Hormonal therapy aims to interrupt the supply of androgens to the tumoural tissue in an effort to stop its growth, and it is normally referred to as androgen deprivation therapy (ADT). This therapeutic option is more commonly used in advanced cases of prostate cancer, including cases where metastasis has developed[53].

Androgen deprivation can be achieved in the clinic via several different methods. Bilateral orchiectomy is a surgical procedure where the main androgen-producing glands (testicles) are removed to halt endogenous production of testosterone. This procedure permanently reduces the production of androgens, but might not be desired due to its permanent nature and requirement of a surgical procedure[54]. Therefore, it is usually reserved for higher risk cases.

Medical castration represents an alternative to the surgical approach. Unlike bilateral orchiectomy, medical castration is reversible and avoids surgery-related issues, making it the favoured choice in the clinics over orchidectomy. Medical castration makes use of agonists of the luteinizing-hormone release hormone (LHRH) with the aims to stop the physiological production of androgens stimulated by the endogenous LH. LHRH agonists are continually administered to keep a sustained stimulation of the LHRH receptor, which causes desensitization by reducing the expressed levels of the receptor. This causes the LHRH driven production of LH in the pituitary to stop. Without circulating LH, testosterone

production in the testicles is then halted[55]. LHRH antagonists that directly block the production of LH are also used as a treatment and possess certain advantages over LHRH agonists such as avoiding the initial testosterone surge caused by LHRH agonists before the desensitization has time to occur[56,57].

Another approach to androgen deprivation is the use of androgen synthesis inhibitors. Abiraterone acetate is the most representative compound of this family of drugs[58]. Once it is administered orally, it is deacetylated in the body and becomes an irreversible inhibitor of the Cytochrome P450 Family 17 Subfamily A (CYP17) enzyme, a protein involved in the first step of androgen synthesis. This enzyme transforms testosterone precursors pregnenolone and progesterone into dehydroepiandrosterone (DHEA) and androstenedione respectively. These compounds are considered “weak” androgens and can be further transformed into testosterone. Abiraterone and other similar drugs target CYP17 with aims to stops the metabolic synthesis of testosterone in all tissues. This constitutes an advantage over the previously described LHRH agonists, as it affects testosterone synthesis in any tissue regardless of its responsivity to the hypothalamic-pituitary-gonadal axis.

Non-steroidal antiandrogens constitute a group of drug molecules with AR antagonistic activity. These compounds bind to the LBD of the AR and impede binding of androgens and the subsequent activation of AR transcriptional activity. They replace steroidal antiandrogens previously used in the clinic, as the latter acted as agonists of other related steroidal receptors such as the glucocorticoid and mineralocorticoid receptors. This caused unwanted secondary effects and could constitute a mechanism of cancer resistance. The newer non-steroidal antiandrogens specifically target AR and block its activation regardless of the available androgen levels. Because of that, they can be effectively used in combination with other previously described approaches to maximize treatment effectiveness[59]. Bicalutamide and enzalutamide[60,61] constitute examples of broadly used non-steroidal antiandrogens.

Androgen deprivation therapy is an effective treatment that allows remission of the tumours in the majority of patients, but unfortunately after 1-2 years a resistant phenotype of prostate cancer emerges that is no longer sensitive to hormone therapy[1]. This resistant variant of prostate cancer is termed castration

resistant prostate cancer (CRPC) and is currently incurable. Treatment after CRPC is considered palliative and looks to extend the life of the patient but total remission after development of CRPC in not achievable today.

Chemotherapy in prostate cancer involves the use of taxanes, mainly docetaxel and cabazitaxel. These agents interfere with the microtubule network and block nuclear translocation of AR and cause phosphorylation of pro-apoptotic protein BCL-2, triggering cell death. Docetaxel is also capable of repressing AR expression by promoting FOXO1 upregulation, a direct transcriptional repressor of AR[62]. The use of these compounds is usually reserved for advanced states of prostate cancer such as metastatic prostate cancer and CRPC, as it is where they are proven to be most effective, and resistance to taxanes emerges when used in previous stages. Chemotherapy in CRPC cases is usually administered in conjunction with ADT agents, and its aim is primarily to increase the overall survival time of the patients[63].

1.4 Molecular Mechanisms of Castration Resistant Prostate Cancer

Castration resistant prostate cancer is an ADT-unresponsive stage of PC. Clinically, it is defined as progression of disease as measured by the rise of PSA levels and progression of lesions despite castrate levels of androgens in the serum[64]. Prostate cancer cells are able to adapt with time to the lack of androgens by using a wide array of molecular mechanisms (Figure 1-3). This heterogeneity in the response mechanisms to ADT is responsible for the current inability to overcome CRPC by treatment, as different agents such as abiraterone and enzalutamide will cause their own set of resistance mechanisms to emerge.

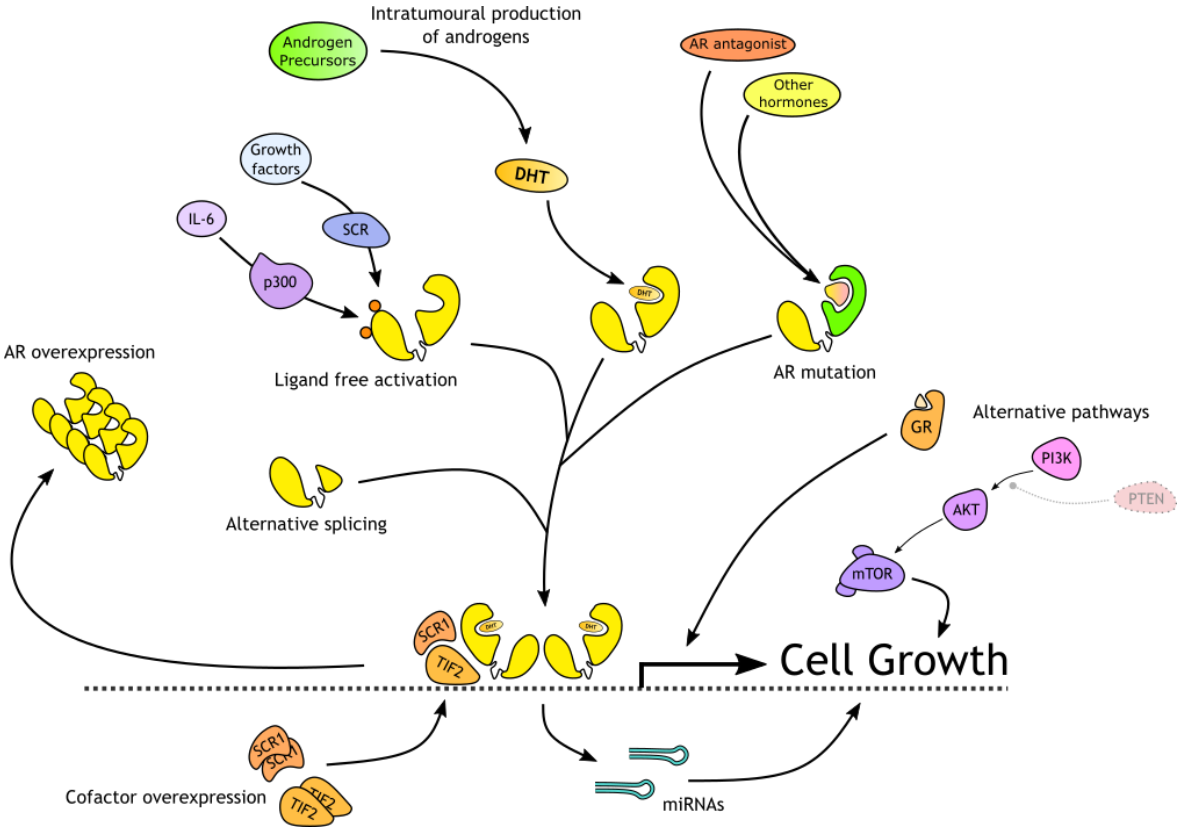

Figure 1-3 – Overview of the molecular mechanisms of CRPC

1.4.1 Intratumoural production of androgens

In absence of circulating testosterone, prostate cancer cells can enable androgen synthesis machinery by upregulating the expression of the necessary enzymes. It has been shown that while ADT is able to reduce androgen levels in the serum by more than 90%, testosterone and DHT levels in the prostate are not as affected. Several studies describe that after ADT, prostate tissue presents a reduction in the androgen levels from 70% to 80%, pointing to an alternative source of androgen synthesis. This testosterone and DHT endogenously synthesized by the prostate combined with the residual levels of androgens after ADT would be enough to activate AR signalling and bypass the need for androgens produced in the testes[65].

The canonical route for testosterone and DHT synthesis involves transforming pregenenolone and progesterone into testosterone precursors dihydroepiandrosterone (DHEA) and androstenedione via the hydrolase and liase activities of CYP17A1. Those precursors are then converted to 5-androstenediol

previous to testosterone or to testosterone directly by action of HSD17B3 and AKR1C3 and HSD3B.

When testosterone synthesis is blocked, there are two main alternative pathways that involve the direct synthesis of DHT from precursors other than testosterone (Figure 1-4). The androstanedione pathway involves the conversion of androstanedione into androstenedione by Steroid 5 Alpha-Reductase (SRD5A), which then can be converted directly to DHT by HSD17B2. The "backdoor pathway" consists of an alternative route starting at progesterone. Progesterone is converted into dihydroprogesterone by SRD5A and then into androsterone by CYP17A1. Androsterone can then be converted into DHT via two different pathways. It can become androstenedione by action of HSD3A and follow the previously described pathway, or it can be transformed into androstanediol by HSD17B3 and subsequently into DHT by HSD3A. Several of these enzymes can be found to be upregulated in absence of androgens enabling the testosterone-independent synthesis of DHT[66].

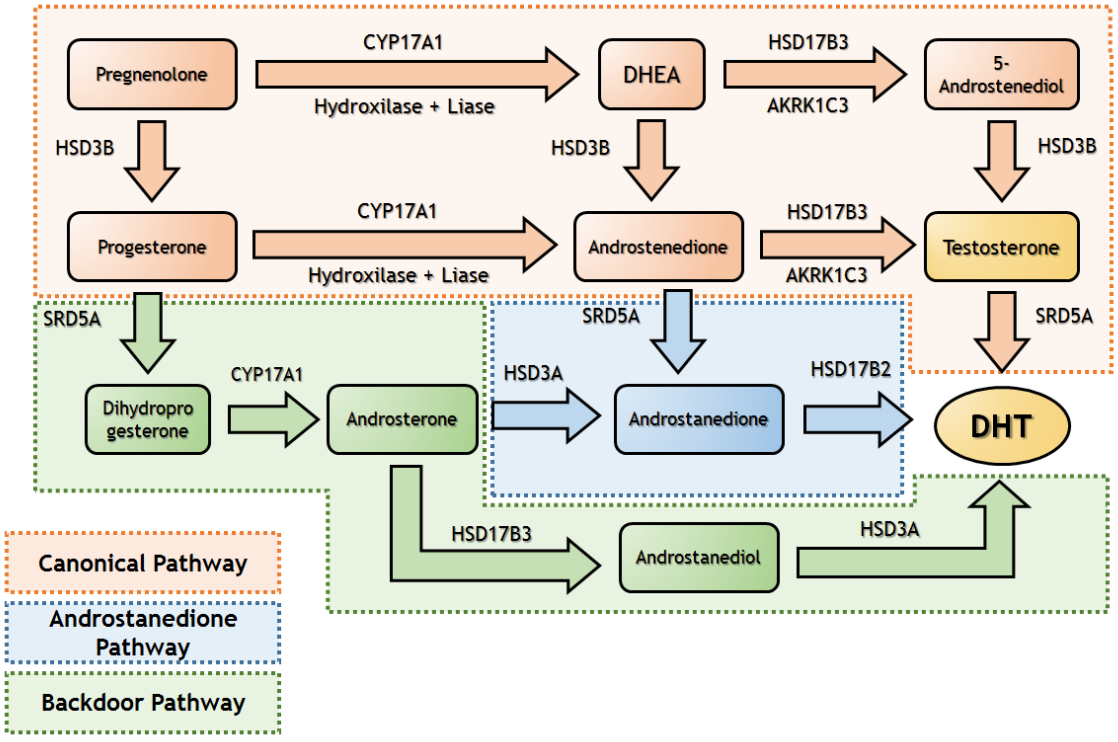

Figure 1-4 – Alternative routes of DHT synthesis in prostate cancer

Figure shows the canonical pathway of DHT synthesis along with the two alternatives, the androstenedione pathway and the backdoor pathway.

These two alternative pathways eliminate the need for testosterone and allow the prostate cancer cells to still engage AR signalling even when endogenous production has been stopped[67]. This type of resistance cannot therefore be considered a true "androgen independence", as DHT and AR signalling are still being required for tumour progression.

1.4.2 AR overexpression

Upregulation of receptor expression constitutes a standard biological response to scarcity of ligand. In the case of AR, the low levels of androgens caused by ADT can force an increase in AR transcription. This can over-sensitize the signalling pathway in order to adapt to the low levels of testosterone available[68]. In the case of prostate cancer, high genomic instability combined with a positive survival selection for increased AR expression can lead to AR gene amplification[69,70]. In some cases, up to 20 copies of the AR gene have been detected in a cell[71]. This process not only sensitizes prostate cancer cells to low levels of testosterone, but can help overcome AR antagonist therapy[72].

1.4.3 AR mutations

The LBD is the most frequent site for gain of function mutations in AR. The selective pressure exerted by low levels of testosterone or treatment with AR antagonists selects for LBD mutations that allow AR to be activated by alternative ligands (promiscuity) and can even transform AR antagonists into agonists[37].

The T877A mutation has been described in the LNCaP cell line and in clinical patients. This AR variant presents increased affinity for estrogens and progesterone, allowing AR activation in absence of testosterone[73]. A double mutation of T877A and L701H has been described that increases sensitivity to cortisol and cortisone, further expanding the possible alternative agonists for AR[74,75]. These mutations often reduce the specificity of the ligand binding pocket by substituting big amino acids for smaller ones that are less structurally restrictive and allow bigger ligands to enter.

In response to treatment with AR antagonists, mutations can emerge that transform them into AR agonists. W714L and W741C have been detected after

treatment with bicalutamide[76], and F876L after treatment with enzalutamide and apalutamide[77]. These mutations increase the ligand pocket size as well, allowing the AR antagonists to bind AR and cause a conformational change that results in an AR-ligand structure similar to that of wild type AR bound to DHT.

Other mutations can increase the binding of coactivators to AR after its activation, leading to an increased transcriptional activity. The V730M mutation affects the coactivator binding motifs, allowing for a stronger response to decreased levels of testosterone and other AR ligands[78].

1.4.4 Alternative splicing

Alternative splicing of AR, although not usual, can happen under non-pathological circumstances. Variant AR45 is an N-terminal truncated variant detected in healthy tissue and encodes an alternative exon 1. This variant lacks the NTD and therefore direct transcriptional activity, but has been shown to interact with the full length AR to inhibit AR mediated gene regulation[79].

The majority of the known harmful AR variants are considered “gain of function” variants and are truncated in their C-terminal end affecting the LBD. This leads to constitutively active AR proteins, as the intact DBD and NTD remain transcriptionally active without the empty LBD stopping nuclear translocation and transcriptional activity[80].

The AR-V7 variant constitutes the most studied alternative splicing variant of AR. It has been detected in clinical cases of CRPC and can serve as a predictor of biochemical recurrence after surgery[81]. AR-V7 is a ligand independent active variant of AR that not only has been shown to recapitulate the transcriptional programme of wild type AR, but is also capable of regulate a novel set of target genes. Activation of abnormal transcriptional programmes can contribute to the adaptation of prostate cancer to ADT, allowing the tumour cells to not only grow in absence of androgens but to also engage in alternative survival strategies[82].

Other LBD-lacking AR variants can also promote CRPC survival beyond directly activating the canonical AR transcriptional programme themselves. The AR^{v567es} variant can stimulate increased expression of wild type AR and interact with it

forming a heterodimer. The AR^{wt}-AR^{v567es} complex can then translocate to the nucleus and be transcriptionally active in absence of androgens[83].

AR23 is a splicing variant that possess an altered DBD and is exclusively cytoplasmic. This variant does not engage in direct transcriptional activity, instead being able to regulate signalling pathways that are non-canonical for AR activity. AR23 has been shown capable of affecting the transcriptional programme of the NF-κB and AP1 transcription factors while remaining in the cytoplasm[84].

Pathological circumstances where AR gene amplification is common favour the occurrence of harmful variants by generating extra copies of the AR gene prone to alternative post-transcriptional processing. ADT also exerts an artificial selection of already present AR-variants that present a proactive role in CRPC. Several AR variants that are present in normal tissue can also be detected in CRPC tissue in vastly increased amounts.

1.4.5 Alternative pathways

Prostate cancer growth can involve several pathways besides AR signalling. Canonical pathways that control growth in most cells are prone to be engaged in CRPC, including pathways regulated by AR in pre-ADT conditions. This altered signalling can promote ligand independent AR activity or completely bypass the need for AR stimulation.

Several growth factors and cytokines can promote AR activation in androgen-deprived conditions. The epidermal growth factor (EGF) and insulin-like growth factor 1 (IGF-1) pathways both activate SRC kinase. SRC kinase is upregulated in cases of CRPC and can phosphorylate and activate AR in absence of ligand[85]. Another receptor belonging to the EGF family, HER2/Neu, is capable of activating AR signalling when overexpressed in cellular models. This activation of AR is unresponsive to AR antagonist treatment, and it has been described to occur via activation of ACK1 kinase and phosphorylation of AR in a similar way as SRC kinase does[86]. The inflammatory cytokine IL-6 can promote prostate cancer growth independently of androgens in presence of downstream target STAT3, leading to activation of AR by the histone acetyltransferase p300[87]. IL-6 is

produced by prostate cancer cells and prostate stroma cells as well, acting as a paracrine signalling that promotes cancer growth in the tumour microenvironment. IL-6 is also able to induce expression of enzymes that allow for intraprostatic androgen synthesis[88] and prime fibroblasts for the creation of metastatic niches[89].

Other mechanisms can circumvent the need for AR signalling completely. The glucocorticoid receptor (GR) belongs to the same receptor family as AR and shares regulatory targets with it[90]. GR can also bind to ARE and promote expression of canonically AR regulated genes[91]. Studies have shown that GR is upregulated in cells treated with AR antagonists and their survival was dependant on GR activity[92].

Loss of PTEN protein in prostate cancer leads to unchecked tumour growth. PTEN is a phosphatase enzyme that transforms the active phosphatidylinositol-3,4,5-triphosphate (PIP_3) into the inactive phosphatidylinositol-4,5-biphosphate (PIP_2), providing a brake on the PI3K/AKT/mTOR growth pathway. When PTEN is not present, the PIP_3 synthetized by PI3K in response to growth factors does not degrade to its inactive form PIP_2, resulting in an exacerbated activation of AKT. The active AKT continually signals for cell growth and survival while inhibiting apoptosis and cell cycle arrest through the mTOR pathway without any counterbalance mechanism[93]. PTEN loss is a common occurrence in several cancer types, including prostate cancer[93]. The *PTEN* gene has been described to be affectedbetween 16% to 41% of prostate tumours, with increased incidence in CRPC[94,95].

In other cases, the effects of AR signalling loss are avoided directly. The antiapoptotic BCL2 protein has been found to be upregulated in cases of prostate cancer and in CRPC. In absence of AR signalling, growth is halted and apoptotic is engaged in the prostate cells[96]. Overexpression of BCL2 blocks the suicide signal and allows the cells to survive, and correlates with survival in prostate cancer[97].

1.4.6 AR cofactors

Coactivators and corepressors of AR are an important part of AR regulation of transcription. Overexpression of coactivators and loss of corepressors can potentially have a role in maintaining AR signalling in CRPC. Increased expression of coactivators TIF2 and SCR1 has been described to occur in prostate cancer. Overabundance of coactivators increases the sensitivity of AR to low levels of testosterone and can enhance the strength of AR activation caused by alternative ligands in mutated ARs[96].

1.4.7 miRNAs

Micro RNAs (miRNAs) are short RNA molecules capable of silencing expression of specific genes by targeting their mRNA, leading to its degradation. This allows miRNAs in CRPC to silence tumour suppressor genes and promote cancer growth. Several miRNAs are found to be upregulated in advanced prostate cancer and high levels associate with poor outcome and increased recurrence after treatment[98].

AR is known to regulate several miRNAs with potential tumorigenic capabilities. miR-125b was described to be moderately to highly expressed in prostate cancer samples. This miRNA supresses the expression of pro-apoptotic gene BAK1, increasing cancer cell survival[99]. Another miRNA, miR-21, presented an increased expression in prostate cancer as well. AR directly regulates expression of miR-21 and overexpression of this miRNA in prostate cells allows them to grow under androgen deprivation conditions[100], as it targets tumour suppressor genes such as PTEN and programmed cell death protein 4 (PDCD4)[101,102].

Other miRNAs such as the miR-34 family are actively supressed by AR and see their levels increased in androgen deprived conditions. These miRNAs are considered to be tumour suppressors, as they are capable to regulate the cell cycle and epithelial to mesenchymal transition and supress AR expression. Their levels in prostate tissue inversely correlate with prostate cancer progression and life expectancy[103].

1.5 Discovery of *SLFN5* and Introduction

1.5.1 Discovery of Schlafen 5 (SLFN5) in CRPC

In the search for an effective treatment of CRPC, its wide molecular heterogeneity constitutes a great obstacle. Current treatments are unable to produce sustained remission of the cancer and in the long-term result in the development of further resistance. The selective pressure exerted by all varieties of ADT drives the emergence of abnormal AR variants and mutants as well as activation of other compensatory mechanisms that allow the cancer to thrive under the treatment.

In order to overcome this diversity, an unbiased approach encompassing several different models of CRPC was required. Dr. Mark Salji, a member of the host laboratory, performed proteomic analysis of three different pairs of orthotopic xenograft CRPC models in search of molecular alterations that occurred across all three models[104]. This experimental design involved the use of isogenic pairs of hormone naïve and castrate resistant PC to study the respective proteomes and to identify altered proteins in CRPC. The CRPC cell lines were injected into castrated CD-1 nude mice, while the hormone naïve cells were injected into the same type of mice without performing castration. The use of these *in vivo* orthotopic models recapitulates clinical prostate cancer and post ADT conditions better than standard *in vitro* 2D culture, providing a more accurate picture of CRPC in a laboratory setting.

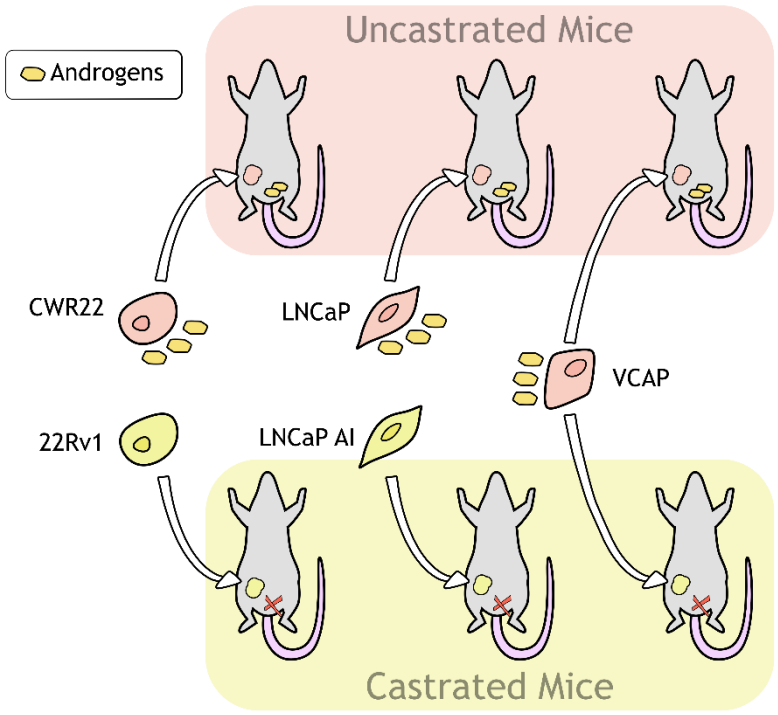

Figure 1-5 – Experimental design of CRPC proteomic screening

The three cell line pair models used were LNCaP/LNCaP AI, CWR22/22Rv1 and VCAP/VCAPCR (Figure 1-5). LNCaP AI were derived from LNCaP through *in vitro* culture in absence of androgens and present certain characteristics such as alternative growth signalling pathways, increased anti apoptotic action, and an altered cell cycle[105,106]. 22Rv1 were derived from a CWR xenograft tumour that relapsed under castrated conditions and was serially propagated in mice. The 22Rv1 cell line also presents the constitutively active V7 variant of Androgen Receptor[107,108]. VCAP constitute a metastatic prostate cancer model, originally derived from a vertebral metastasis of prostate cancer[109]. VCAPCR tumours consist of regular VCAP cells injected into castrated mice.

After proper establishment and development of the tumour (10-12 weeks), samples were flash frozen for conservation and their proteome was analysed by liquid chromatography – mass spectrometry (LC-MS). CRPC altered proteins were defined comparing the proteome of the CRPC models to their respective isogenic counterpart and selecting significantly altered hits. The lists of altered expression proteins for each model pair were then compared and a list of

commonly altered hits in the three models was obtained. One of such commonly altered proteins was SLFN5. This protein presented a fold change of >2 in CRPC across all three model pairs. SLFN5 was being overexpressed in LNCaP AI, 22Rv1 and VCAPCR in comparison with their respective androgen naïve models LNCaP, CWR22 and VCAP.

The emergence of SLFN5 as an upregulated protein across all three models of CRPC, regardless of which resistance mechanisms are engaged, signalled a potential importance of this protein in CRPC.

1.5.2 The Schlafen family

SLFN5 belongs to the relatively novel Schlafen family. This group of genes was first discovered in 1998 by Dr David A. Schwarz and colleagues when they were studying the quiescent state of peripheral T-cells[110]. Schwarz and colleagues characterised six murine Schlafen (*Slfn1-4, Slfn6-7*) genes in these mice and suggest the existence of another gene (*Slfn5*). Some members of the family were described to be transcriptionally upregulated or downregulated after positive selection of the T-cell clones in mice, and Slfn1 was found to affect development of the thyme and cause cell cycle arrest. The German word for "to sleep", Schlafen, was coined by Schwarz to name the family due the effect Slfn1 had on the cell cycle.

Further studies of the Schlafen family by Peter Geserick and colleagues in 2008 expanded the number of family members when they identified murine *Slfn5*, *Slfn8*, *Slfn9* and *Slfn10*[111]. These novel genes contained additional domains that were absent in the previously discovered Schlafen genes and were classified into a distinct subgroup. Structural homology analysis of those exclusive domains revealed a putative function as a DNA/RNA helicase and capacity to bind ATP, further expanding the potential functions of the Schlafen family to include RNA mediated transcription regulation.

In 2009, Olivia Bustos and colleagues performed a genomic study of the Schlafen family across multiple organisms[112]. They describe the Schlafen genes clustering in a region related with immune functions and suggest a degree of functional redundancy based on the similarities in the sequences of the family members.

Bustos and colleagues identified Schlafen genes in 28 animal species, including mouse and human. Phylogenetic analysis points to multiple gene duplications as the origin of the several groups of Schlafen. The group suggests that the family is under a selective pressure that causes a rapid adaptive evolution and even loss of Schlafen genes in each organism, leading to a high divergence between different species. Interestingly, they also describe a case of horizontal transmission of a Schlafen gene from rodents to orthopoxviruses, at the same time they rule out a viral origin of the Schlafen genes.

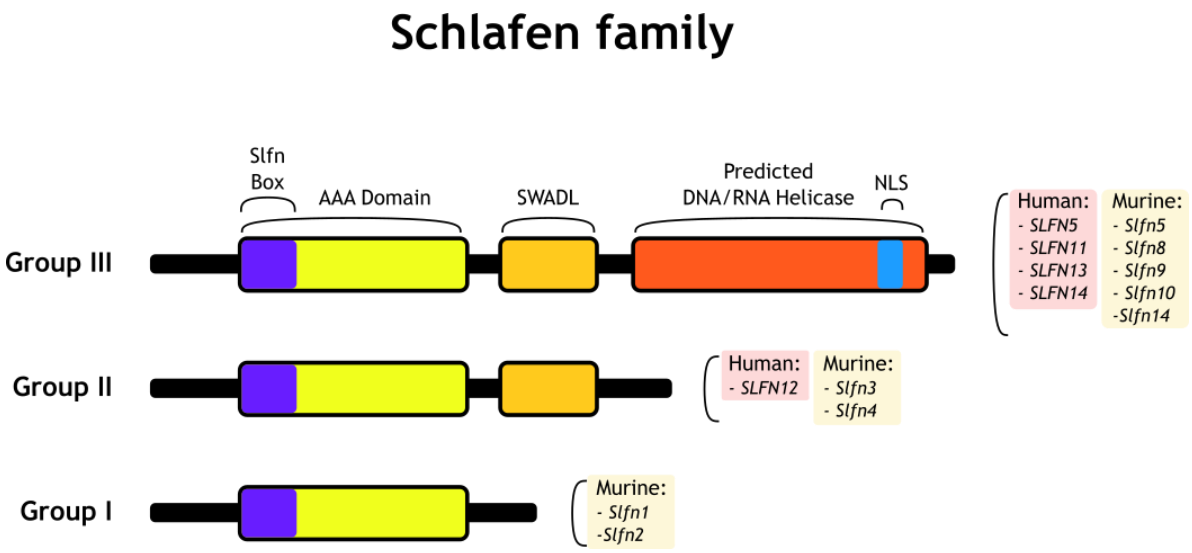

Figure 1-6 – Structure, groups and members of the Schlafen family

According to their structure and domains, the Schlafen family members are classified into three distinct groups[113] (Figure 1-6). Schlafen family Group I are the smallest members of the family, and contain domains that are shared across all members of the family. These proteins are formed by an AAA domain, predicted to interact with ATP or GTP, and the domain exclusive to the Schlafen family, termed Slfn box. This domain has a currently unknown function, but it is present only in the members of the Schlafen family. Schlafen family Group II members are comprised of the same domains as Group I, but contain an additional domain termed SWADL, also exclusive to members of the Schlafen family. The name of this domain derives from the sequence of amino acids that comprises the domain, Serine-Tryptophan-Alanine-Aspartate-Leucine, and its function has not been characterised as well. Finally, Schlafen family Group III encompasses the bigger members of the family. In addition to all the previously

described domains from groups I and II, they possess an extended C-terminal tail containing the aforementioned DNA/RNA helicase predicted domain and a nuclear localisation signal. Due to the presence of this NLS, members of the Group III are found in the nucleus, while members of the groups I and II are localised in the cytoplasm[114].

1.5.3 SLFN5

Human SLFN5 belongs to the group 3 of the Schlafen family and has been scarcely been studied in the literature. The first SLFN5-centric studies started to emerge during this last decade. Therefore, the available body of literature about SLFN5 is limited; what is known about its role and function is considerably variable. Regarding cancer, *SLFN5* has been described to act as both a tumour suppressor and a pro tumorigenic agent, with no previous existing studies about *SLFN5* in prostate cancer. This suggests a context dependent protein with biological effects result from its interaction with other active players present.

Regulation of Schlafen family members by type I interferon signalling has been described by several sources in distinct biological contexts[115]. Human SLFN5 expression was characterised in 2010 to be induced by interferons alpha and beta (IFN-α/β). A study in malignant melanoma cells showed that IFN-α/β can affect cell growth and invasion via upregulation of SLFN5 expression. Stable knockout models of *SLFN5* in these cells showed increased anchorage independent growth and invasion in a collagen matrix are a result of SLFN5 loss, although no clear molecular mechanism was established[116]. Further studies revealed that IFN-α/β-induced SLFN5 expression represses invasiveness and motility in renal carcinoma cells through suppression of matrix metalloproteinases 1 and 13. On the other hand, SLFN5 does not affect cell proliferation or morphology in this model, restricting its function to repression of the migratory properties of the cell[117]. Further studies revealed that the anti-invasive properties of SLFN5 were also found in other cancer cell models including breast, lung and colorectal cancer. Removing SLFN5 expression in these models results in increased AKT/GSK3β/β-catenin pathway activation, as well as enhanced invasive and migratory properties. This same study found SLFN5 expression to be lower in highly invasive models of fibrosarcoma and renal

clear cell cancer. Overexpression of SLFN5 in these models resulted in reduced matrix metalloproteinase 14 expression, invasion and migration[118].

In contrast with a tumour suppressor role for SLFN5 just described, several studies show *SLFN5* as a potential oncogene. A transcriptomic analysis of both acute and chronic lymphoblastic leukaemia revealed *SLFN5* as one of the 10 common upregulated genes in these pathologies in comparison with normal CD19+ B cells and samples from the thymus, suggesting an active role for *SLFN5* in this pathologies[119]. Another study showed that *SLFN5* expression in the immune cells that reside in the cancerous tissue can promote tumorigenesis as well. Following the discovery of the correlation between IFN-α induced *Slfn4* in mouse immune cells and development of intestinal metaplasia, an analysis of human samples revealed that a high expression of SLFN5 in T-lymphocytes in the inflamed gastric mucosa correlated with the development of intestinal metaplasia as well. This pathology is considered a gastric cancer precursor lesion as it carries a high probability of further development of gastric cancer[120]. Further studies on this subject suggest that both SLFN5 along with SLFN12 interfere with cell differentiation mediated by hedgehog signalling pathway in order to cause the aforementioned pathological developments[121].

A recent paper (2019) described *SLFN5* as the driver of epithelial-mesenchymal transition (EMT) in lung cancer. EMT results in loss of epithelial characteristics of the cells in favour of acquiring more a more mesenchymal phenotype. This process reduces the strength of cell-to-cell connections and tissue integrity, resulting in further disorganization and increased potential for mobility and migration. In the end, the effects of EMT lead to cancer metastasis and further disease progression. Overexpression models of SLFN5 in lung cancer cell line A549 displayed several hallmarks of EMT such as upregulation of vimentin, loss of E-cadherin, and translocation of ß-catenin to the cell nucleus. This resulted in the SLFN5 overexpressing cells to display a mesenchymal like morphology, and enhanced the migratory and invasive capabilities of these cells, in direct contrast with the migration suppressor role described avobe[122].

The complexity and apparent contradictory actions of SLFN5 extend as well to its currently described molecular mechanisms. Two recent studies (2017 and 2020) have described two different action mechanisms for SLFN5. Arslan A.D.

and colleagues characterized SLFN5 as a transcriptional co-repressor of STAT-1 transcription factor[123]. They showed that SLFN5 promotes invasiveness and motility in glioblastoma multiforme via transcriptional repression through a direct interaction with STAT-1. Type I interferon signalling engages STAT-1 driven transcription at the same time it induces SLFN5 expression. In the described case, SLFN5 acts as a negative feedback agent, repressing the type I interferon signalling. Suppression of SLFN5 expression in this model led to strengthened antineoplastic responses induced by type I interferon signalling.

On the other hand, Wan G. and colleagues performed chromatin immunoprecipitation followed by sequencing (ChIP-Seq) analysis of SLFN5 in breast cancer cells which led to the identification of several SLFN5-binding motifs in the DNA[124]. This discovery suggests a direct regulatory function of transcription mediated by the interaction between SLFN5 and the DNA strand. As proof of concept, they show that SLFN5 supresses EMT in breast cancer by directly repressing the expression of transcription factor ZEB1 by binding to one of the identified motifs present in *ZEB1* promoter region.

Overall, previous literature on SLFN5 does not present a clear and consistent functionality across different types of cancer, but at the same time, provides evidence of certain molecular functions that can help in further characterization studies of SLFN5 in CRPC.

1.6 The mTOR Pathway

The mTOR (mammalian target of rapamycin) pathway is described as a "nutrient sensor" pathway as well as a master regulator of cell growth (Figure 1-7). The mTOR pathway is activated by a combination of inputs that signal appropriate conditions for cell growth and division. Nutrient availability and external signals (such as insulin, other hormones and growth factors) are the main signals integrated by the mTOR pathway, and the adequate combination of these stimuli will engage mTOR signalling. Once engaged, the mTOR pathway coordinates signals that instruct the cell to proceed with an anabolic program to support growth and division, while supressing unnecessary catabolic processes. Two main protein complexes are described in which mTOR is a component. mTOR complex 1 (mTORC1) is the main node of the pathway signalling and the main canonical targets of the mTOR pathway sit directly downstream of mTORC1. Accompanying mTOR in this complex several proteins are found. Raptor acts as the main scaffold agent of the complex, and aids in the recruitment of downstream phosphorylation targets. Another protein, mLST8, allows the complex to interact with upstream activators of the complex. Two other proteins that function as mTORC1 repressors can also be found in the complex, PRAS40[125] and Deptor[126].

On the other hand, mTOR complex 2 (mTORC2) is a less characterised complex that contains different associated proteins and possesses a different signalling programme. It can be activated by PIP_3 and partially by AKT, as well as inhibited by mTORC1. At the same time it can phosphorylate AKT to promote its activation[127].

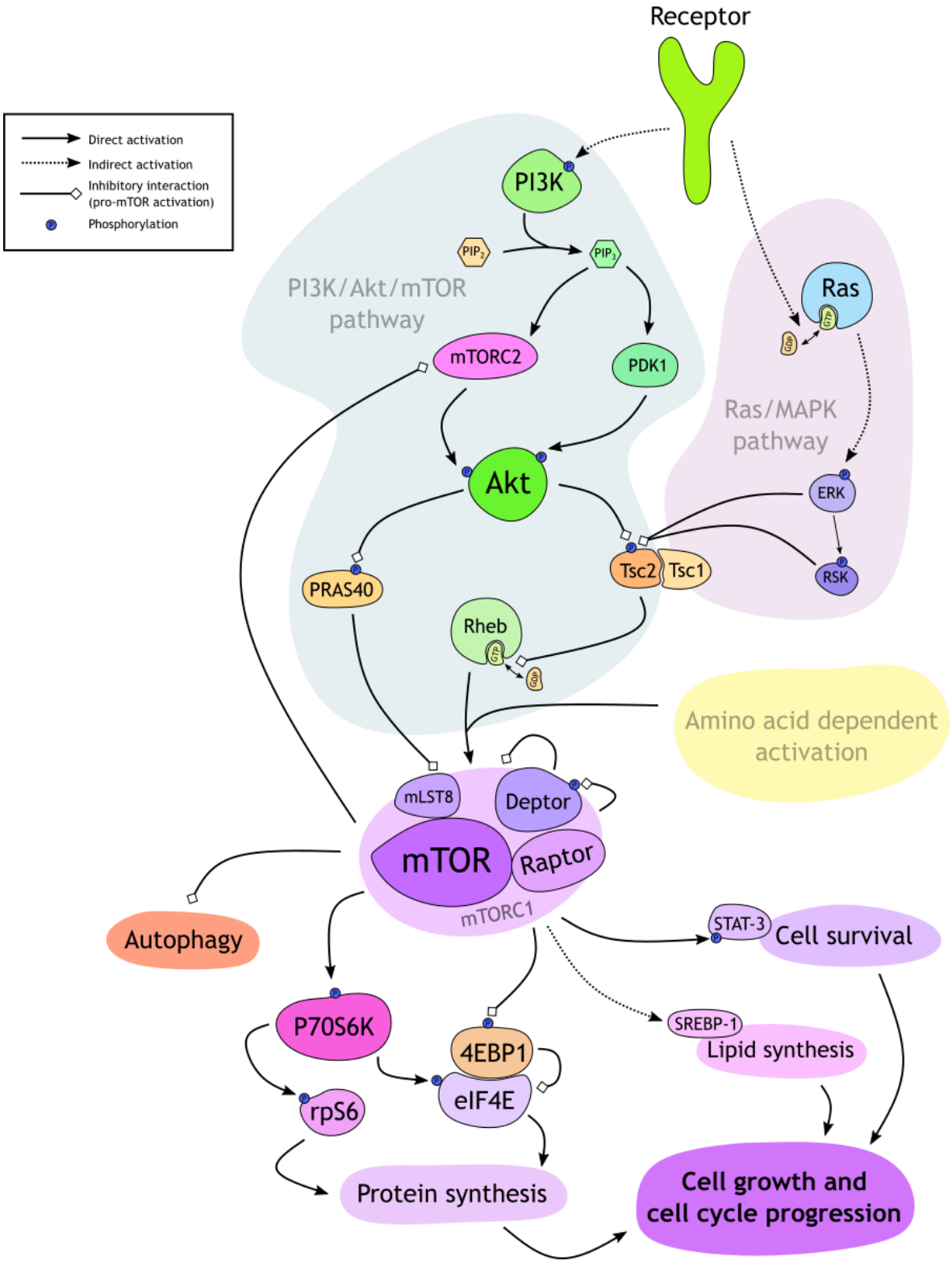

Figure 1-7 - Main activation pathway of mTORC1 signalling and downstream effects

The two main downstream targets of mTOR are the P70-S6 kinase 1 (P70S6K) and eukaryotic translation initiation factor 4E-binding protein 1 (4EBP1). The mTOR protein in the mTORC1 directly phosphorylates these two proteins[128,129], resulting in several downstream effects related with protein translation and

overall cell growth. As its own name indicates, P70S6K directly phosphorylates ribosomal protein S6 (rpS6). This protein is part of the 40S subunit of the ribosome and its phosphorylation promotes protein synthesis and polysome formation and has a key role in cell growth[130]. The actual mechanism of action of rpS6 is has not been completely characterized and contradictory results exist. Some other studies also suggest that it enhances translation of only a certain subset of mRNAs[131]. Apart from rpS6, P70S6K phosphorylates a wide array of other proteins involved in protein synthesis, including the eukaryotic translation initiation factor 4E (eIF4E).

4EBP1 in its unphosphorylated form is bound to eIF4E. This translation initiation factor is necessary to direct the interactions between the ribosome and the mRNAs. While 4EBP1 is bound to eIF4E, it is inhibiting eIF4E pro transcriptional activity. When mTORC1 phosphorylates 4EBP1, the complex dislodges and eIF4E is free to help protein synthesis.

Apart from protein synthesis, mTORC1 is capable of regulating several other processes that will aid and promote cell growth and division[132]. STAT-3 is a transcription factor capable of promoting cell proliferation and survival and can be activated by phosphorylation via mTORC1. SREBP-1 is a transcription factor that mediates the expression of lipogenic genes. Enhanced SREBP-1 expression and activation can be a consequence of mTORC1 activation, which helps the cells meet the lipid demands required for the formation of new membranes in the growth process[133].

1.6.1 Activation of mTOR signalling

The main activation route for mTOR is through the PI3K/AKT/mTOR pathway[134]. When one of the mTOR activating ligands binds its membrane receptor, PI3K is recruited to the site and activated by phosphorylation. The molecular activity of PI3K consists on the phosphorylation of lipid PIP_2, converting it into the active messenger molecule PIP_3. PIP_3 causes PDK1 and mTORC2 to phosphorylate and activate AKT. Finally, active AKT will phosphorylate mTORC1 inhibitors Tsc2 and PRAS40, supressing their inhibitory action over the complex and allowing its activation. Tsc2 exists in a complex with Tsc1, with the latter being responsible of maintaining the complex together. The way Tsc2 exerts its inhibitory function

over mTOR is by keeping the Rheb protein inactive. Rheb is a GTP binding protein that requires to be bound to GTP in order to activate the mTORC1. Tsc2 enzymatic activity catalyses the transformation of Rheb bound GTP into GDP, inactivating Rheb. It is the phosphorylation of Tsc2 by AKT what causes a halt of that activity, allowing GTP bound Rheb to activate mTORC1[135,136]. Once mTORC1 is activated, it will phosphorylate the Deptor protein marking it for degradation and supressing its inhibition (Figure 1-7).

The mTOR pathway can also be activated by external ligands via the Ras/MAPK/ERK signalling pathway. In this case, the Ras protein is activated in response to ligand binding on the appropriate receptors, which leads to downstream phosphorylation of ERK and RSK. Both this kinases have the ability to phosphorylate Tcs2, stopping its inhibitory action over Rheb[137] (Figure 1-7).

External growth signals by themselves are not enough to activate mTOR signalling. The pathway works to make sure that the increase in the nutritional demands of cell growth is going to be met before engaging the molecular machinery. In order to accomplish this signal integration, activation of the mTOR pathway is also dependent on the available levels of amino acids. This nutrient sensing capability constitutes an independent activation pathway that needs to be engaged in order for any growth signals to be able to promote cell growth via mTOR. The Rheb protein is localised mainly in the lysosomes, and mTORC1 needs to move from the cytosol to the lysosomal surface in order to be activated by Rheb. This process is controlled by a sensor system in the lysosome that reacts to amino acid availability and allows anchorage of mTORC1 to the lysosome, allowing its subsequent activation by Rheb[138].

A Rag protein complex formed by RagA and RagB controls the recruitment of mTORC1 to the lysosomal surface via interaction with Raptor. These Rag proteins are GTPases whose activation is controlled by the levels of amino acids in the cell. The RagA/B complex is kept in the lysosomal membrane bound to a protein complex known as Ragulator. This complex possesses guanine exchange activity that will directly activate the RagA/B complex by addition of GTP in response to amino acid levels. Once this has occurred, the active Ragulator/RagA/B complex will allow the docking of mTORC1 to the lysosomal membrane via interaction with Raptor and the subsequent activation of mTORC1 by Rheb[139].

The main amino acid sensing capabilities of this system are mediated by the Vacuolar H^+-ATPase (v-ATPase). The presence of this protein in the lysosomal membrane and its ATPase activity has been proved to be essential for mTORC1 activation by the Ragulator/RagA/B complex[139,140]. The v-ATPase directly interacts with the RagA/B complex and Ragulator in an amino acid dependent manner. The mechanism by which the v-ATPase senses amino acids levels has not been completely characterized, but seems to involve the disassembly of both v-ATPase subunits in response to amino acids being accumulated inside the lysosome[141].

The intralysosomal accumulation of amino acids, especially leucine, seems to be a key factor for regulation of v-ATPase assembly and interaction with Ragulator and RagA/B. When amino acids were exported out of the lysosome either by transporter overexpression or membrane permeability, it disrupted mTORC1 recruitment and activation[140]. Further studies demonstrated that the essential amino acid (EAA) leucine seems to be the most powerful activator of this sensing machinery. When comparing the phosphorylation of mTOR downstream targets it was found that when added at the same concentration, leucine produced the highest mTOR activation effect among all the EAA tested[142].

Transport of leucine into the lysosomal compartment is carried on mainly by the LAT1 amino acid transporter. Earlier studies showed that treatment with LAT1 inhibitors interrupted the leucine mediated activation of mTOR[143]. Further experiments demonstrated that a dual transport system was required. For LAT1 to import leucine, it needs to transport glutamine in the opposite direction, meaning accumulation of glutamine was necessary for LAT1 mediated leucine transport. Transporter ASCT2 (*SLC1A5*) was identified as the glutamine transporter responsible of such activity. After that, it was finally demonstrated that the localisation and activity of both LAT1 and ASCT2 in the lysosomal membrane are necessary for leucine-dependent activation of mTOR, proving that the lysosome is the main site where amino acid levels are sensed by the mTOR activating machinery[144,145] (Figure 1-8).

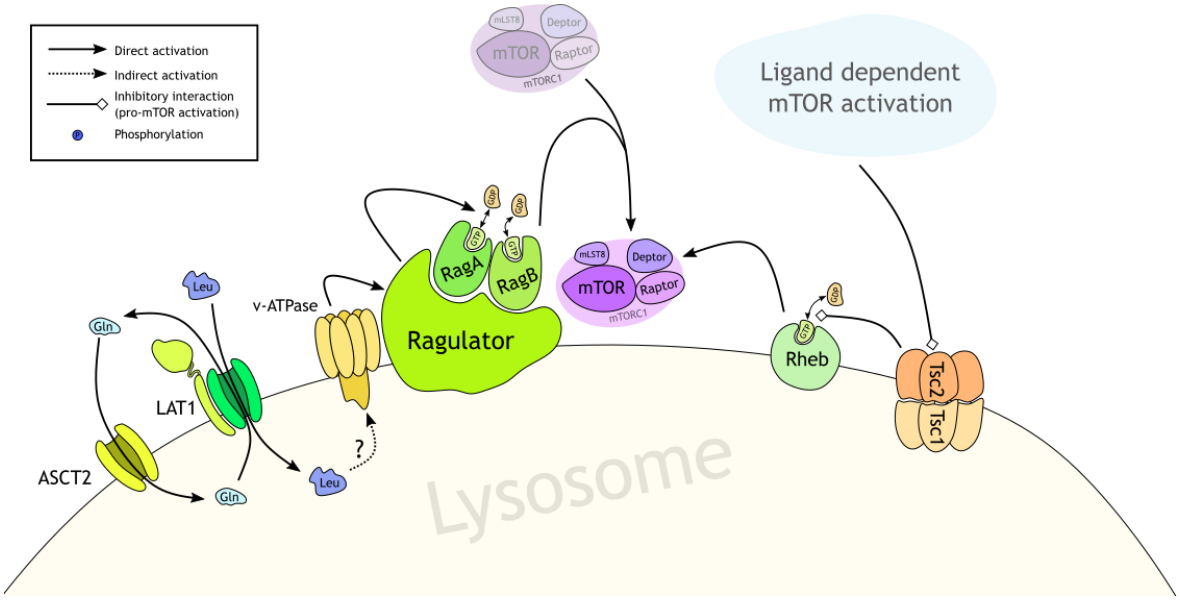

Figure 1-8 – Lysosomal amino acid sensing machinery controls mTOR localisation and activation

1.6.2 mTOR and prostate cancer

As described previously in this work, activation of the mTOR pathway in advanced prostate cancer is a common occurrence as a result of PTEN loss. This leads to the unchecked production of PIP_3 and subsequent activation of mTORC1 induced growth signalling. Genomic studies highlighted alterations in the PI3K/AKT/mTOR pathway are a common event in invasive prostate cancer. A study from 2010 analysed samples from 218 tumours and discovered alterations related with the PI3K/AKT/mTOR pathway in ~50% of the primary samples and in all of the metastatic samples[146]. At the same time, they observe the *PTEN* alteration rate to be around 40%, similar to what had been previously reported in other studies[147,148]. *In vivo* studies using double PTEN/mTOR knockout confirmed the need of a functioning mTOR for PTEN loss driven tumorigenesis and tumour progression in prostate cancer[149]. Furthermore, ribosome profiling in mTOR driven PC3 prostate cancer cells revealed that the main processes regulated by mTOR driven genes were translation, cell invasion and metastasis[150].

The role of the PI3K/AKT/mTOR pathway activation in prostate cancer is not confined to the replacement of the AR-mediated growth that is lost after ADT. A reciprocal inhibitory interaction between both pathways has been reported in

prostate cancer cells[151,152]. Activation of the PI3K/AKT/mTOR pathway in prostate cancer leads to reduced expression of the HER2 kinase. As mentioned previously, HER2 can directly phosphorylate AR, promoting its stability and activation. At the same time, active AR signalling inhibits PI3K/AKT/mTOR activation by promoting the expression of PHLPP, an AKT phosphatase (Figure 1-9). This regulatory feedback between both pathways can help explain the unsatisfactory results of treating of CRPC with PI3K/AKT/mTOR pathway inhibitors, but at the same time sheds light on the high prevalence of PTEN loss and other PI3K/AKT/mTOR alterations in prostate cancer. Combination therapy aimed at supressing both AR and PI3K/AKT/mTOR signalling has been studied but with mixed results, and further research on the nature of this relationship and the development of novel drugs that involve mTORC2 is suggested in the literature[153,154].

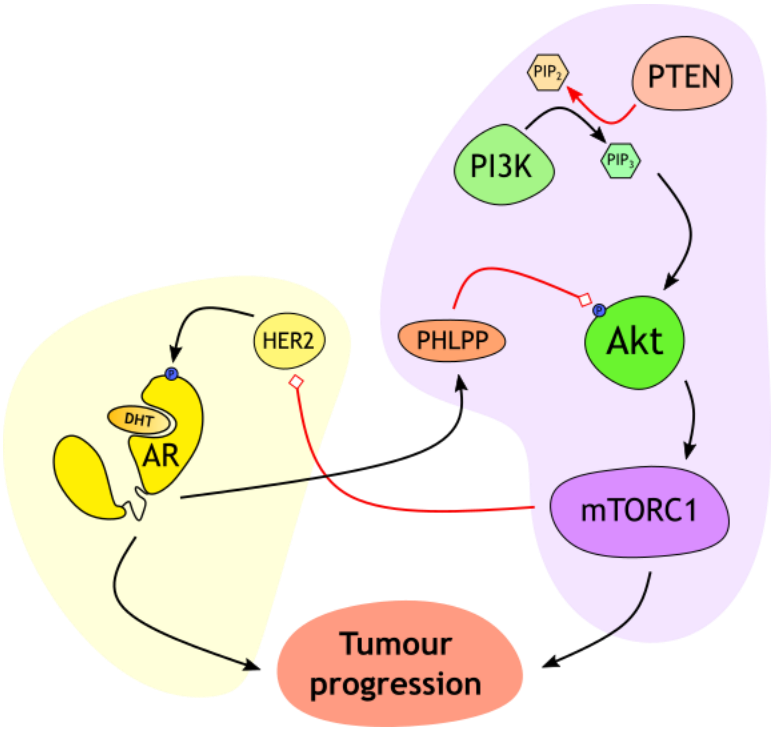

Figure 1-9 - Inhibitory interactions between the AR and the PI3K/AKT/mTOR pathways

1.6.3 Autophagy

Autophagy is a process in which the cells degrade their own organelles and proteins, recycling damaged and obsolete cell parts into useful metabolites. This process is engaged in response to nutrient scarcity and metabolic stress,

providing a way to overcome those challenges. Internal vesicles called autophagosomes are formed, containing cellular material. Once the autophagosomes are completed they proceed to fuse with lysosomes, forming autolysosomes. Inside these vesicles, the digestive enzymes of the lysosomes act on the contents of the autophagosomes, degrading them and obtaining basic nutrients such as free amino acids.

As mentioned previously, an active mTORC1 represses autophagy, as mTOR activation occurs in response to growth signals and adequate nutrient levels. There are several regulation steps that mTORC1 disrupts impeding the engagement of autophagy[155,156]. The more preeminent process blocked by mTORC1 is the autophagosome formation. This process requires the successive action of two protein complexes, the ULK complex, and the PIK3C3 complex, activated by the former. The ULK complex is inhibited by phosphorylation of the ULK1/2 and ATG13 proteins by mTORC1. The PIK3C3 complex causes the synthesis of PIP3 in the autophagosome surface leading to subsequent recruitment of the proteins needed for the finalisation of the autophagosome. In addition to the reduced ULK activity, mTORC1 phosphorylates AMBRA1 and ATG14L directly inhibiting the activity of the PIK3C3 complex as well. Furthermore, mTORC1 also affects the transcription of autophagy related genes by causing the Transcription Factor EB (TFEB) to remain in the cytoplasm. This transcription factor controls the expression of several lysosome and autophagosome related genes.

The role of autophagy in cancer has been described as context dependent, or more precisely, stage dependent. In the early stages of cancer development, inhibition of autophagy can cause inadequate responses to cellular stress leading to the accumulation of free radicals. These free radicals promote cellular alterations and mutations that will result in more tumorigenic phenotypes. At the same time in advanced stages of prostate cancer, engagement of autophagy aids in dealing with the increased nutrient demands and metabolic challenges suffered by cells in the centre of tumoural growths[157].

In the case of prostate cancer, autophagy is described to be supressed by AR signalling. Consequently, under androgen deprivation prostate cancer cells have been reported to engage autophagy and undergo apoptosis in response to

autophagy inhibitors[158]. At the same time, enzalutamide resistant cells are shown to be more sensitive to autophagy inhibition and exhibited reduced mTOR activation[159].

On the other hand, a more recent study reports that AR activation causes engagement of autophagy and describes that the expression of several autophagy related genes (including TFEB) is promoted by AR signalling. Furthermore, it correlates the expression of those autophagy related genes with cancer progression and metastasis[160]. All these seemingly contradictory statements can be explained by the fact that androgen deprivation causes considerable cellular stress, which also results in autophagy activation[161]. On top of that, as previously mentioned the effect of autophagy in cancer development and progress is dependent on cancer stage. The seemingly contradictory roles of autophagy in prostate cancer remain to be fully defined, constituting an interesting object of study.

1.7 LAT1 Amino Acid Transporter

LAT stands for Large Amino acid Transporter. LAT1 (also known as CD98) is an amino acid transporter formed by the association of two proteins, SLC7a5 and SLC3a2/4F2hc. SLC7a5 is the main protein of the unit and defines LAT1, while SLC3a2 can bind to other proteins to form other transporters.

LAT1 function was first reported in 1963[162]. It transports mainly neutral and branched amino acids in a Na+ and pH independent manner. Its main substrates are phenylalanine, tryptophan, leucine, isoleucine, methionine, histidine, tyrosine and valine[163]. Its transport function is not restricted to these amino acids, as it has been show to transport other amino acids with reduced affinity as well as other molecules such as L-Dopa, thyroid hormones and drugs like baclofen and melphalan[164].

SLC3a2/4F2hc is required for SLC7a5 to act as a transporter[165]. SLC3a2 is a glycoprotein that binds SLC7a5 with a disulphide bond in order to stabilize it and localize it to the plasma membrane[166]. SLC3a2 itself does not have any transport activity[167]. SLC3a2 can also bind the SLC7a8 to form LAT2, another amino acid transporter with similar kinetics and substrate affinity[168]. SLC3a2 by itself has as

well been found to be a marker of poor prognosis[169], and not all of its biological effects can be explained by its bond with the LAT transporters, pointing to biological roles for SLC3a2 beyond the stabilisation of LAT complexes[170].

Intake of substrate by LAT1 is usually performed in exchange of glutamine, which is exported out of the cell. This makes LAT1 function dependent on the availability of glutamine within the cells, linking its activity to that of glutamine importers such as ACST2/SLC1a5[171]. Other molecules are known to be able to be used as exchange currency for extracellular amino acids, but glutamine is the most prevalent in human cells.

One of the main functions of LAT1 is to provide the cell with several EAA so growth can occur, as amino acids are necessary both for energetic and anabolic reasons[172]. The cell depends on EAA because they cannot be synthetized endogenously, and the only alternative is to obtain them from the environment. Interestingly, while LAT1 is not associated with amino acid absorption from the diet (which is mediated by other transporters), it is involved in amino acid transport and homeostasis across the blood-brain barrier[173] and the placenta[174]. It has also been found to regulate and promote angiogenesis when expressed by endothelial cells[175,176]. In addition to these roles, LAT1 is also necessary for the amino acid sensing system of the mTOR pathway, as described before. Its transport of leucine into the lysosome is required for the localisation of mTORC1 into the lysosomal surface.

1.7.1 LAT1 and cancer

LAT1 has been found to be expressed in several cancer types including thymic carcinoma[177], glioblastoma[178], gastric carcinoma[179], pancreatic ductal adenocarcinoma[180,181], non-small cell lung cancer[182] and prostate cancer[183]. Its expression has been associated with bad prognosis, disease severity, metastasis and resistance to treatment. The increase in LAT1 expression in cancer is in keeping with the surge in metabolic needs caused by tumour growth. Cancer cells need keep up growth under the increasingly stressful conditions caused by tumour expansion and the activation of growth-driving signalling pathways such as the PI3K/AKT/mTOR pathway.

In the specific case of prostate cancer, it has been shown that LAT1 correlates with cancer differentiation as measured Gleason score[184]. A study by Qian and colleagues in 2011 characterised a mechanism by which LAT1 expression emerges in androgen independent prostate cancer. Qian and his group observed that LAT1 expression in hormone naïve LNCaP cells was low, and that the main transporter for leucine uptake was another member of the LAT family, LAT3. On the other hand, in the androgen-insensitive PC-3 cell line they observed an increased expression of LAT1 and dependence on its transport function. They proposed a model in which the cellular stress caused by androgen deprivation causes a switch from LAT3 to LAT1, mediated by the ATF4 transcription factor[185]. It is unknow why a pro anabolic hormone such as DHT reduces the intake of an amino acid transporter. It can be speculated that LAT3 is a more efficient transporter or that LAT1 is more a pro-homeostasis transporter than a intake driver under normal circumstances. Another study by Xu and colleagues found LAT1 expression correlated with shorter time to develop CRPC after ADT. They also observe high levels of LAT1 in PC-3 and other androgen independent cell lines such as C4-2 and DU145. Furthermore, they observe that silencing AR expression increases LAT1 levels, and that addition of DHT reduces LAT1 expression[186]. Altogether, the literature strongly points to LAT1 expression being an important factor in the development and survival of the CRPC phenotype.

Chapter 2 - Materials and Methods

2.1 Cell culture

Human hormone naïve prostate cancer cell lines LNCaP and CWR22 and human melanoma cell line A375 were cultured in RPMI 1640 with Phenol Red, no Glutamine (Gibco, 31870025). Media for hormone naïve cells was supplemented with 2 mmol Glutamine and 10% Foetal Bovine Serum (FBS). This media formulation will be referred as FBS media throughout this text.

Human castration resistant prostate cancer cell lines LNCaP AI and 22Rv1 were cultured in RPMI 1640 without Phenol Red nor Glutamine (Gibco, 34204014), supplemented with 2 mmol Glutamine and 10% Charcoal Stripped Foetal Bovine Serum (CSS) (Gibco, 10706143). This serum does not contain androgens and Phenol Red is removed from the formulation to avoid any interference with Androgen Receptor signalling[187]. This media formulation will be referred as CSS media throughout this text.

22Rv1 (ATCC CRL-2505) and LNCaP (ATCC CRL-1740) were obtained from ATCC. LNCaP AI cells were obtained from Newcastle University, UK. CWR22 cells were obtained from Case Western Reserve University, Cleveland, Ohio.

To perform passing on the cells, Trypsin 0.25% was added to the cells and they were left from 5 to 10 minutes at 37ºC until all cells were detached from the bottom. Appropriate media supplemented with serum was added to stop the Trypsin activity. For the 22Rv1, resuspended cells were passed at this stage through a 40µm filter to avoid clumping and issues regarding plate attachment. Cells were then seeded in culture flasks at roughly 30-40 % confluence.

2.2 Development of knockout and overexpressing cell lines

2.2.1 CRISPR/Cas9 Knockout

Commercial plasmids Slfn5 CRISPR/Cas9 KO Plasmid (sc-408333), Slfn5 HDR Plasmid (sc-408333-HDR) and appropriate control plasmids (Santa Cruz Biotechnology) were transfected into 22Rv1 and LNCaP AI cells to develop stable

SLFN5 knockout clones. Transfection was performed on 10^6 cells at a time using Cell Line Nucleofector Kit V (Lonza, VCA-1003) and a Nucleofector 2b Device (Lonza, AAB-1001), program T-013. After transfection, cells were resuspended in CSS media to a final volume of 10mL and seeded into 6 cm plates. 24 hours after that, fresh media containing 0.5µg/mL Puromycin was added to the cells. Cells were kept under this selection media until visible and isolated colonies developed. These colonies were individually picked and expanded to develop stable clonal cell lines. Loss of expression of SLFN5 was validated by Western Blot.

2.2.2 SLFN5 and SLC7a5 overexpressing cell lines

Hormone naïve LNCaP and CWR22 cells were transfected with the SLFN5 (NM_144975) Human MYC-Tagged ORF Clone plasmid (Origene, RC216330). 22Rv1 SLFN5 KO cells were transfected with the SLC7A5 (NM_003486) Human Tagged ORF Clone plasmid (Origene, RC207604). The corresponding empty vector (Origene, PS100001) was used to develop adequate clonal controls. Transfection was performed on 10^6 cells at a time using Cell Line Nucleofector Kit V (Lonza, VCA-1003) and a Nucleofector 2b Device (Lonza, AAB-1001), program T-013. After transfection, cells were resuspended in FBS media to a final volume of 10mL and seeded into 6 cm plates. 24 hours after that, fresh media containing 1mg/mL G418 was added to the cells. Cells were kept under this selection media until visible and isolated colonies developed. These colonies were individually picked and expanded to develop stable clonal cell lines. Expression of the exogenously introduced protein was validated by Western Blot using antibodies against SLFN5 and SLC7a5 along with MYC-tag.

2.3 Western Blotting

Protein expression was measured using western blotting. Cell lysates were obtained scrapping cells or suspending tissue in 1% SDS supplemented with PMSF 57µL as protease inhibitor and 1 tablet of PhosSTOP™ (MERCK, 4906837001) per 10 mL of solution. Cells were briefly sonicated afterwards to achieve liquid consistency of the lysate. Lysates were quantified using Pierce BCA Protein Assay Kit (Thermo Fisher, 23225). NuPAGE™ LDS Sample Buffer (4X) (Thermo Fisher, NP0007) supplemented with NuPAGE Sample Reducing Agent (10X) (Thermo

Fisher, NP0004) was added to the samples. 10 to 30 µg were loaded into 4%-12% gradient gels or 4%/10% gels and run at 110V for 80 to 120 minutes. Proteins were then transferred from the gel to an Immobilon-FL PVDF Membrane (MERCK, IPFL00010) using 35V for 120 minutes. Membrane was then blocked with 5% powdered milk in 1% TBST for 20 minutes, and further washed 3 times with 1% TBST. Primary antibodies were added 1:1000 in 5% BSA containing 0.05% Sodium Azide and left on overnight on a roller at 4ºC (Table 2-1). Primary antibodies were washed 3 times with 1% TBST and secondary antibodies were added according to the visualization method (Table 2-2). Membrane was washed 3 times with 1% TBST and visualized using a LI-COR Odyssey CLx Imaging system (LI-COR Biosciences) or a MyECL machine (Thermo Fisher Scientific) using Pierce™ ECL Plus Western Blotting Substrate (Thermo Fisher Scientific, 32132).

Table 2-1 - Primary antibodies used in Western Blot

Target	Species	Company	Reference	MW
4EBP1	Rabbit	Cell Signaling	9644S	15-20
AKT	Rabbit	Cell Signaling	4685S	56
AR	Rabbit	Santa Cruz	sc-816	120, 80 (V7 var.)
HSC70	Mouse	Santa Cruz	sc-7298	70
LC3	Rabbit	Cell Signaling	12741P	14, 16
p-4EPB1 (Thr37/46)	Rabbit	Cell Signaling	2855S	15-20
P70	Rabbit	Cell Signaling	9202	70, 85
p-AKT (Thr308)	Rabbit	Cell Signaling	9275S	56
p-P70-S6k (Thr389)	Rabbit	Cell Signaling	9234S	70, 85
p-S6 (Ser235/236)	Rabbit	Cell Signaling	4856	32
p-S6 (Ser240/244)	Rabbit	Cell Signaling	2215	32
SLC3a2	Rabbit	Sigma	SAB1400263	80
SLC7a5	Rabbit	Cell Signaling	5347S	38
SLFN5	Rabbit	Abcam	ab121537	110
Tubulin-α	Mouse	Santa Cruz	sc-8035	50
p-JAK1 (Tyr1034/1035)	Rabbit	Cell Signaling	D7N4Z	130
p-STAT1 (Tyr 701)	Rabbit	Cell Signaling	58D6	84, 91
MYC-tag	Rabbit	Cell Signaling	2276	Variable
ATF4	Rabbit	Cell Signaling	D4B8	38

Table 2-2 - Secondary antibodies used in Western Blot

Target Species	Method	Company	Reference
Rabbit	LI-COR Odyssey CLx Imaging system	LI-COR	IRDye® 680RD Goat anti-Rabbit IgG Secondary Antibody

Mouse	LI-COR Odyssey CLx Imaging system	LI-COR	IRDye® 800CW Goat anti-Mouse IgG Secondary Antibody
Rabbit	Pierce™ ECL Plus Western Blotting Substrate	Cell Signaling	Anti-rabbit IgG, HRP-linked Antibody #7074
Mouse	Pierce™ ECL Plus Western Blotting Substrate	Cell Signaling	Anti-mouse IgG, HRP-linked Antibody #7076

2.4 qPCR

Cells were scraped in 350µL RLT buffer and processed using QIAshredder homogeniser columns (Qiagen, 79654). At this point, samples could be kept at -20ºC. RNA extraction was performed using RNeasy Mini Kit (Qiagen, 74104) with on-column DNase digestion (Qiagen, RNase-Free DNase Set, 79254) following the manufacturer´s protocol. RNA concentration was determined using a Nanodrop machine. 4 µg of RNA were used to prepare cDNA. A High-Capacity cDNA Reverse Transcription Kit (Thermo Fisher Scientific, 4368814) was used to synthetize cDNA following provided instructions. The qPCR was performed using TaqMan Universal Master Mix (Thermo Fisher Scientific, 4305719) and the appropriate probe from Universal ProbeLibrary (Roche) corresponding to each primer (Thermo Fisher Scientific) (Table 2-3). The qPCR was performed in an ABI 7500 FAST qPCR system (Thermo Fisher Scientific).

Table 2-3 - Primer sequences and corresponding probes

Gene	F Sequence	R Sequence	Probe
CASC3	ggggttccagttaatacaagtttc	gccagctgtatttctcttctgag	84
SLFN5	agcaagcctgtgtgcattc	ctggctggcagatgtttttc	84
AR	gccttgctctctagcctcaa	ggtcgtccacgtgtaagttg	14
SLC7a5	ttatacagcggcctctttgc	tgatcatttcctctgtgacga	88
SLC3a2	agccaaggctgacctcct	aggcgttccagctcaaga	20
NCCRP1	tgacgaacaaccagccatta	cagcagccagacatgcag	42
NDNF	gtcaaaacctgcagaaagca	catccagcaggtaagatttgc	41
TFPI	gcctgggcaatatgaacaat	ccacctggaaaccattcg	47
KCNH5	tttttggagaacatcgtcagg	caggccaatccacaatctg	48
NCMAP	gggggataccaccttcttct	tgatgatgacaaccaccaca	50
STRBP	aacaaggggagcttttgttg	ggggcagctgtgctgtaa	68
ORAI2	gatggaagtgcttggatgc	aggcacgttaagctcagcac	58
ATF4	tctccagcgacaaggctaa	ccaatctgtcccggagaa	76
ACACB	gtttgcggattcccaattt	cctcggatggacagttcct	2
CFAP61	ctggaaacgcgctctgtag	caggcataagtcagggaagg	64
FLRT2	gcaccaagaaggacaactcc	aggagacgatctgaaaactggt	80

MYC	tgctccatgaggagacacc	cctcatcttcttgttcctcca	77

2.5 siRNA transfection

To perform transient silencing of genes, Lipofectamine RNAimax (Thermo Fisher Scientific, 13778150) was used following the provided protocol. The siRNA was added to 750.000 cells seeded in 6-well plates. ON-TARGETplus smartpool siRNAs against AR (L-003400-00), SLFN5 (L-027164-01), MYC (L-003282-02) and ATF4 (L-005125-00), as well as non-targeting siRNA (D-001810-01-20) were purchased from Dharmacon. 72 hours after transfection, RNA or protein were extracted as described for qPCR analysis and Western Blot, respectively.

2.6 Immunofluorescence staining

Cells are seeded in 12 well plates containing sterile 19mm coverslips and grown to 40-60% confluence. Cells were then washed with cold PBS 1x and fixed by adding a 1:1 Acetone/Methanol solution and leaving the plate at -20°C for 20 minutes. The fixing solution was carefully aspirated and cold PBS 1x was added to the cells for 5 minutes three times. Blocking solution (10% FBS, 0.5% BSA, 0.3% Triton X-100 in PBS 1x) was applied and left for 1 hour. Cells were washed in PBS 1x following previous instructions. Primary antibody solution (1% BSA, 0.3% Triton X-100, 2µg/mL of primary antibody in PBS 1x) was added and left overnight at 4°C. Cells were washed again in PBS and secondary antibody solution (1% BSA, 0.3% Triton X-100, 1:100 anti-rabbit Alexa 555 antibody in PBS) was added and left for 1 hour at room temperature. Finally, cells were washed again in PBS and mounted into microscopy slides using mounting media containing 4',6-diamidino-2-phenylindole (DAPI). Pictures of the preparations were acquired using a Nikon A1R Z6005 (Nikon Instruments) and further processed using ImageJ software. Primary antibodies for SLFN5 and MYC-Tag used can be found in Table 2-1.

2.7 Immunohistochemistry of human samples

A cohort of 537 prostate cancer samples was kindly provided by Dr. Ladan Fazlin and Dr. Martin Gleave from the Vancouver Prostate Centre. SLFN5 protein expression was assessed by performing immunohistochemistry using an automated staining platform, Ventana DISCOVERY Ultra (Ventana Medical

Systems). FFPE TMA sections were baked, deparaffinized, and incubated in antigen retrieval solution CC1 (Ventana) at 95ºC for 64 min. Following, primary antibody anti-SLFN5 antibody (abcam, ab121537) was added 1:100 and incubated at room temperature for 1 hour. UltraMap DAB anti-Rb or anti-Ms Detection Kit (Ventana) were used for detection. Stained slides were scanned using a Leica Aperio AT2 (Leica Microsystems). Aperio ImageScope software (Leica Biosystems) was used to quantify positively stained cells by a scoring algorithm measuring intensity and pixel count in hand annotated areas. For the analysis, PSA recurrence was defined as by the American Society for Therapeutic Radiology and Oncology (ASTRO), which is 3 successive rises in PSA above nadir, with the date of recurrence designated as the midpoint between the nadir and the first measurements[188].

2.8 In vitro cell growth assessment

2.8.1 Cell proliferation

To asses cell proliferation in 2D culture, 70.000 cells per well were seeded in 24 well plates. T=0 cells were counted 24 hours after the initial seeding to stablish an accurate initial number. Fresh media was added at t=0 to the rest of the wells. Cells were then counted at 24, 48 and 72 hours after t=0. A CellDrop Cell Counter (DeNovix) was used to automatically count the number of cells in each well.

2.8.2 Cell confluence

Cells were plated at a 10-30% confluence and left overnight to attach to the substrate. The next day before inserting the plates into the Incucyte system, fresh media and any treatment of interest were added to the cells. Cell confluence was then measured at stablished intervals (1-2 hours) using an IncuCyte ZOOM live-cell analysis system or an IncuCyte S3 live cell analysis system (Essen Bioscience Ltd). Confluence was analysed used confluence masks specifically calibrated for the assessed cell lines.

2.8.3 Anchorage independent growth

Assessment of anchorage independent growth was performed using a protocol modified from Horibata et al. 2015[189]. Sterile 3% agarose in distilled water was prepared and autoclaved before use. In preparation to the addition of cells to the wells, a bottom layer was formed by adding 2mL of 0.6% agarose to each well of 6-well cell culture plates. The 0.6% agarose for the bottom layer was prepared by mixing the premade 3% agarose with warm culture media in a 1:4 ratio just before the addition. The bottom layer was allowed to solidify by placing the plates in a flat surface at 4ºC for 1 hour. Before the addition of the cell layer, the plates were kept at 37ºC for at least 30 minutes. To prepare the cell layer, cells were resuspended using Trypsin and diluted to a concentration of 40.000 cells/mL and mixed in a 1:1 ratio with 0.6% agarose, prepared as described before. To each well, 1 mL of the cell-agarose mixture was added. Plates were left on a flat surface at 4ºC for 15 minutes to allow the cell layer to solidify, after which the plates were moved to a 37ºC degree 5% CO_2 incubator. A week after the cell layer was added, 1 mL of feeder layer was added. This layer was prepared mixing the 3% agarose solution with culture media in a 1:10 ratio to obtain 0.3% agarose. After adding the feeder layer, plates were left on a flat surface at 4ºC for 15 minutes before placing them back on the incubator. A week after the addition of the feeder layer (2 weeks after the cell layer was added), images were taken using a contrast phase microscope. Colony size and number were analysed using Colony Counter plugin (https://imagej.nih.gov/ij/plugins/colony-counter.html, Bruno Vieira, University of Lisbon) for ImageJ.

2.9 Transwell migration assay

For 24 hours before the seeding, cells were nutrient starved by being kept in serum-free media. To prepare the well, 500µL of serum containing media were added to wells on 24 well plates and Corning transwell polycarbonate membrane cell culture inserts (MERCK, CLS3413) were then inserted into the wells. Cells were resuspended in serum-free media at a concentration of 10^6 cells/mL, and 500µL (500.000 cells) were added to the well of each membrane insert. After 24 hours, the inserts were fixed by adding 100% methanol and placing the cells at -20°C for 30 minutes. To stain the cells, the membranes were submerged in

filtered haematoxylin for 30 minutes. T membranes were then washed using tap water and cells on the internal side of the membrane (cells that have not migrated) were scrapped with a wet cotton bud. Membranes were washed again in tap water and left to dry for exactly 15 minutes. Membranes were removed from the insert and mounted onto microscopy slides, the bottom side (where cells that have migrated remain) facing upwards. Images were taken with a Zeiss AXIO microscope (Zeiss) at 2.5x magnification and further analysed using ImageJ.

2.9.1 Cell count of transwell migration assay

Cells were automatically counted in Image J using a custom pipeline. An image comprising the entire membrane was created by merging images with Adobe Photoshop (Adobe). The composed image was further processed in ImageJ performing the following instructions:

Image>Color>Split Channels. Red and Blue channel images are discarded, and all following work is performed on the Green channel image.

Process>Enhance Contrast 0.3%

Process>Filters>Unsharp Mask 1, 0.6

Process>Math>Max>200

Four 370x370 pixel areas are selected from each membrane image and new image files are created from them (*File>New>Internal Clipboard*). Further processing was done individually in each one of these images.

Image>Adjust>Threshold (Default parameters)

Process>Binary>Watershed

Analyze>Analyze Particles: *Size:25-Infinity* and *Show:Masks*. This will output the number of cells detected in each image.

2.10 In vivo experiment (surgical procedure, measurement, sampling)

To develop an *in vivo* orthograft model, 14x10^6 cells 22Rv1 cells per mice were injected into the anterior prostate lobe of CD1-nude mice (Charles River Laboratories). Androgen depletion was produced by performing an orchidectomy on the same surgery as the injection. In preparation for the injection, the cells were suspended in serum-free RPMI medium and mixed in a 1:1 proportion with Matrigel (Corning). 50 µl of cell suspension containing the appropriate number of cells were injected orthotopically into the mice. Tumours were allowed to grow for 9 weeks after injection, after which mice were sacrificed and samples harvested. The endpoint was decided by monitoring the size of the tumours and executed before an endpoint diameter of 1.2 cm was reached by any tumour. Tumour growth was monitored weekly starting at the third week after surgery to allow for tumour establishment. Ultrasound imaging was used to monitor and collect size data, performed with the Vevo3100 ultrasound imaging system (Fujifilm Visualsonics). At the end of the experiment, mice were euthanised by excess of CO2 and tumours were collected. Half of the tumour material was snap-frozen in liquid nitrogen for further analysis, while the other half was fixed in 10% formalin for histological procedures.

2.11 Transcriptomics

RNA was extracted from samples using RNeasy Mini Kit (Qiagen, 74104) after homogenisation with QIAshredder homogeniser columns (Qiagen, 79654). DNA was degraded with RNase-Free DNase Set (Qiagen, 79254). Quality of the purified RNA was then measured on a 2200 Tapestation (Agilent) using RNA screentape.

Preparation of libraries for cluster generation and DNA sequencing was done with an adapted method derived from Fisher et al. 2011[190] using Illumina TruSeq Stranded mRNA LT Kit (Illumina, 20020594). Quality and quantity of the DNA libraries was assessed using a 2200 Tapestation (D1000 screentape) and Qubit (Thermo Fisher Scientific, Q32851) respectively. The libraries were run on the Illumina Next Seq 500 using the High Output 75 cycles kit (2 x 36 cycles, paired end reads, single index).

Fastq files were generated from the sequencer output using Illumina's bcl2fastq. Quality checks on the raw data were performed using FastQC and Fastq Screen. RNA-Seq paired-end reads were aligned to the human genome, version GRCh38 and annotated using Tophat. Expression levels were analysed with HTSeq, and R environment with packages from the Bioconductor data analysis suite and differential gene expression analysis based on the negative binomial distribution using the DESeq2 package. Further data analysis and visualisation was conducted using the Bioconductor and R packages. Gene set enrichment analysis was performed with GSEA software.

2.12 Proteomics

2.12.1 SLFN5 KO tumours sample preparation for MS analysis

Proteins from total cell lysates were processed with DTT for reduction and Iodoacetamide for alkylation. Alkylated proteins were then precipitated using a 24% and a 10% solution of trichloroacetic acid subsequently. During the precipitations, pellets were kept at 4°C for 10 minutes and then centrifuged for 5 minutes at 15,000g. Supernatants were carefully aspirated, and pellets were washed with water until the reaching a neutral pH in the supernatant, as a measure of complete removal of trichloroacetic acid from the pellet. Pellets were reconstituted and further digested with Endoproteinase Lys-C (Alpha Laboratories, 125-05061) for 1h at RT and then with Trypsin (Promega, V5111) O/N at 35 °C.

2.12.2 MS analysis of SLFN5 KO tumours.

The following method has been adapted from Blomme et al. 2020[191]. Digested peptides were desalted using StageTip[192]. Separation was performed by nanoscale C18 reverse-phase liquid chromatography performed on an EASY-nLC 1200 (Thermo Fisher Scientific, LC140) coupled to an Orbitrap Fusion Lumos mass spectrometer (Thermo Fisher Scientific). Elution was carried out using a binary gradient with buffer A (water) and B (80% acetonitrile), both containing 0.1% of formic acid. The peptide mixtures were separated at 300 nl/min flow, using a 50 cm fused silica emitter (New Objective) packed in-house with ReproSil-Pur C18-AQ, 1.9µm resin (Dr Maisch). Packed emitter was kept at 50°C

by means of a column oven integrated into the nanoelectrospray ion source (Sonation). The gradient used start at 2% of buffer B, kept at same percentage for 3 minutes, then increased to 23% over 180 minutes and then to 32% over 40 minutes. Finally, a column wash was performed ramping to 95% of B in 10 minutes followed by a 5 minutes re-equilibration at 2% B for a total duration of 238 minutes. The eluting peptide solutions were electrosprayed into the mass spectrometer via a nanoelectrospray ion source (Sonation). An Active Background Ion Reduction Device (ESI source solutions) was used to decrease ambient contaminant signal level.

Samples were acquired on an Orbitrap Fusion Lumos mass spectrometer (Thermo Fisher Scientific). The mass spectrometer was operated in positive ion mode and used in data-dependent acquisition mode (DDA). Advanced Peak Determination was turned on and Monoisotopic Precursor Selection was set to "Peptide" mode. A full scan was acquired at a target value of 4e5 ions with resolution R = 120,000 over mass range of 375-1500 amu. The top twenty most intense ions were selected using the quadrupole, fragmented in the ion routing multipole, and finally analysed in the Orbitrap, using a maximum injection time of 35 ms or a target value of 2^4 ions.

2.12.3 SLFN5 KO tumours data analysis

The MS .raw files were processed with MaxQuant software[193] version 1.6.3.3 and searched with Andromeda search engine[194], querying UniProt[195] Homo sapiens (30/04/2019; 42,438 entries). The database was searched requiring specificity for trypsin cleavage and allowing maximum two missed cleavages. Methionine oxidation and N-terminal acetylation were specified as variable modifications, and Cysteine carbamidomethylation as fixed modification. Unique and Razor peptides were used for protein group quantification. The FDR for peptide, protein and site identification was set to 1%.

MaxQuant proteingroups.txt output file was further processed using Perseus software[196] version 1.6.2.3. The common reverse and contaminant hits (as defined in MaxQuant output) were removed. Only protein groups identified with at least one uniquely assigned peptide were used for the analysis. For label-free quantification, proteins quantified in all 3 replicates in at least one group were

measured according to the label-free quantification algorithm available in MaxQuant[197].

2.13 Metabolomics

To perform metabolite analysis, 10^6/well cells were seeded in 6 well plates in triplicate. 24 hours after the seeding, fresh media was added to the cells. 48 hours after fresh media was added, samples were washed 3 times with cold PBS 1x (4°C), taking care of aspirating as much as possible as PBS can cause interference in the chromatography. Once washes are performed, 1mL of ice cold (-20°C) extraction solution (50% Methanol, 30% Acetonitrile, 20% H20) was added to the cells and plates were put in a shaker for 5 minutes at 4°C to allow metabolite extraction. The extraction solution was then collected and kept at -75°C prior centrifugation. This step forces impurities to crystalize and allows for their removal in the centrifugation step. Samples were centrifuged at 16.000g for 10 minutes at 4°C and supernatant was transferred to HPLC glass vials. In parallel, 1% SDS was added to the plates after removing the extraction buffer to extract proteins. These samples were then quantified using the BCA protein assay kit (Thermo Fisher Scientific, 23225) and used to normalise the LC-MS data.

The LC-MS phase was performed according to a previous protocol[198]. In summary, an Q Exactive Orbitrap mass spectrometer (Thermo Scientific) coupled to a Thermo Ultimate 3000 HPLC system was utilised for data acquisition. The HPLC setup was composed of a ZIC-pHILIC column (SeQuant, 150 × 2.1mm, 5µm), with a ZIC-pHILIC guard column (SeQuant, 20 × 2.1mm) and an initial mobile phase of 20% 20 mM ammonium carbonate, pH 9.2, and 80% acetonitrile. 5 µl of sample were injected and metabolites were separated over a 15 minutes mobile phase gradient, decreasing the acetonitrile content to 20%, at a flow rate of 200 µl/min and a column temperature of 45°C. All metabolites were detected across a mass range of 75-1000 m/z using the Q Exactive mass spectrometer at a resolution of 35,000 (at 200 m/z), with electrospray (ESI) ionization and polarity switching to allow detection of both positive and negative ions in a single run. The mass accuracy for all metabolites was < 5 ppm. Acquisition of data was done with Thermo Xcalibur software.

Metabolites were identified by a combination of the known ion mass and retention time in the chromatography column. The peak areas of different metabolites were measured using Thermo TraceFinder v. 4.0 software. Commercial standards of several of the detected metaboliteshad been analysed previously on the same LC-MS system, providing a reference for metabolite identification.

2.14 Proximity ligation assay

22Rv1 cells were cultured on coverslips, washed with cold PBS 1x and fixed by addition of cold methanol and resting 20 minutes at -20°C. All incubations were performed in a humidity chamber. Blocking was done with 0.1% tween-TBS with 1% BSA for 1 hour at 37°C. After addition of primary antibodies against SLNF5 (121537, abcam) and ATF4 (E4QAE, Cell Signaling), samples were incubated overnight at 4°C. P-LISA staining was performed as previously described in Gauthier et al 2015[199]. Secondary antibodies linked to probes PLA Probe Anti-Mouse PLUS (DUO92001, Sigma-Aldrich, France) and PLA Probe Anti-Rabbit MINUS (DUO92005, Sigma-Aldrich, France) were used for detection. The ligation and amplifications steps were performed according to manufacturer's recommendations. Several washes using 0.1% tween-TBS were performed between each step. Nuclei were then stained with DAPI and slides mounted with Fluoromount Aqueous Mounting Medium (F4680, Sigma Aldrich) and images were captured using a Zeiss LSM microscope confocal (Zeiss).

2.15 Statistical analysis

Analysis of experimental data was performed using GraphPad PRISM software v8.4.0 (GraphPad Software Inc) and Microsoft Excel (Microsoft).

Chapter 3 - Characterisation of SLFN5 role in prostate cancer

3.1 Characterisation of SLFN5 in Prostate Cancer

3.1.1 SLFN5 expression is controlled by androgens via Androgen Receptor

To validate the elevated SLFN5 expression in CRPC models, the protein levels of SLFN5 were assessed in the LNCaP/LNCaP AI and CWR/22Rv1 pairs. The androgen responsive LNCaP and CWR were cultured in media to which foetal bovine serum (FBS), containing androgens, is added. The castration resistant LNCaP AI and 22Rv1 were cultured in absence of androgens with charcoal stripped serum (CSS) added to the media instead of FBS. This filtered additive contains no androgens and lacks some other small molecules[200] and proteins[201].

CRPC is often driven by alterations in AR signalling. The identification of SLFN5 in all three pairs of isogenic hormone naïve and castration resistant orthografts raises the possibility that SLFN5 expression may be modulated by AR function.

All four cell lines were cultured in both FBS and CSS containing media for 72 hours, after which, SLFN5 protein expression was assessed by western blot. Consistent with the results of the *in vivo* discovery experiment, LNCaP AI and 22Rv1 cells express SLFN5 at a higher level than LNCaP and CWR respectively regardless of the culture conditions. In the case of LNCaP and LNCaP AI, the presence or absence of androgens in the media affected the expression of SLFN5, with both cells displaying higher levels of SLFN5 protein when cultured under androgen deprivation in comparison to culture in presence of androgens (Figure 3-1).

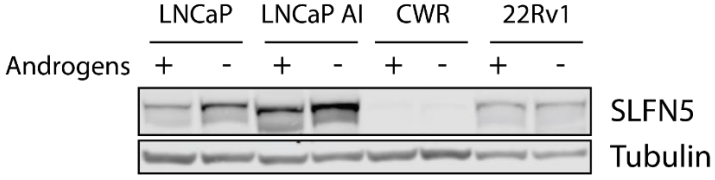

Figure 3-1 - SLFN5 expression in prostate cancer cells cultured in vitro

Cells were cultured for 72 hours in the presence or absence of androgens in the culture media, as indicated. Figure shows representative Western Blot of SLFN5 of an n=3. Tubulin was used as a loading control.

To further test if androgens were responsible for repressing the expression of SLFN5 and that the observed effects were not caused by any other compound missing in the CSS media, androgen independent cell lines LNCaP AI and 22Rv1 were treated with endogenous di-hydro-testosterone (DHT) for 72 hours. This timeframe was chosen as we wanted to observe effects androgen had in the expression of SLFN5 beyond the short term. Figure 3-2.a shows that adding exogenous androgens reduces SLFN5 protein expression in LNCaP AI and 22Rv1. Furthermore, depriving LNCaP cells of androgens for 72 hours caused a fourfold increase in the transcript levels of *SLFN5*, and a 24 treatment with DHT could rescue the reduced levels of expression (Figure 3-2.b).

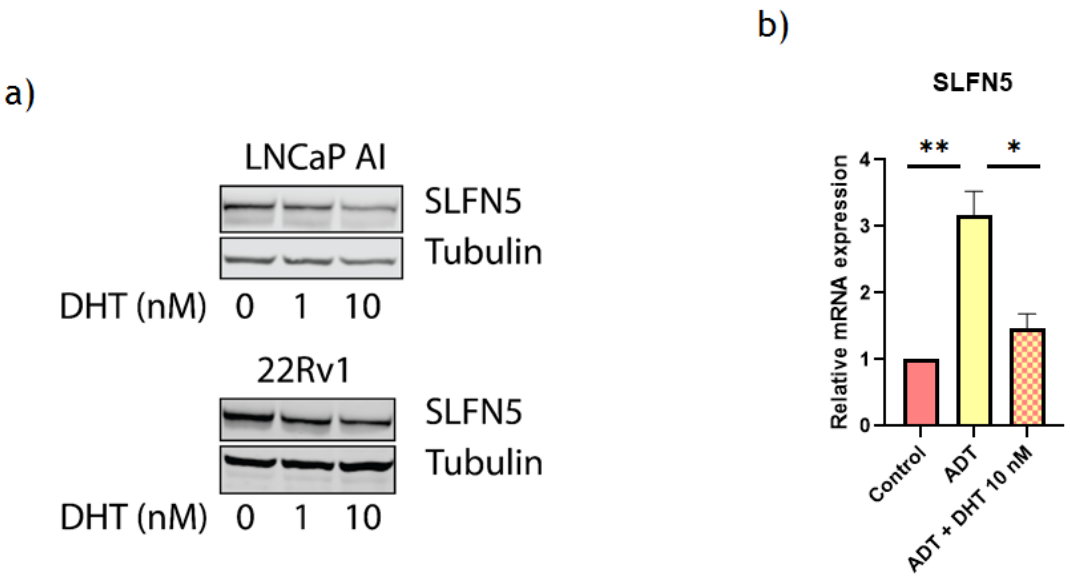

Figure 3-2 - SLFN5 expression in DHT treated cells

a) LNCaP AI and 22Rv1 Cells were treated with 1 nM and 10 nM DHT for 72 hours. Figure shows representative Western Blot of SLFN5 of an n=2. Tubulin was used as a loading control. b) LNCaP cells were grown in presence of androgens (Control), placed in androgen deprived media for 48 hours (ADT) and treated for 24 hours with DHT after 24 hours in androgen deprived media (ADT+DHT 10nM). *CASC3* was used as a reference gene for normalisation and the fold change compared to average of control is shown. (* = <0.05, ** = <0.005, Tukey´s multiple comparisons test). Error bars represent Standard Deviation, n=2.

Given that androgens such as DHT can affect other signalling systems, especially in non-physiological concentrations, we tested the implication of AR in SLFN5

expression itself, as DHT could be exerting its effect through another receptor. Short term silencing (72 hours) of *AR* was performed on the androgen responsive LNCaP and CWR cell lines, and *SLFN5* mRNA expression was measured by qPCR. Supressing *AR* significantly upregulated *SLFN5* mRNA expression by two-fold (Figure 3-3).

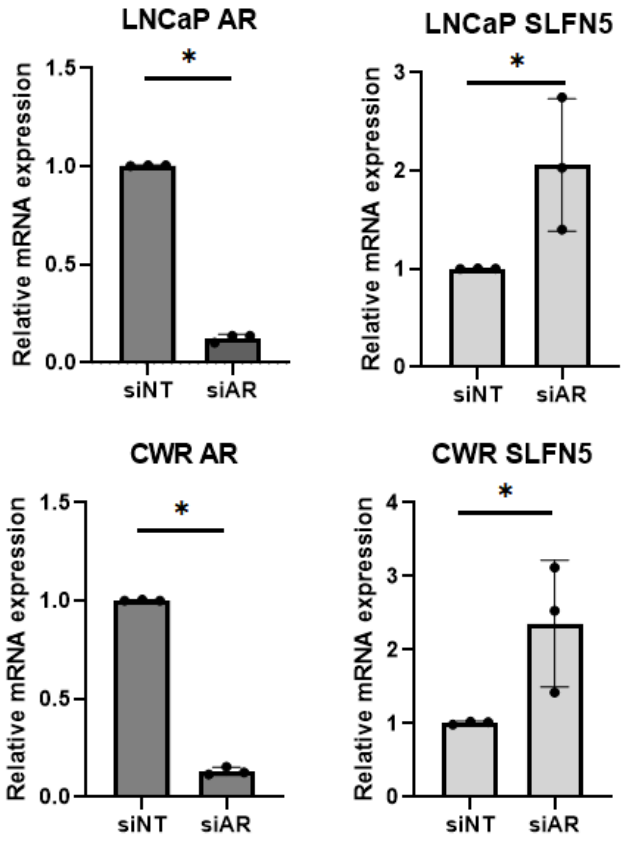

Figure 3-3 - SLFN5 expression under Androgen Receptor silencing

Transcript levels of *AR* and *SLFN5* in LNCaP and CWR cells were examined by PCR after being treated with siRNA targeting *AR* for 72 hours. Reduction in the levels of *AR* resulted in an increase of at least two-fold in *SLFN5* transcript levels (*= <0.05, Mann-Whitney test). Each dot represents a technical replicate from a total of 3 biological replicates. Error bars represent Standard Deviation.

Taken together, this data reveals SLFN5 levels respond to AR activity. This relation suggests the reason why tumours derived from CRPC cell lines present increased expression of SLFN5 could be due to the lack of androgen activated AR signalling.

3.1.2 SLFN5 is localised in the nucleus of prostate cancer cells

SLFN5 possesses a nuclear localisation signal (NLS) and has been previously shown to reside in the nucleus of other human cell lines[122]. Immunofluorescence staining was used to study the subcellular localisation of this protein in the LNCaP, LNCaP AI and CWR cell lines.

SLFN5 in LNCaP AI is mainly localised in the nucleus (Figure 3-4.a). Furthermore, nuclear localisation of SLFN5 in androgen sensitive LNCaP and CWR was not altered by the presence or absence of androgens in the culture media (Figure 3-4.b).

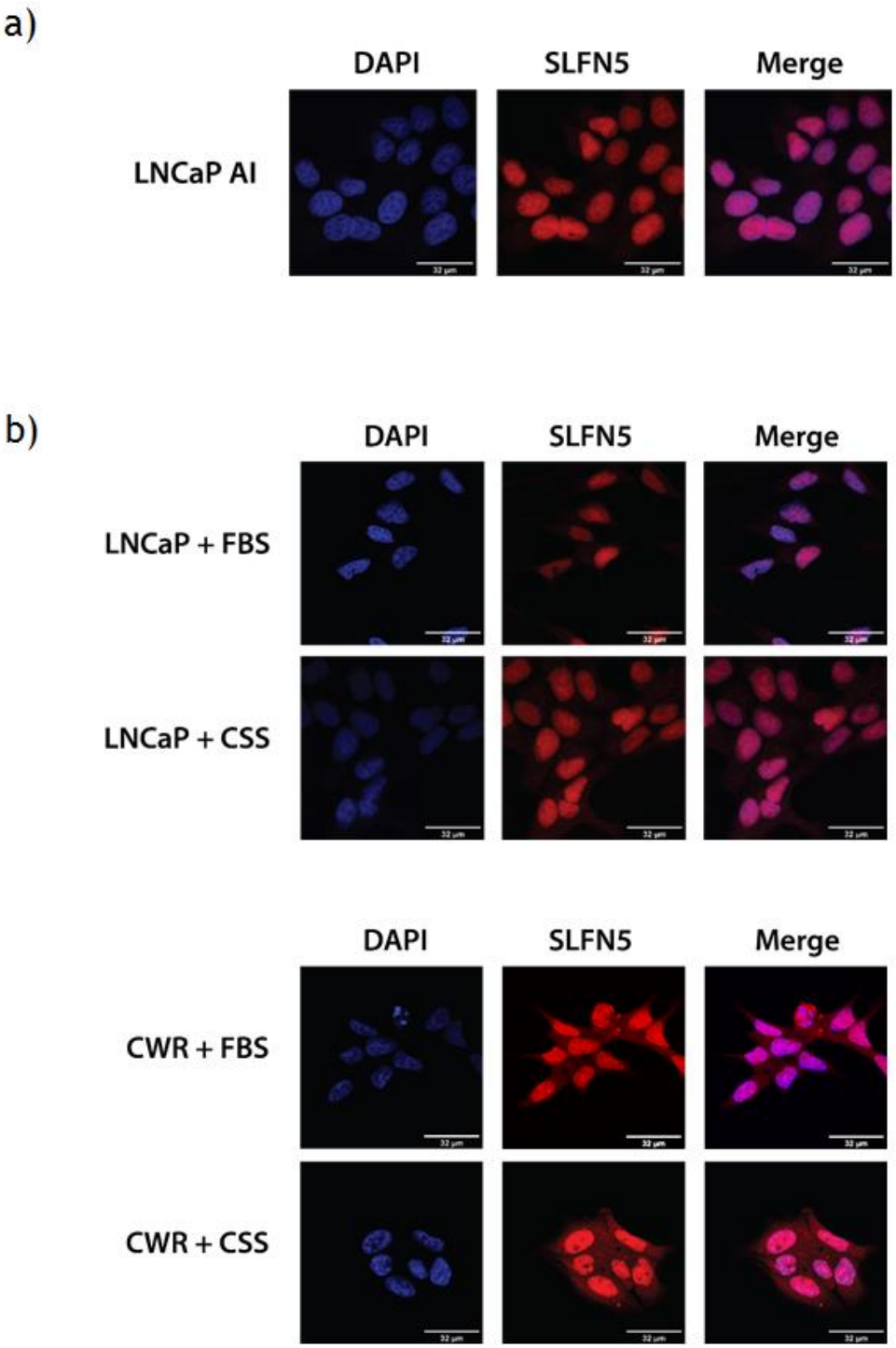

Figure 3-4 – Immunofluorescence staining of SLFN5

a) LNCaP AI cells were seeded in wells containing round 19 mm coverslips. After 72 hours, the cells were fixed and stained with anti SLFN5 antibody and mounted in DAPI containing media. b) LNCaP and CWR cells were cultured as described for the LNCaP AI cells in presence (FBS) or absence (CSS) of androgens in the media for 72 hours. DAPI was used as a nuclear stain. Scale bar measures 32 µm. Contrast was modified during image processing to accurately compare localisation between differently treated cells.

3.1.3 SLFN5 is not regulated by IFN-a in prostate cancer cell lines

The main regulatory pathway for SLFN5 expression that has been described until now is Interferon Type-1 signalling[116]. Experiments were performed to assess if Interferon alpha (IFN-α) was capable of altering the expression of SLFN5 in PC cell lines through this signalling pathway.

A375 cells were used as a positive control for IFN-α treatment. As described in the literature, A375 melanoma cells are sensitive to treatment with IFN-α[202]. SLFN5 protein levels showed an increase after 6 hours compared to no IFN-α treatment. IFN-α downstream phosphorylation targets JAK1 and STAT1 were shown to be phosphorylated after IFN-α treatment, indicating activation of Type-1 Interferon signalling (Figure 3-5).

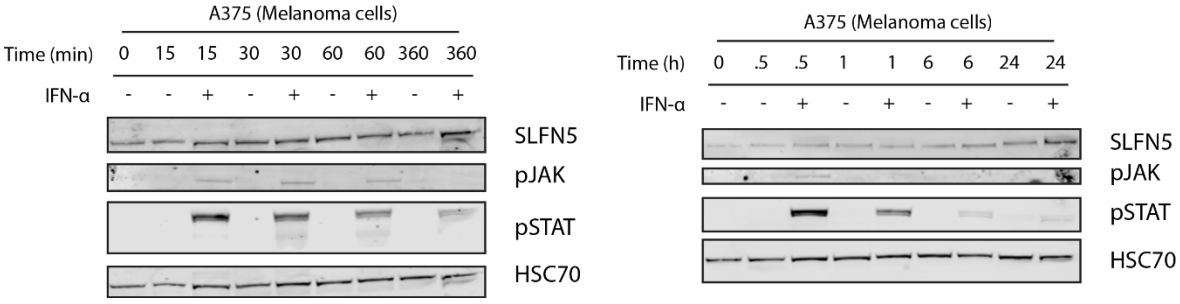

Figure 3-5 - IFN-α affects expression of SLFN5 in A375 cells

This experiment was performed once as a positive control for the effects of IFN-α on SLFN5 expression. IFN-α was added 24 hours after the initial seeding with fresh media at a concentration of 500 U/mL. Protein samples were then taken at different time points, ranging from 15 minutes to 24 hours. Phosphorylation of JAK1 and STAT1 was used as a measure of Type-1 Interferon signalling activation by Western Blot. HSC70 was used as a loading control. Panel a) shows short term effects (0h to 6h) and panel b) shows long term effects (0h to 24h).

Prostate cancer cells were treated with 500 Units/mL of IFNα for 72 hours to mirror the previous DHT treatment, and protein levels were measured by Western Blot. Figure 3-6 shows the addition of interferon does not affect the levels of SLFN5, nor of AR in PC cell lines. AR expression was studied to account for the possibility of IFN-α regulating SLFN5 through AR signalling. After treatment with IFN-α, there was no activation of the Type-1 Interferon signalling in these cells as measured by phosphorylation of the downstream target JAK1, as phosphorylation of STAT1 decreases after 24h, as shown in Figure 3-5. This

indicates that PC cell lines are not sensitive to IFN-α, at least at the studied concentration. These preliminary results suggest Type-1 Interferon signalling is not the main cause of the increased levels of SLFN5 observed in CRPC models.

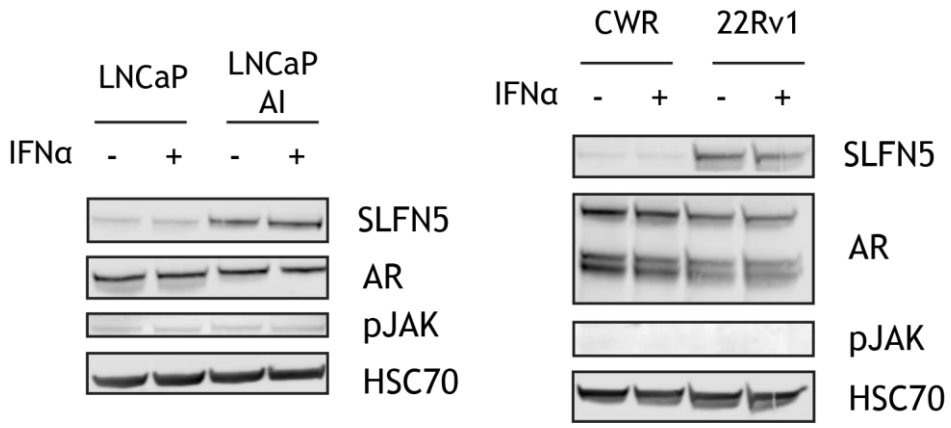

Figure 3-6 - Addition of IFN-α does not affect expression of SLFN5 in PC cell lines.

LNCaP, LNCaP AI, CWR and 22Rv1 cells were added fresh media containing 500U/mL of IFN-α 24 hours after the initial seeding. They were kept on that condition for 72 hours, after which protein expression was analysed by Western Blot. Figure shows representative Western Blot of an n=1. Phosphorylated JAK1 was used as a measure of Type-1 Interferon signalling activation. HSC70 was used as a loading control.

3.1.4 SLFN5 is highly expressed in clinical CRPC cases

The previous results confirm that SLFN5 is highly present in several CRPC models. It has also been shown to be repressed by the presence of androgens and activated androgen receptor. Taken together, these data suggest that there is an inverse association between SLFN5 expression and androgen levels/AR signaling. These circumstances exist when prostate cancer patients undergo androgen deprivation therapy, where either androgen production or AR signalling is targeted to be inhibited by several compounds. Consistent with these results, LNCaP variants that were chronically cultured in various antiandrogens and therefore considered ‘castration resistant’ presented elevated levels of SLFN5 protein (Figure 3-7).

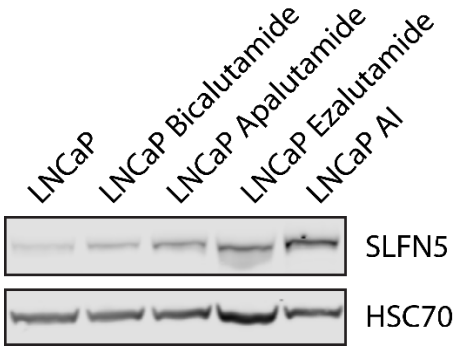

Figure 3-7 – SLFN5 expression in LNCaP resistant to anti-androgens

LNCaP cells were chronically grown in 10μM bicalutamide (Casodex), apalutamide (ARN-509) or enzalutamide. Cell lysates were kindly procured by Dr. Arnaud Blomme. HSC70 was used as loading control.

To study SLFN5 in a clinical context, a cohort of 537 samples was kindly provided by Dr. Ladan Fazlin and Professor Martin Gleave from the Vancouver Prostate Centre. Samples from 537 patients were categorised by treatment, Gleason score, development of CRPC or neuro endothelial prostate cancer (NEPC), and were immunostained for SLFN5 followed by scoring of its expression by trained pathologists (Table 3-1). The cohort showed that SLFN5 immunoreactivity is significantly increased in CRPC tumours in comparison with untreated cases and cases treated with neoadjuvant hormonal therapy (NHT), matching the expectations of the previous work in the cell line models (Figure 3-8.a). SLFN5 expression was also confirmed to be nuclear in human samples of prostate cancer, as observed in the *in vitro* models (Figure 3-8.b).

Survival analysis based on high and low SLFN5 expression revealed that patients who had higher levels of SLFN5 expression also showed shorter relapse free survival, as measured by the time to PSA recurrence. This suggests that SLFN5 expression is associated with disease progression including the development of a CRPC phenotype (Figure 3-9.a).

Furthermore, SLFN5 expression in this cohort was also analysed in relation with Gleason score, survival status, development of metastases, cancer recurrence and lymph node status. Higher SLFN5 was found to significantly correlate with more advanced cancers (as measured by Gleason sum score >7), the presence of metastases and with overall survival (Figure 3-9.b).

Altogether, the analysis of SLFN5 expression in this cohort of patients shows that expression of SLFN5 is associated with more advanced and aggressive cases of prostate cancer, and with the development of CRPC. These results confirm what has been suggested by the studies about SLFN5 in prostate cancer in our laboratory. As CRPC cellular models present higher SLFN5 expression than their hormone naïve counterparts, so do clinical cases of CRPC. High levels of SLFN5 expression are associated with reduced time to disease relapse, markers of aggressive disease (including the presence of metastasis) as well as increased risk of cancer associated mortality.

Table 3-1 – SLFN5 expression in clinical cohort

SLFN5 Tissue Microarrays	Untreated	1-3 m NHT	4-6 m NHT	>7m NHT	All NHT Treated	CRPC	NEPC
Number of cases	151	90	64	141	348	45	29
Minimum	0	0	0.02	0	0	0	0
25% Percentile	0.09	0.0975	0.09	0.08	0.09	0.205	0.165
Median	0.15	0.165	0.2	0.17	0.17	0.35	0.25
75% Percentile	0.26	0.3225	0.3	0.31	0.32	0.44	0.365
Maximum	0.7	0.57	0.84	1	1	0.79	0.62
Mean	**0.1879**	**0.2164**	**0.2392**	**0.2124**	**0.225**	**0.332**	**0.28**
Std. Deviation	0.1444	0.1545	0.1825	0.1775	0.1748	0.1751	0.1568
Std. Error of Mean	**0.01175**	**0.01629**	**0.02281**	**0.01494**	**0.009368**	**0.0261**	**0.02911**
Lower 95% CI of mean	0.1647	0.1841	0.1936	0.1829	0.2066	0.2794	0.2204
Upper 95% CI of mean	0.2111	0.2488	0.2848	0.242	0.2434	0.3846	0.3396

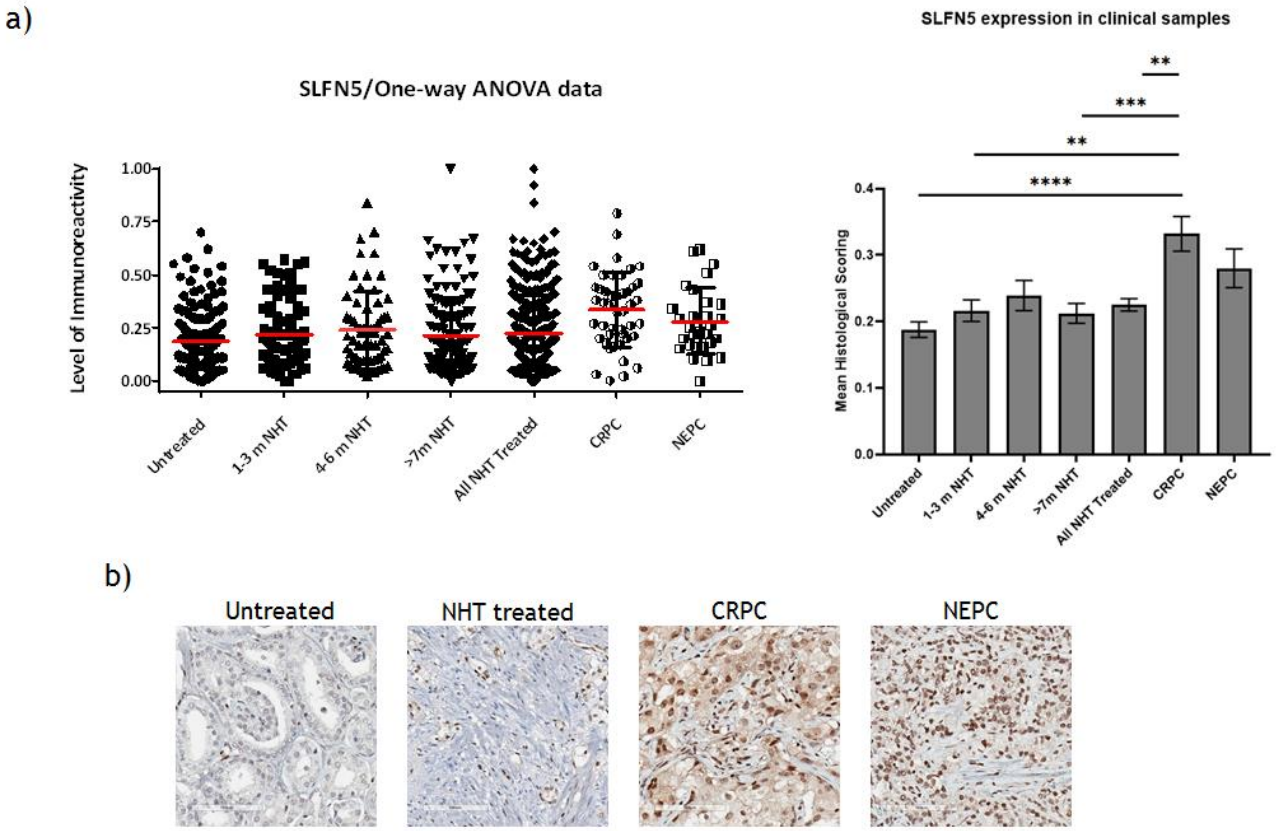

Figure 3-8 - SLFN5 expression is higher in CRPC clinical cases

a) Scoring of SLFN5 expression in all the samples of the cohort. SLFN5 expression was significantly higher in CRPC cases compared to untreated and those treated with NHT (= <0.005, *** = <0.0005, **** = <0.0001, Tukey´s multiple comparison test). Error bars represent standard error of mean. b) Representative staining of *SLFN5* in each case group. Staining was performed by Sonia Kung and scoring was performed by Dr. Ladan Fazlin and Dr. Martin Gleave from the Vancouver Prostate Centre.**

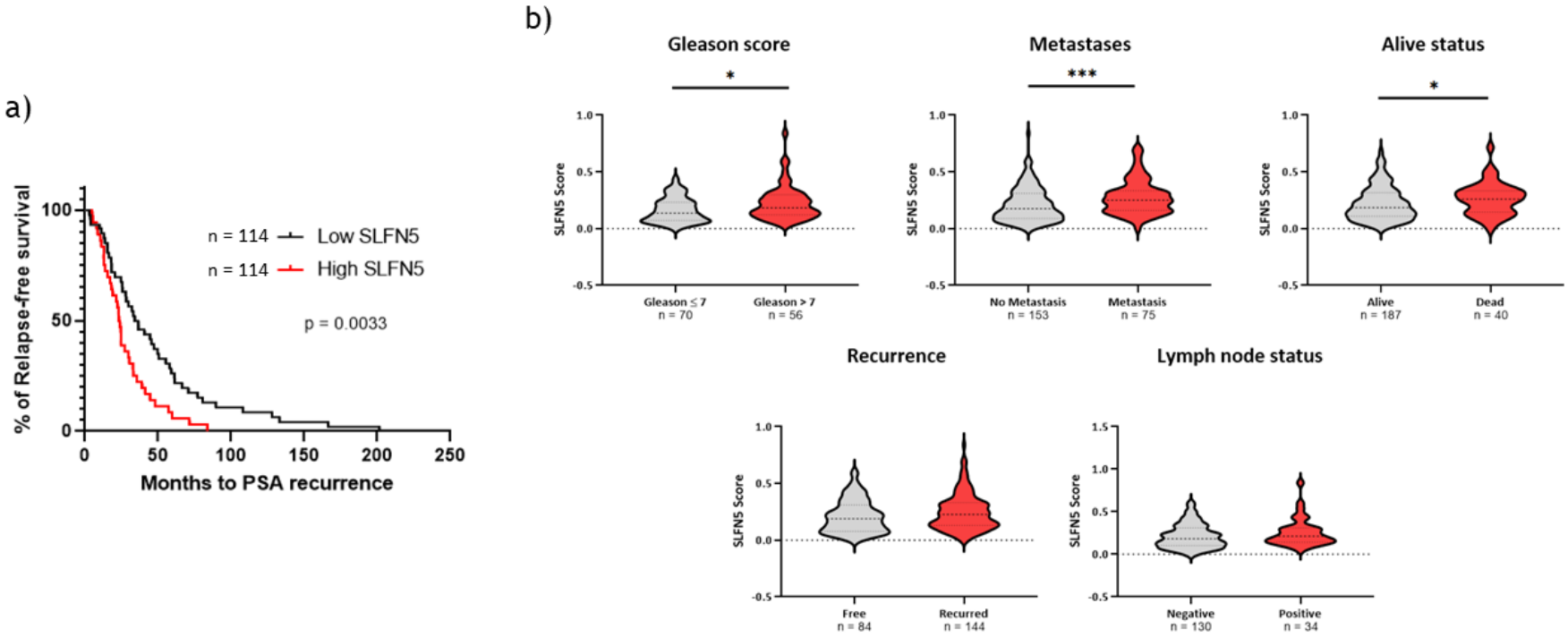

Figure 3-9 – High SLFN5 expression reduces time of relapse free survival, and correlates with Gleason score, metastases development and survival

a) Patients were categorised in low and high SLFN5 categories using the median value for the entire population (n=144 for each group). Relapse free survival was measured as time to PSA recurrence. Analytical comparison was made using the Logrank/Mantel-Cox test. b) SLFN5 expression was compared among patient groups based on low and high Gleason sum scores, survival status and the development of metastases, cancer recurrence and lymph node status using Mann Whitney test. Significance is defined as $p < 0.05$ (* = <0.05, * = <0.0005).**

3.2 Generation and Characterization of *SLFN5* Knockout and Overexpression cell lines

3.2.1 Development of SLFN5 Knockout cell lines

In order to study the role of SLFN5 in the growth and survival of prostate cells under castration-like conditions, the CRISPR/Cas9 system was used to establish 22Rv1 and LNCaP AI derived cell lines that completely lack expression of SLFN5. This model allows the study of these androgen independent cells with permanently and totally absent SLFN5 expression, allowing for long term and *in vivo* experiments.

After transfection and selection, western blot was used to confirm complete loss of SLFN5 expression in single clones of both 22Rv1 and LNCaP AI. Several LNCaP AI and 22Rv1 clones were identified as complete SLFN5 knockouts (Figure 3-10).

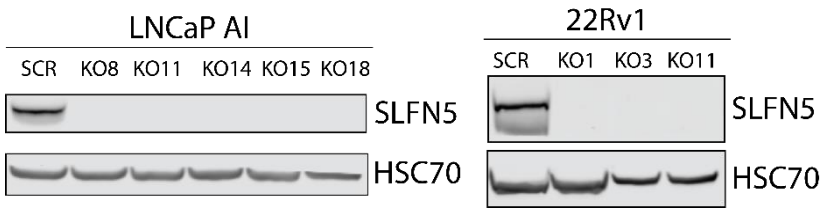

Figure 3-10 – Validation of CRISPR/Cas9 Knockout of SLFN5

Figure shows western blot of clones that have lost protein expression of SLFN5. HSC70 was used as a loading control.

3.2.2 Characterization of SLFN5 Knockout in vitro phenotype

Since SLFN5 expression increases under castrated conditions, we wondered if the absence of this protein affected the growth of LNCaP AI and 22Rv1 cells under androgen deprivation. LNCaP AI and 22Rv1 SLFN5 KO cells were cultured in standard 2D cell culture conditions and cell numbers were monitored every 24 hours for 72 hours after the initial measurement. Under these growth conditions, LNCaP AI KO clones saw their growth impaired by the lack of SLFN5 expression, while 22Rv1 KO did not present a significant difference in growth in both clones at the same time (Figure 3-11).

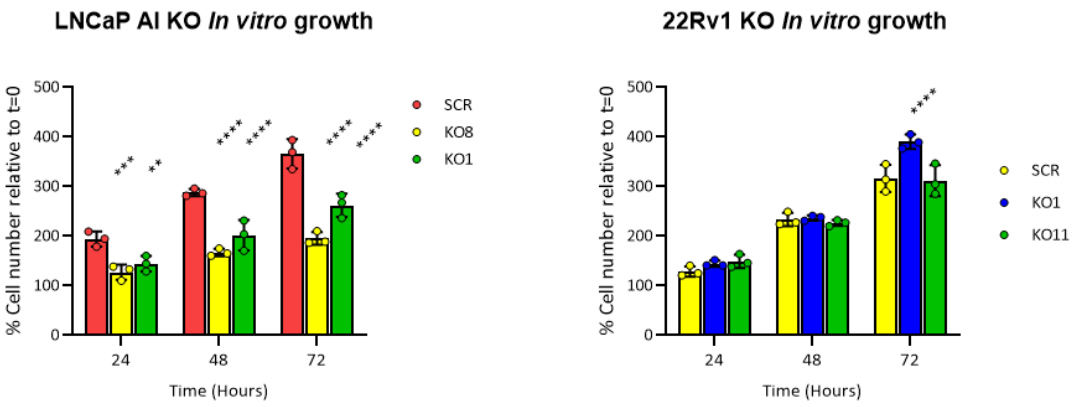

Figure 3-11 - *In vitro* cell growth of SLFN5 knockout cells

Both LNCaP AI KO and 22Rv1 KO cells were seeded at the same initial concentration of 70.000 cells per well and grown for several days. Cells were counted every 24 hours. Shown in the figure are representative experiments of an n=3. Significance is defined as p<0.05 by Dunett´s multiple comparison test to the SCR sample (= p<0.005, *** = p<0.0005, **** = p<0.0001).**

To study cell growth in an anchorage independent way, cells were cultured in an agar based medium. When cultured this way, the cells tend to grow forming a spherical colony instead of forming a single monolayer. Culture under these conditions entails a different interaction with the environment than 2D growth and can mimic several factors that are at play during *in vivo* growth, such as nutrient availability gradients. Nevertheless, when 22Rv1 KO cells were cultured in agar, there was not a significant difference between the size of the colonies established (Figure 3-12).

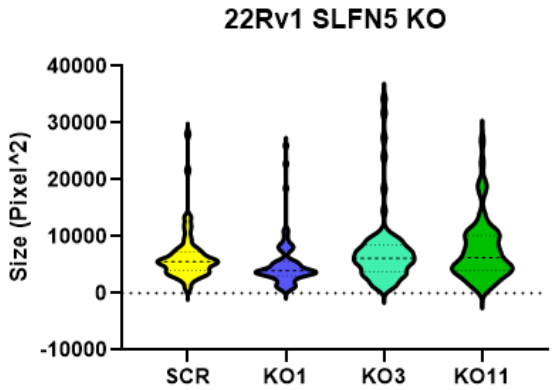

Figure 3-12 - Anchorage independent growth of 22Rv1 KO cells

22Rv1 KO cells were seeded in androgen free media containing 0.3% agarose and left in culture for 11 days. After that, several pictures were taken, and colony size was measured using ImageJ. Dunett´s multiple comparison test to the SCR sample analysis showed no significant (p < 0.05) difference between the size of any SLFN5 KO clone to the control cell line. Shown in the figure is a representative experiment of an n=2.

SLFN5 has been described to affect cell migration in models from non-prostate tissues[117]. To study the effect SLFN5 depletion has in the migratory properties of prostate cancer cells, transmembrane well assays were performed on LNCaP AI KO cells. Cells were placed in serum free media for 24 hours and then added to transmembrane assay well inserts containing media with serum on the other side of the porous membrane. After membrane processing, the number of cells that had migrated to the serum rich side of the membrane was counted using an ImageJ pipeline. LNCaP AI cells that lacked SLFN5 migrated in lower numbers than the control cell lines (Figure 3-13), indicating that SLFN5 provides an advantage in serum driven migration.

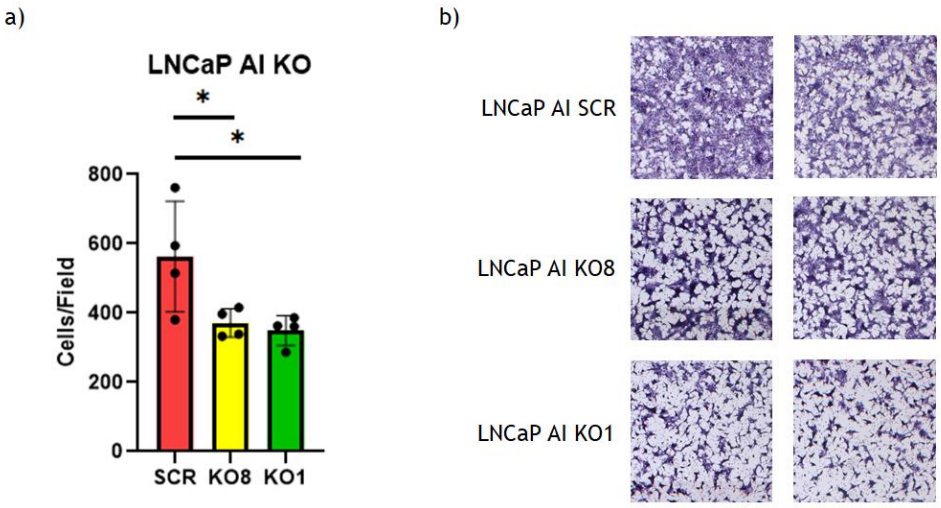

Figure 3-13 – Migratory properties of LNCaP AI KO cells

LNCaP AI KO cells were starved for 24 hours and then 500.000 cells were seeded on a transmembrane assay well insert with serum containing media on the other side of the membrane. 48 hours after seeding, the cells were fixed to the membrane and stained with filtered haematoxylin. a) Graph shows count of cells from n=2 biological replicates with n=2 technical replicates each, 4 measured fields per replicate. Error bars represent Standard Deviation. (* = p<0.05, Holm-Sidak´s multiple comparisons test) Cell count shows that LNCaP AI cells that lacked SLFN5 expression had reduced migratory capabilities compared to the SLFN5 expressing control. b) Representative images of fields selected for analysis (2.5x magnification).

3.2.3 Development of SLFN5 overexpressing cell lines

To study if increasing SLFN5 levels had any phenotypic effect in the androgen naïve cells, we introduced a *SLFN5* expression plasmid to the LNCaP and CWR cell lines. Several clones that presented an increased expression of SLFN5 were obtained (Figure 3-14). From now on, cell lines that overexpress SLFN5 will be

denoted as “OE” followed by a unique clone number, or “EV” from empty vector for the non-SLFN5 overexpressing control.

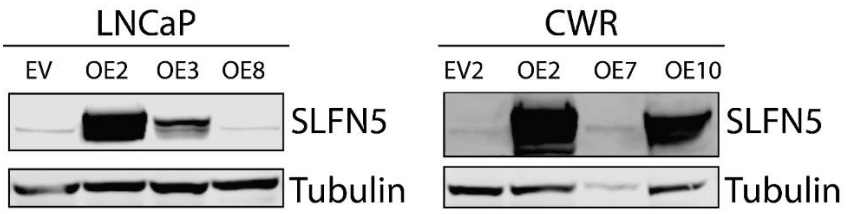

Figure 3-14 – Validation of SLFN5 overexpressing clones

Figure shows the Western Blot of one control clone transfected with an empty vector plasmid (EV) and three clones of each cell line that were transfected with the plasmid for the expression of *SLFN5* (OEs), presenting varied levels of SLFN5 expression, including clones considered negative for SLFN5 overexpression (LNCaP OE8, CWR OE7). Tubulin was used as a loading control. Clones LNCaP OE8 and CWR OE7 were considered negative for SLFN5 overexpression and were subsequently used as negative controls in the following experiments.

3.2.4 Characterization of SLFN5 Overexpression in vitro phenotype

The effects of introducing exogenous overexpression of SLFN5 to a model with low basal expression of this protein were characterised. First, standard monoculture growth was assayed in a similar manner used for the SLFN5 KO cells. As showed in Figure 3-15, neither LNCaP OE nor CWR OE cells grew differently to their respective empty vector control transfected cells. An increase of SLFN5 levels in these cells does not seem to affect growth rate under the regular conditions where androgens are present in the media.

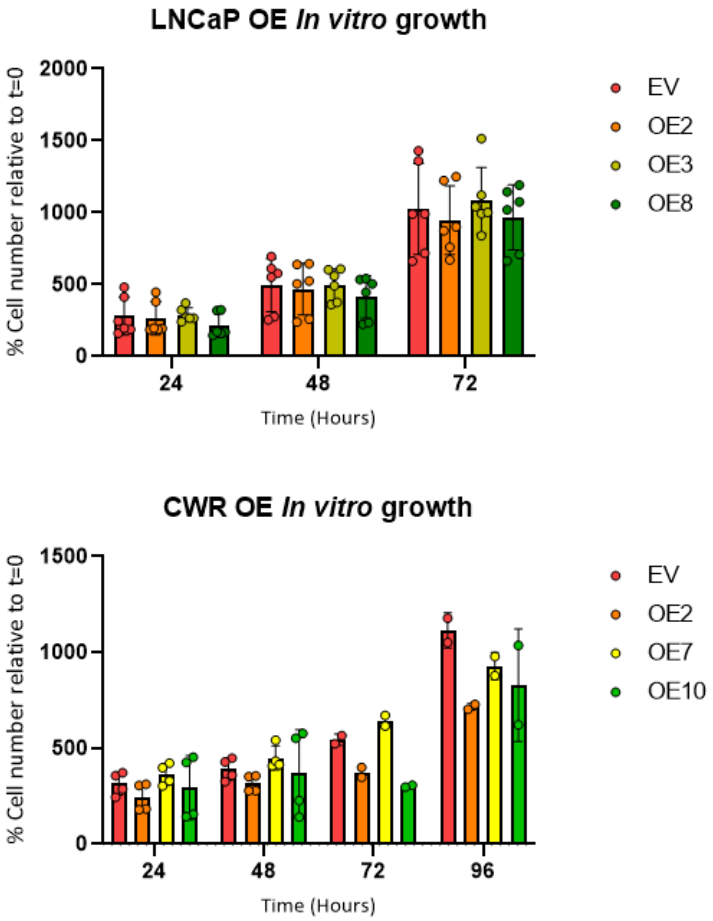

Figure 3-15 – *In vitro* cell growth of SLFN5 overexpressing cells

LNCaP and CWR overexpressing SLFN5 were seeded at the same initial concentration of 70.000 cells per well for the LNCaP and 140.000 c/w for the CWR. Cells were counted every 24 hours after the initial seeding. The different clones did not show any significant difference ($p<0.05$, Dunett´s multiple comparisons test) in cell division rate. For LNCaP SLFN5 OE n=3, for CWR SLFN5 OE n=2. Error bars represent Standard Deviation.

Since prostate cancer cells naturally increase their expression of SLFN5 under androgen deprivation, it was hypothesized that its effect might be evident under such conditions. LNCaP OE cells were subjected to androgen deprivation for 72 hours, and cell confluence was measured every two hours using an Incucyte system. LNCaP cells overexpressing SLFN5 at different levels (Figure 3-14) did show reduced growth in the absence of androgens, but there was no difference between the SLFN5 overexpressing cells and the control (Figure 3-16).

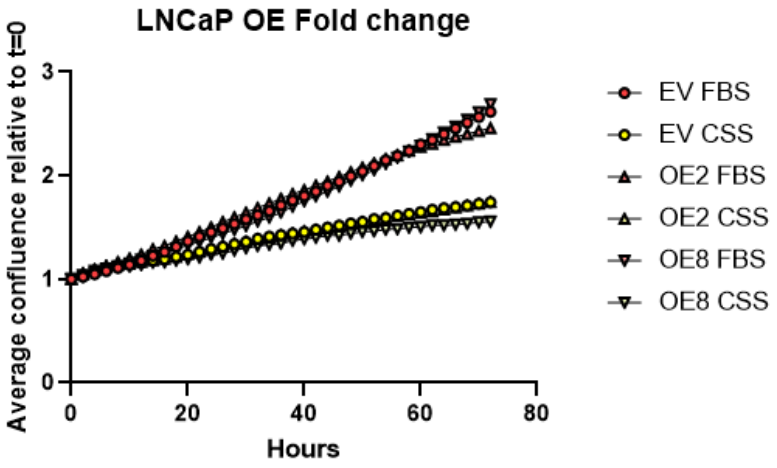

Figure 3-16 - Growth of LNCaP OE cells under androgen deprivation

LNCaP OE cells were seeded in 96 well plates, and after 24 hours, fresh culture media supplemented with serum containing androgens (FBS) or without androgens (CSS). Shown in the figure is a representative experiment showing the average fold change of 6 wells. Error bars (not visible due to reduced size) represent Standard Deviation.

Finally, anchorage independent growth in agar was assayed in LNCaP OE cell lines. This revealed that only one clone (OE2) out of three grew significantly more than the other cell lines under presence of androgen, but this might be due to the statistical power of a small number of outliers and further replicates should be conducted. This difference was not present when cells were grown in absence of androgens, where all clones behaved the same as the control cell line (Figure 3-17).

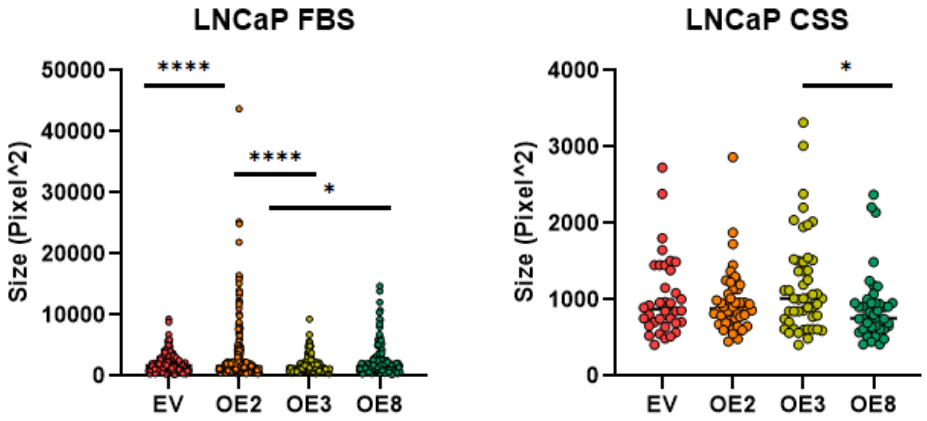

Figure 3-17 – Anchorage independent growth of LNCaP OE cells

LNCaP OE cells were seeded in androgen containing (FBS) or androgen free (CSS) media containing 0.3% agarose and left in culture for 14 days. After that, several pictures were taken, and colony size was measured using ImageJ. n=1. (* = <0.05, ** = <0.0001, Tukey´s multiple comparisons test).**

Interestingly, when SLFN5 subcellular localisation was probed in the LNCaP OE models using anti MYC-tag antibodies, there was a discrepancy between the localisation of SLFN5 among the clones. MYC-tagged SLFN5 in clone OE 2 localised predominantly in the nucleus, while in clone OE 3 it was detected mainly on the cytosol (Figure 3-18). This cytoplasmic localisation was not observed in any other prostate cancer model surveyed nor is it described in the literature. This discrepancy could be the cause of the different behaviour of the clones suggested by the anchorage independent growth assay.

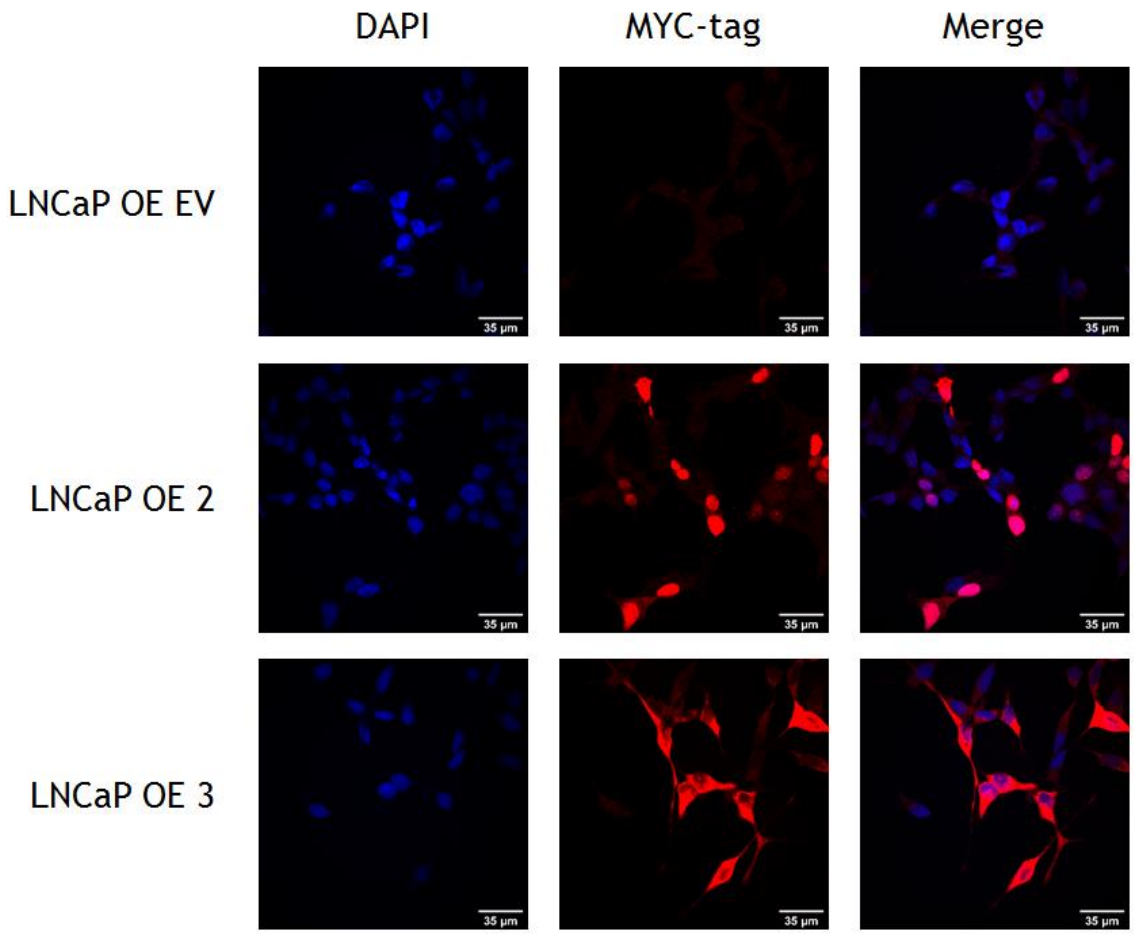

Figure 3-18 – Subcellular localisation of MYC-tagged SLFN5 in the LNCaP OE model

Shown in the figure is a representative image of an n=2. DAPI was used as a nuclear stain. A secondary antibody conjugated to Alexa-555 was used to detect the MYC-tag primary antibody.

3.2.5 Absence of SLFN5 causes reduced tumour growth under androgen deprivation

SLFN5 in CRPC was first discovered on a study where three different pair of cell models were used to generate orthograft tumours. The proteome of these tumours was studied and compared to find shared alterations in protein expression among all three *in vivo* models of CRPC, in order to overcome the heterogeneity in CRPC. Studying SLFN5 KO cells in *in vitro* conditions is limiting due to said conditions being unable to fully represent how castration affects the whole body of the host organism. The absence of androgens alters several biological processes that may indirectly affect cancer cell growth in an androgen depleted microenvironment. To study how prostate cancer cells behave under castration conditions in an organism when they do not express SLFN5, an *in vivo* orthograft experiment was carried out.

CD1-nude mice were injected with 22Rv1 KO cells into the anterior prostate and were at the same time castrated to mimic the effects of androgen deprivation therapy in patients. Two different SLFN5 knockout clones were used to mitigate potential non-relevant effects related to the monoclonal origin of the 22Rv1 KO cells. The tumours were then allowed to develop for three weeks, after which weekly volume measurements were taken using ultrasound scanning (Figure 3-19.a).

The experiment was terminated after the 7th week of ultrasound assessment, before the biggest tumour could reach endpoint size (longest diameter of 1.2 cm length on ultrasound imaging). Tumours were then harvested along with blood, liver, kidneys, epiploic fat, lungs and lymph nodes. Tumours were measured and weighted after extraction (Figure 3-21.b). One half was fixed in formalin for further histological analysis (Figure 3-20). The other half was snap frozen in dry ice.

Analysis of the weekly change in volume revealed a significant decrease in growth for the SLFN5 knockout clones (Figure 3-21.a). After 7 weeks, 22Rv1 KO tumours had scarcely increased in size. The biggest fold change among KO1 tumours was 1.7 and for KO11 clones it was 1.8. The average fold change for the control (SCR) tumours was 2.1, the highest being 3.4 (Figure 3-21.c).

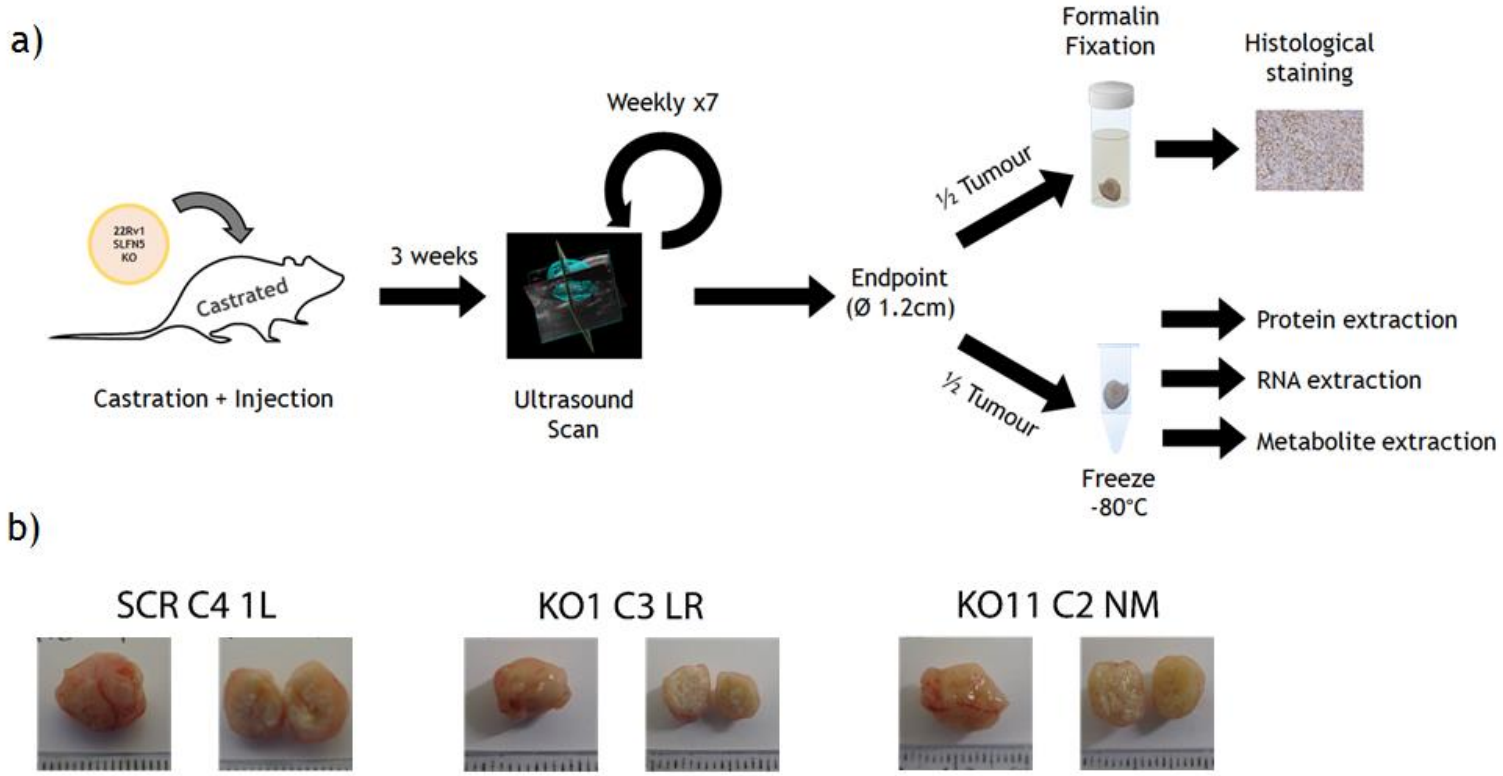

Figure 3-19 – Workflow of 22Rv1 SLFN5 KO orthograft experiment

a) Workflow of the experiment. b) Representative photographs of tumours taken right after extraction, whole and after being cut in halves.

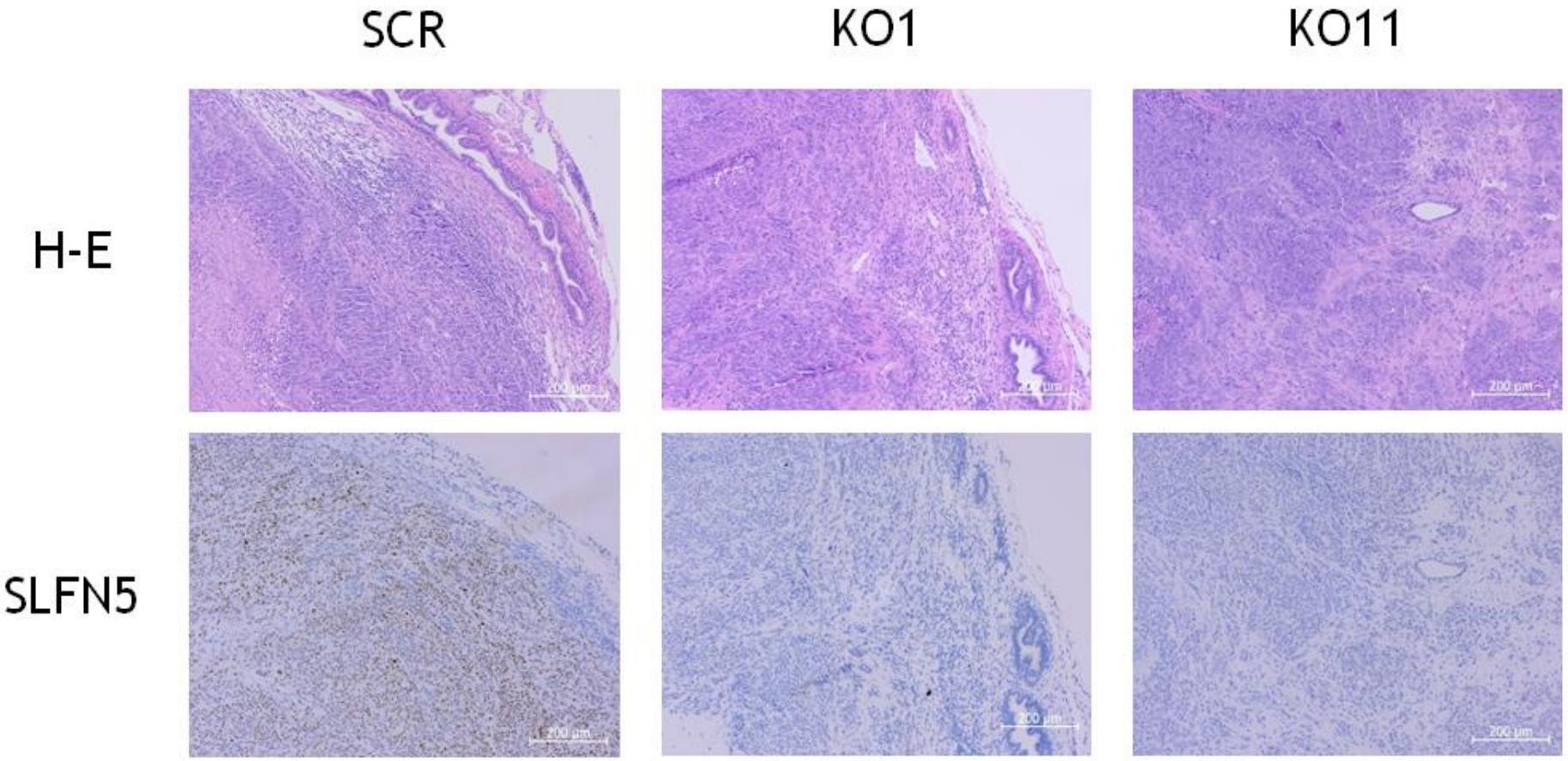

Figure 3-20 - Histological analysis of 22Rv1 KO tumours

Figure shows Haematoxylin and Eosin staining (top) and SLFN5 Immunohistochemistry (bottom) of a representative sample from each clone used in the experiment. Scale bar measures 200 µm.

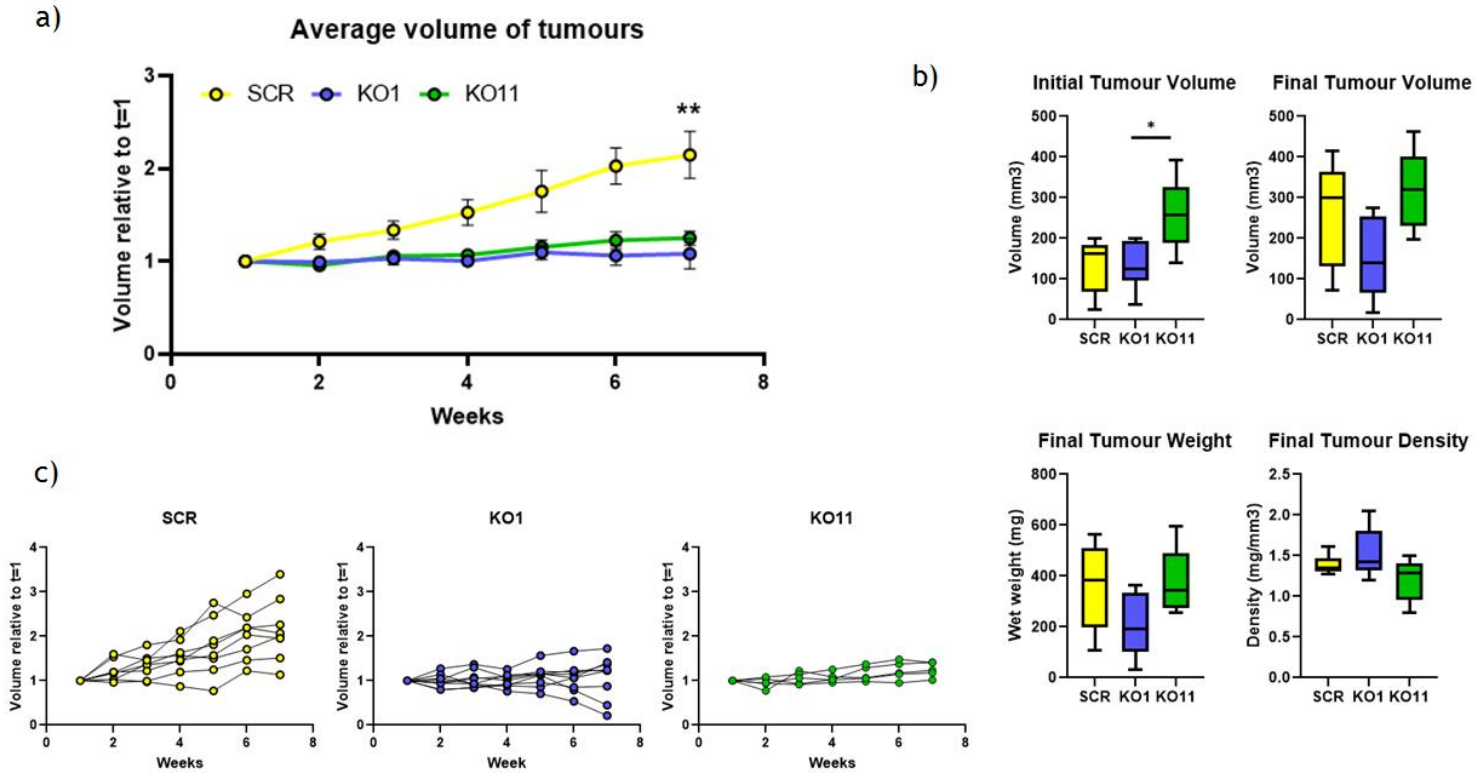

Figure 3-21 – Growth analysis of 22Rv1 KO orthografts

Volumes were measured weekly using VEVO Lab Software to define the surface of the tumour and calculate the total volume. a) Average fold changes ± SEM of the tumours derived from each clone. Fold change is defined as the ratio to volume at t=0. One-way ANOVA showed significant (= $p < 0.005$) difference between both KO clones and the control. There was no significant difference between the growth of KO1 and KO11. b) Initial volume, final volume, weight and density (final weight divided by final volume) of the tumours. There was only a significant (* = $p < 0.05$, Kruskal-Wallis test) difference between sizes at the beginning, between the KO1 derived tumour and the ones from KO11. c) Fold change plots of each tumour separated by cell line.**

Chapter 4 - Omics Analysis of 22Rv1 SLFN5 KO Identifies a Role for SLFN5 in LAT1 Expression via ATF4

4.1 Transcriptomic Analysis of 22Rv1 SLFN5 KO Models

In order to gain an unbiased understanding of the effects of SLFN5-mediated functions in prostate cancer, transcriptomic analysis was performed on the 22Rv1 KO cells and orthografts. The use of two different SLFN5 clones helped exclude potential false hits caused by the clonal selection. Analysing data from both *in vitro* and *in vivo* models further strengthened the confidence of the obtained hits. The resulting data were compared and selected following the workflow described in Figure 4-1. First, only the genes whose mRNA was significantly altered ($p < 0.05$) in the same direction (increase or decrease over control sample) in both KO clones (KO1 and KO11) were considered as true hits. Then, the results obtained in the analysis of the tumour samples and the *in vitro* samples were compared in order to find which and how many genes were consistently altered across both models, and what genes were only altered in each particular condition (Table 4-1). This analysis yielded a list of 64 genes whose expression is confidently altered when SLFN5 is removed from the cells (Table 4-2).

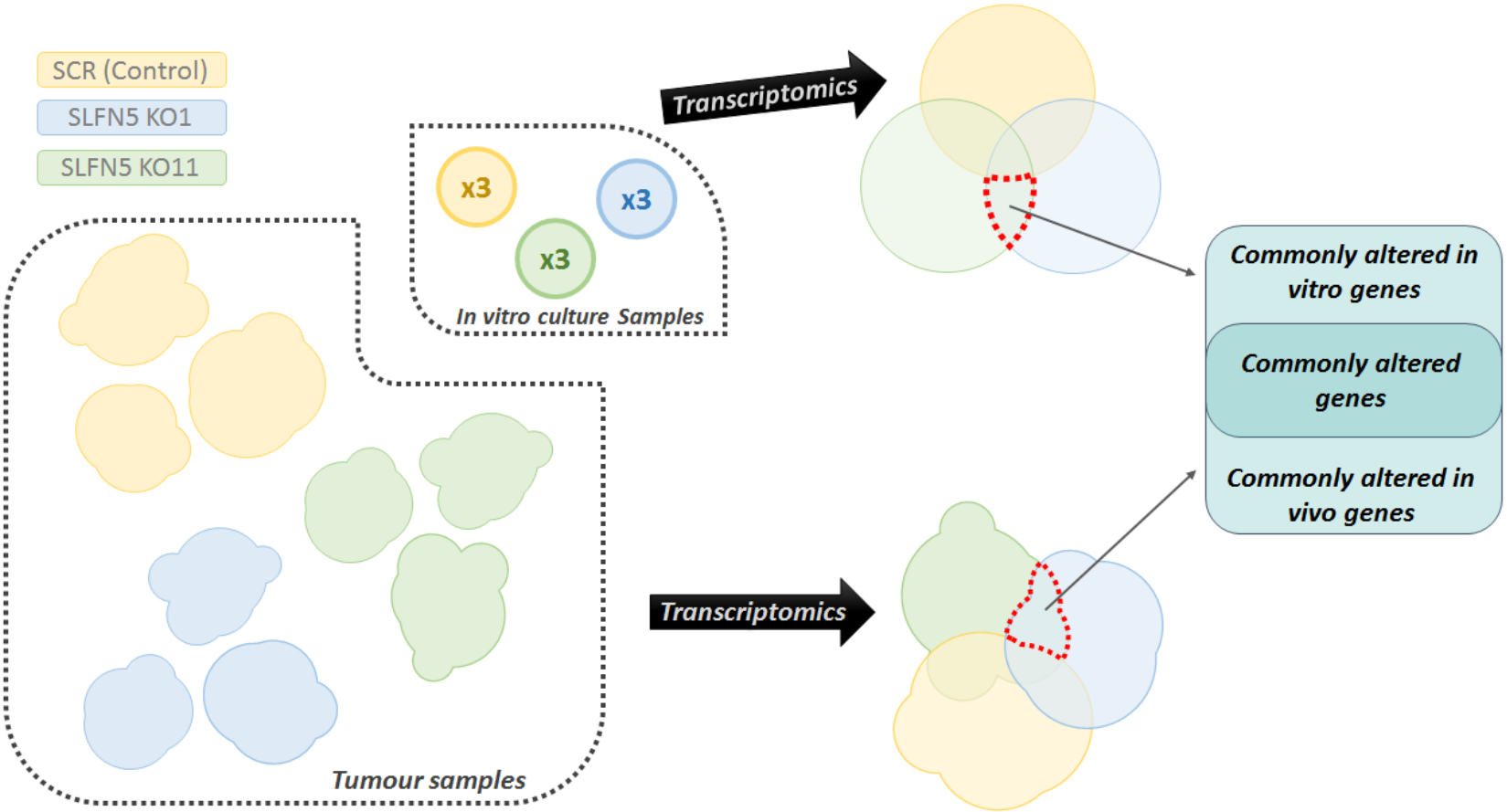

Figure 4-1 – Comparison workflow of transcriptomic analysis of 22Rv1 KO models

Representative samples from three tumours derived from each 22Rv1 KO clone, as well as three biological replicates of each 22Rv1 KO clone culture in *in vitro* conditions were processed for RNA extraction and then had their transcriptome analysed. Significance was defined as $p < 0.05$ in a T-test analysis comparison of the transcript detection intensity between the samples. Analysis was performed in collaboration with Ann Headley.

Table 4-1 – Number of transcripts identified for each defined criteria

Table shows the number and % over total identified transcripts for each comparison performed. Significance was defined as $p < 0.05$ in a T-test analysis comparison of the transcript detection intensity between the KO samples and the SCR control ones.

	# of Identified Transcripts	% of Total	Name	Definition Criteria
	37455	100.00%	Total	All identified transcripts (Over 58425 total detected)
In vitro analysis	1416	3.78%	KO1 Up In vitro	Significant, positive fold
	676	1.80%	KO1 Down In vitro	Significant, negative fold
	2092	5.59%	KO1 Up+Down In vitro	Significant
	1947	5.20%	KO11 Up In vitro	Significant, positive fold
	2348	6.27%	KO11 Down In vitro	Significant, negative fold
	4295	11.47%	KO11 Up+Down In vitro	Significant
	521	1.39%	KO1 + KO11 Up In Vitro	Significant, same direction
	211	0.56%	KO1 + KO11 Down In Vitro	Significant, same direction
	732	1.95%	In vitro Up + Down	Significant, same direction
In vivo analysis	477	1.27%	KO1 Up In Vivo	Significant, positive fold
	319	0.85%	KO1 Down In Vivo	Significant, negative fold
	796	2.13%	KO1 Up+Down In Vivo	Significant
	240	0.64%	KO11 Up In Vivo	Significant, positive fold
	409	1.09%	KO11 Down In Vivo	Significant, negative fold
	649	1.73%	KO11 Up+Down In Vivo	Significant
	85	0.23%	KO1 + KO11 Up In Vivo	Significant, same direction
	30	0.08%	KO1 + KO11 Down In Vivo	Significant, same direction
	115	0.31%	In Vivo Up + Down	Significant, same direction
In vitro + In vivo	12	0.03%	KO1+KO11 Up In vivo + In vitro	Significant, same direction
	52	0.14%	KO1+KO11 Down In vivo + In vitro	Significant, same direction
	64	0.17%	All Up + Down	Significant, same direction

Table 4-2 – Significantly altered transcripts in 22Rv1 KO model in both *in vivo* and *in vitro* conditions

Red coloured fold changes indicate reduced expression in KO clones, green indicates increased expression in KO clones.

	In vitro				*In vivo*			
	KO1		KO11		KO1		KO11	
Gene	Fold change	p value	Fold change	p value	Fold change	p value	Fold change	p value
NDNF	-375,497	4,3E-203	-444,491	3,3E-196	-74,5781	3,13E-59	-161,281	1,75E-79
KCNH5	-69,8793	1,2E-134	-224,953	1,62E-83	-57,7291	1,03E-46	-131,017	1,64E-31
NCMAP	-79,7554	7,7E-161	-90,3863	2,7E-156	-46,4657	8,36E-50	-66,9673	9,06E-60
SLC40A1	-58,1427	4,9E-193	-91,7175	2,2E-228	-19,9005	1,48E-40	-12,0208	1,93E-27
TFPI	-168,903	3E-98	-315,13	1,21E-24	-19,5526	6,19E-40	-4,64382	4,8E-10
CFAP61	-10,6493	3,12E-37	-17,8862	9,87E-43	-10,3722	1,4E-12	-11,696	3,54E-14
DCN	-8,72552	9,7E-27	-12,4927	7,57E-30	-11,1441	1,04E-17	-8,38263	2,35E-13
MIR600HG	-10,5136	5,7E-105	-14,857	6,1E-135	-6,5985	3,56E-12	-9,13772	6,73E-17
SLC7A5	-9,15767	2,05E-54	-6,49413	5,65E-39	-6,70841	7,31E-18	-7,41572	1,26E-19
FLRT2	-4,92569	3,09E-33	-6,26239	4,5E-44	-3,90536	8,48E-08	-10,0178	4,47E-23
FOXN4	-3,35061	5,58E-06	-12,4459	1,89E-13	-5,61315	6,43E-06	-7,66165	2,28E-08
NCCRP1	-14,9969	2,07E-13	-10,1861	2,33E-12	-6,86656	1,32E-05	-5,16655	0,000143
ORAI2	-10,4294	4E-167	-11,4865	4,6E-180	-6,31583	3,05E-19	-5,31852	1,46E-15
ACACB	-6,28105	9,24E-45	-6,89029	1,92E-49	-5,91949	1E-17	-5,44615	6,16E-16
CCDC68	-12,9596	6,33E-34	-34,7054	7,88E-63	-7,15365	9,47E-15	-4,15825	2,49E-07
PCDH15	-9,55738	2,22E-08	-13,3815	1,61E-06	-5,7029	0,000156	-5,27746	0,002206
LUM	-323,185	2E-172	-52,5058	2,7E-156	-5,64754	1,18E-08	-5,18034	1,19E-07
STRBP	-6,07483	6,05E-52	-8,38615	2,96E-72	-5,15893	3,84E-15	-5,33716	1,28E-15
BMPR1B	-3,8684	1,21E-12	-8,55952	1,28E-30	-4,62356	6,03E-10	-3,97466	6,12E-08
LRFN5	-2,2598	2,36E-10	-2,25693	1,85E-10	-3,67002	1,44E-06	-4,58874	4,64E-09
RCAN3	-2,25504	2,62E-05	-5,35692	5,08E-22	-2,98952	4,47E-05	-5,064	1,98E-11
CRB2	-4,25263	2,69E-09	-5,1135	1,22E-10	-2,83678	0,012356	-4,94765	4,09E-06
KCNC4	-3,53518	1,18E-09	-4,10478	8,37E-12	-2,33875	0,017632	-5,36435	1,42E-09
CRNKL1	-3,56173	2,8E-30	-3,32226	2,83E-27	-3,72807	6,3E-15	-3,72211	9,81E-15
DPYD	-1,90141	0,000671	-13,0121	8,14E-49	-2,5503	0,010309	-4,52036	5,97E-07
TFCP2	-5,06257	2,68E-28	-2,45216	2,77E-09	-2,53774	0,004202	-4,46423	4,85E-08
UBAP2	-4,37828	5,32E-42	-5,04998	7,66E-51	-3,69375	3,67E-13	-3,02065	4,34E-09
BMP5	-6,1082	8,53E-11	-2,86092	9,89E-05	-2,9713	0,01236	-3,70539	0,000817
SLC3A2	-5,2055	1,78E-22	-3,34222	2,91E-12	-3,00551	8,64E-06	-3,21452	1,95E-06
CD9	-3,38547	6,79E-42	-2,90222	3,36E-32	-2,41738	0,000709	-3,53636	5,08E-08
ENPP1	-4,75603	4,24E-18	-2,43871	2,47E-06	-2,7657	5,67E-05	-3,18358	1,7E-06
NEDD4L	-1,94412	8,7E-06	-3,74871	1,17E-22	-2,61687	6,7E-08	-2,97055	4,9E-10

	In vitro				*In vivo*			
	KO1		KO11		KO1		KO11	
Gene	Fold change	p value	Fold change	p value	Fold change	p value	Fold change	p value
CCL28	-1,79545	0,011385	-2,65343	3,52E-06	-2,53248	0,002197	-2,93455	0,000174
TACC2	-3,02977	1,52E-20	-3,92644	1,28E-31	-2,73671	7,65E-07	-2,65536	2,52E-06
FAM161A	-2,50425	0,000248	-3,22996	5,19E-07	-3,03152	0,000872	-2,27176	0,03761
C10orf143	-4,40347	4,74E-37	-3,21342	1,48E-23	-2,94608	0,000212	-2,29603	0,011998
RGPD2	-9,18958	4,64E-18	-9,79586	7,82E-17	-2,69807	0,010888	-2,5204	0,020421
IFT57	-5,01217	9,29E-33	-3,29293	3,6E-18	-2,90529	1,08E-07	-2,27582	0,000199
LRWD1	-2,29186	2,94E-10	-1,71601	9,94E-05	-2,35634	0,000326	-2,80875	4,07E-06
DEGS1	-3,52919	5,22E-34	-3,43148	9,07E-33	-2,4044	0,00026	-2,67042	2,38E-05
PAK4	-2,40466	3,01E-16	-1,84111	3,84E-08	-2,29687	3,05E-05	-2,56048	1,14E-06
TMCC3	-3,2597	1,43E-16	-6,60953	6,88E-40	-2,75612	4,59E-05	-1,86558	0,048408
PCGF2	-3,29065	5,03E-30	-2,58647	2,67E-19	-2,71186	7,57E-05	-1,87994	0,048863
USP34	-1,73938	0,035144	-3,04802	1,37E-07	-2,31023	3,48E-05	-2,20885	0,000155
FADS2	-2,41313	5,24E-12	-1,75315	3,09E-05	-1,70226	0,043209	-2,79857	2,68E-07
FAM43A	-1,7121	0,000486	-2,22371	1,29E-08	-1,97391	0,004806	-2,52641	1,48E-05
GLRX3	-2,49522	3,44E-15	-1,78202	2,09E-06	-2,01708	0,000538	-2,25855	2,42E-05
CSRNP2	-2,87758	8,77E-11	-3,51539	1,68E-15	-2,19614	0,000597	-1,86525	0,016943
GLRX3P2	-2,47819	2,85E-10	-1,72552	0,000376	-1,75367	0,037768	-2,05446	0,002905
NVL	-2,03612	6,71E-11	-1,68789	3,1E-06	-1,95422	0,001556	-1,79683	0,010806
ALDH3A2	-2,14863	6,66E-11	-2,23293	2,76E-12	-1,75984	0,012188	-1,81927	0,007355
ASNSD1	-1,7387	9,61E-08	-1,72397	1,09E-07	-1,59217	0,040253	-1,74355	0,008317
FGF14-AS2	2,246343	4,56E-05	2,883102	1,18E-08	1,903745	0,033913	1,895117	0,037252
OSER1-DT	3,337768	1,49E-07	2,448904	0,000173	1,941289	0,027462	1,991504	0,020085
FLOT2	2,692671	1,47E-17	3,812836	1,54E-32	2,06807	0,018331	1,964852	0,038845
TUBA4A	1,940677	0,010613	1,861238	0,010055	2,33779	0,000935	1,895437	0,03387
CFAP157	3,116314	1,66E-07	3,145898	9,59E-08	2,089496	0,017834	2,182245	0,011213
FXYD5	2,607771	2,32E-07	1,924332	0,000852	2,214427	0,016557	2,172151	0,023395
CCDC154	2,170411	0,013505	1,822949	0,042854	2,171523	0,049528	2,382966	0,021227
MYO15B	3,007733	5,92E-08	2,192122	0,000211	2,182311	0,019241	2,455873	0,004625
COL26A1	3,690706	4,01E-13	2,842741	1,92E-08	2,513712	0,006464	2,224408	0,029725
SUSD4	20,91355	1,01E-49	12,87256	1,38E-35	2,812209	0,000474	2,327286	0,010048
SUSD2	8,568531	2,11E-43	2,131762	2,01E-05	3,127108	0,003104	2,642673	0,019753
SLC34A3	4,14387	2,29E-12	8,448456	3,39E-28	6,09321	6,29E-10	2,684283	0,005212

4.1.1 Validation of 22Rv1 KO transcriptomic results

Twelve genes from the final list of SLFN5 KO affected genes were selected for analysis based on low expression and cell function, and primers were designed to validate their mRNA expression. Among the genes selected, all of them proved to be significantly downregulated in at least one of the 22Rv1 KO clones, and 8 had significantly reduced expression in both 22Rv1 KO clones as measured by qPCR (Figure 4-2, Table 4-3).

Given the CRISPR/Cas9 KO model produces a total and long-term absence of SLFN5 in the cells, we wanted to study the short-term effects of reducing SLFN5 levels. Wild type 22Rv1 cells were treated with *SLFN5* siRNA for 72 hours, and the expression of several of the aforementioned genes was studied. Of the 7 probed genes, 3 of them (*SLC7a5*, *KCNH5*, *NCMAP*) had significantly reduced expression. Interestingly, 2 of them (*NDNF*, *TFPI*) had increased mRNA levels (Figure 4-3.a).

Table 4-3 – Analysis of gene expression on the KO1 and KO11 genes as measured by PCR

Adjusted P Value correspond to Holm-Sidak method (Multiple t-test) comparisons, significance being defined as p < 0.05. In blue is data for KO1, in green for KO11.

	Adjusted P Value	Significant?	Mean of SCR	Mean of KO1	Difference	SE	Adjusted P Value	Significant?	Mean of SCR	Mean of KO11	Difference	SE	Significant reduction in both?
SLFN5	<0.000001	Yes	1.002	0.2142	0.7882	0.065	<0.000001	Yes	1.002	0.1494	0.853	0.062	Yes
SLC7a5	<0.000001	Yes	1.009	0.4307	0.5788	0.065	<0.000001	Yes	1.009	0.5102	0.4992	0.062	Yes
SLC3a2	<0.000001	Yes	1	0.4794	0.5209	0.063	<0.000001	Yes	1	0.6195	0.3808	0.06	Yes
ACACB	0.000261	Yes	1.006	0.7984	0.2076	0.063	0.001661	Yes	1.006	1.207	-0.201	0.062	No
CFAP61	<0.000001	Yes	1.003	1.547	-0.5447	0.063	<0.000001	Yes	1.003	0.2455	0.7571	0.06	No
FLRT2	0.320395	No	1	0.9472	0.05298	0.063	<0.000001	Yes	1	0.6338	0.3664	0.06	No
KCNH5	<0.000001	Yes	1.001	0.2418	0.7595	0.063	<0.000001	Yes	1.001	0.07569	0.9257	0.06	Yes
NCCRP1	<0.000001	Yes	1.002	0.07745	0.9243	0.063	<0.000001	Yes	1.002	0.07117	0.9306	0.06	Yes
NCMAP	<0.000001	Yes	1.001	0.6152	0.3853	0.063	<0.000001	Yes	1.001	0.459	0.5415	0.06	Yes
NDNF	<0.000001	Yes	1.002	0.03298	0.9691	0.063	<0.000001	Yes	1.002	0.03032	0.9717	0.06	Yes
ORAI2	<0.000001	Yes	1.003	0.6492	0.3539	0.063	0.000698	Yes	1.003	0.7877	0.2154	0.06	Yes
STRBP	<0.000001	Yes	1.021	0.5231	0.4979	0.078	0.075806	No	1.021	0.8954	0.1256	0.074	No
TFPI	<0.000001	Yes	1.003	0.004572	0.9984	0.065	<0.000001	Yes	1.003	0.000903	1.002	0.064	Yes

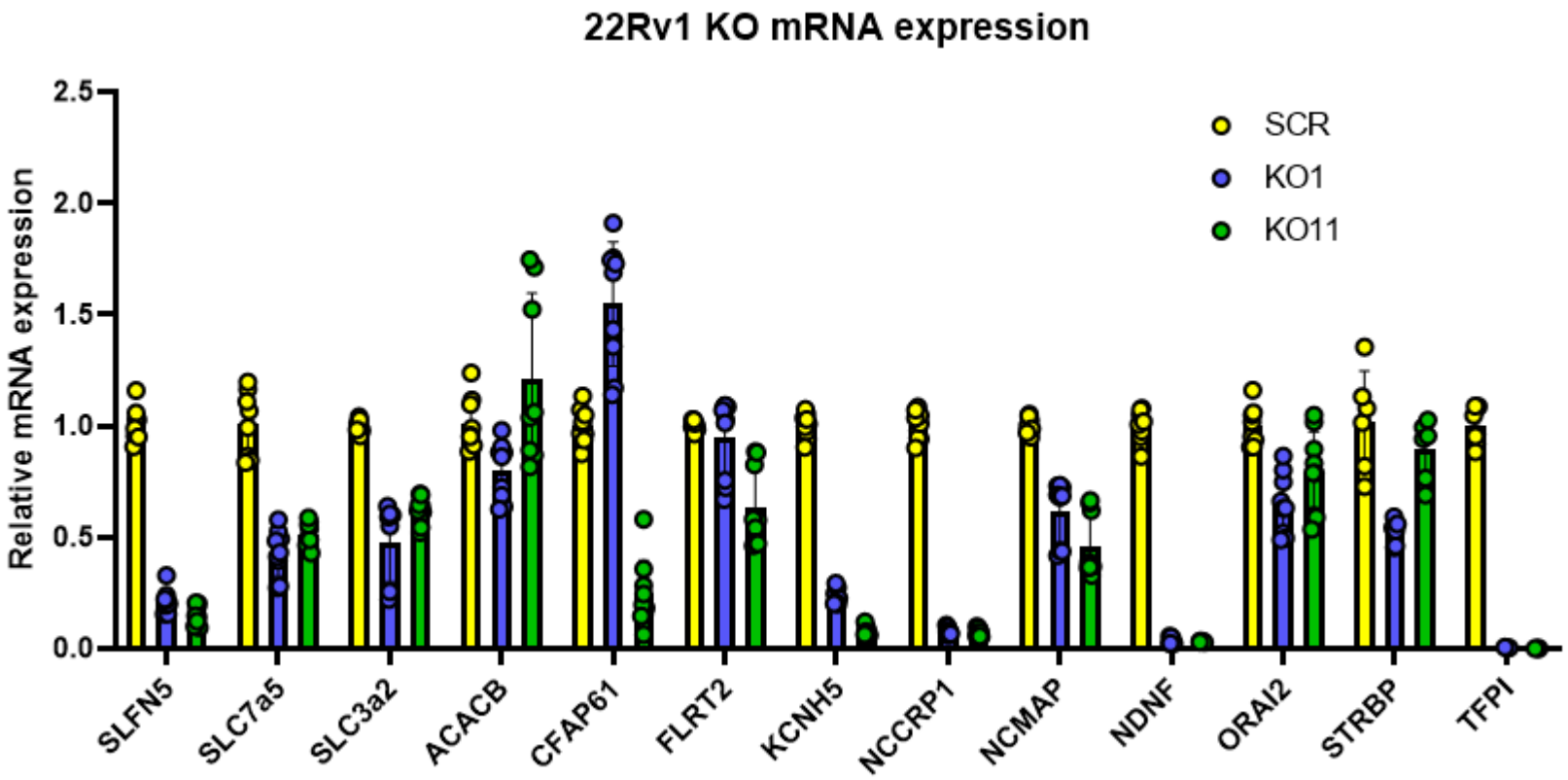

Figure 4-2 - Gene expression in 22Rv1 KO cells as measured by PCR

Figure shows data points from each technical replicate for each of the analysed genes, for significance data refer to Table 4-3. *CASC3* was used as a reference gene for normalisation and the fold change compared to control average is shown. Error bars represent Standard Deviation, n=3, three technical replicates per n.

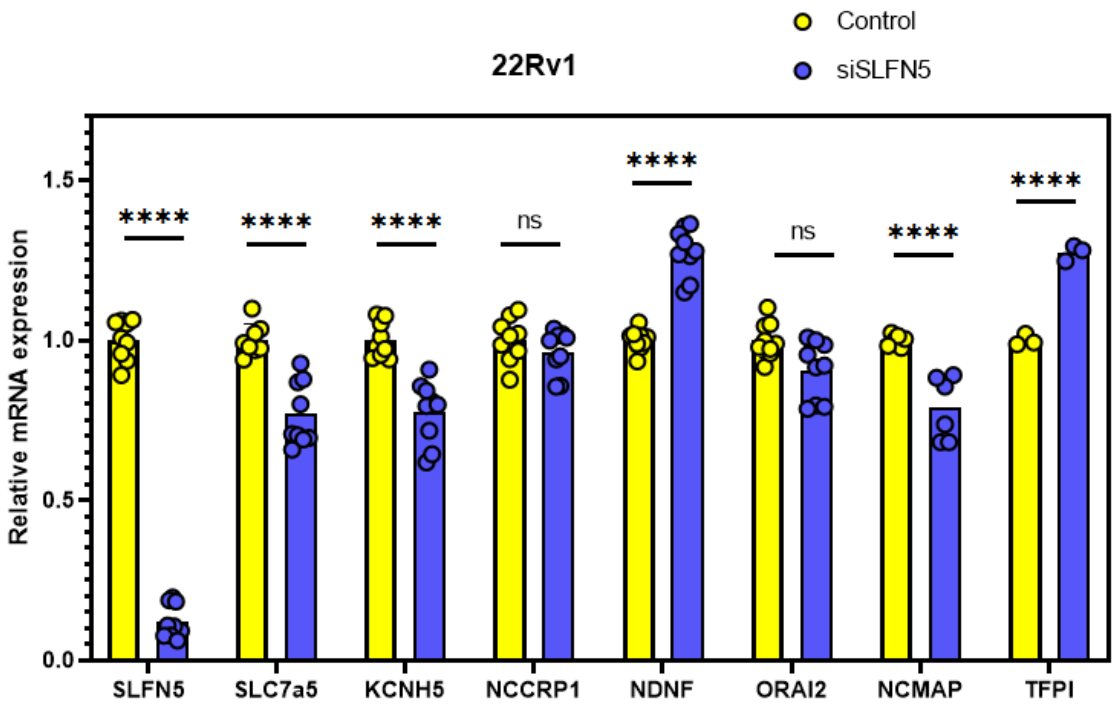

Figure 4-3 – Silencing of SLFN5 in 22Rv1 cells

a) Expression levels of the selected genes after treating the cells with SLFN5 siRNA for 72 hours. (** = p<0.00005, Holm-Sidak method of multiple t-test comparisons). Figure shows data points from each technical replicate. *CASC3* was used as a reference gene for normalisation and the fold change compared to average of control is shown. Error bars represent Standard Deviation, n=3, three technical replicates per n.**

4.2 Proteomic Analysis of SLFN5 KO Orthografts

To further validate the findings of the transcriptome analysis the proteomes of three tumour samples of each 22Rv1 KO clone were compared, following an analysis pipeline similar to the one used for transcriptomic data. Only significantly ($p < 0.05$) altered genes with a matching pattern of expression in both KO samples (upregulated or downregulated) were considered hits. Using this criteria, 38 proteins were found to be significantly altered in tumours from both KO clones when compared to the control orthografts. 19 out of those 38 proteins were detected in lesser amounts in the KO samples than in the control (Table 4-4). This list was then compared with the transcriptomic data, looking to find commonly altered hits in both the tumour samples and the *in vitro* cultured clones. That resulted in 9 proteins commonly altered across all three omic analyses, 8 of them being downregulated in the KO samples in comparison with the control (Table 4-5). Reduced expression of four of them (SLC7a5, SLC3a2, STRBP and NDNF) had been previously validated by PCR (Table 4-3, Figure 4-2).

Table 4-4 – Significantly altered proteins in SLFN5 KO orthografts

Orange and red coloured negative fold changes indicate reduced expression in KO clones, green coloured positive fold indicates increased expression in KO clones.

Gene names	Difference KO1 vs SCR	pvalue KO1 vs SCR	Difference KO11 vs SCR	pvalue KO11 vs SCR
NDNF	-5,34	0,0000	-5,28	0,0004
UBAP2	-3,90	0,0020	-2,50	0,0107
PAK4	-3,61	0,0005	-2,61	0,0387
SLC7A5	-3,28	0,0462	-5,08	0,0090
STRBP	-2,79	0,0005	-3,59	0,0004
RAB27B	-2,61	0,0004	-1,92	0,0091
SLC3A2	-2,54	0,0001	-3,18	0,0002
EIF2B1	-2,42	0,0003	-2,87	0,0018
CD63	-1,89	0,0364	-1,97	0,0153
CD9	-1,76	0,0171	-2,09	0,0089
NFYA	-1,74	0,0110	-1,18	0,0435
PRPSAP1	-1,42	0,0447	-1,02	0,0187
EPHA4	-1,31	0,0368	-1,97	0,0137
IGFBP2	-1,13	0,0023	-0,47	0,0022
ATP5H	-0,93	0,0311	-0,86	0,0237
TFRC	-0,83	0,0328	-1,29	0,0309
ALDH3A2	-0,70	0,0211	-0,51	0,0240
UBR5	-0,45	0,0468	-0,66	0,0053
TM9SF2	-0,19	0,0043	-0,44	0,0380
EIF2S3;EIF2S3L	0,18	0,0407	0,36	0,0164
GSTO1	0,30	0,0346	0,53	0,0448
GSN	0,42	0,0179	0,56	0,0266
FTH1	0,62	0,0241	1,15	0,0245
CPNE1	0,84	0,0126	0,81	0,0131
CENPV	0,88	0,0389	1,07	0,0108
GMPPA	1,29	0,0325	1,57	0,0217
FN1	1,34	0,0192	1,04	0,0400
FAHD2A;FAHD2B	1,43	0,0100	0,89	0,0193
CLU	1,55	0,0207	2,58	0,0037
CNN2	1,55	0,0168	2,38	0,0038
ITGB5	1,63	0,0301	1,02	0,0344
PRSS23	1,76	0,0391	3,96	0,0005
NUP214	1,88	0,0231	2,19	0,0295
STXBP2	2,04	0,0045	1,90	0,0043
FLOT2	2,21	0,0059	2,51	0,0042
GBE1	2,60	0,0002	3,11	0,0000
FLOT1	2,73	0,0000	2,67	0,0058
TGFBI	3,43	0,0010	4,04	0,0002

Table 4-5 – Significantly altered hits across all omic analyses

Orange and red coloured fold changes indicate reduced expression in KO clones, green indicates increased expression in KO clones.

	In vivo Proteomics				*In vivo* Transcriptomics				*In vitro* Transcriptomics			
Gene name	KO1 Fold	KO1 pvalue	KO11 Fold	KO11 pvalue	KO1 Fold	KO1 pvalue	KO11 Fold	KO11 pvalue	KO1 Fold	KO1 pvalue	KO11 Fold	KO11 pvalue
NDNF	-5,34	0,0000	-5,28	0,0004	-74,58	0,0000	-161,28	0,0000	-375,50	0,0000	-444,49	0,0000
UBAP2	-3,90	0,0020	-2,50	0,0107	-3,69	0,0000	-3,02	0,0000	-4,38	0,0000	-5,05	0,0000
PAK4	-3,61	0,0005	-2,61	0,0387	-2,30	0,0000	-2,56	0,0000	-2,40	0,0000	-1,84	0,0000
SLC7A5	-3,28	0,0462	-5,08	0,0090	-6,71	0,0000	-7,42	0,0000	-9,16	0,0000	-6,49	0,0000
STRBP	-2,79	0,0005	-3,59	0,0004	-5,16	0,0000	-5,34	0,0000	-6,07	0,0000	-8,39	0,0000
SLC3A2	-2,54	0,0001	-3,18	0,0002	-3,01	0,0000	-3,21	0,0000	-5,21	0,0000	-3,34	0,0000
CD9	-1,76	0,0171	-2,09	0,0089	-2,42	0,0007	-3,54	0,0000	-3,39	0,0000	-2,90	0,0000
ALDH3A2	-0,70	0,0211	-0,51	0,0240	-1,76	0,0122	-1,82	0,0074	-2,15	0,0000	-2,23	0,0000
FLOT2	2,21	0,0059	2,51	0,0042	2,07	0,0183	1,96	0,0388	2,69	0,0000	3,81	0,0000

4.3 LAT1 protein expression correlates with *SLFN5* levels in prostate cancer models

Since both components of the LAT1 transporter (SLC7a5 and SLC3a2) were found to be consistently downregulated in both *in vivo* and *in vitro* samples of 22Rv1 KO cells, we wondered if the expression of these proteins could be correlated with SLFN5 expression and/or CRPC status in other prostate cancer models. Protein levels of both genes were then studied by Western Blot in several models. Western Blot of the 22Rv1 KO derived orthografts corroborated transcriptomic and proteomic data, both SLC7a5 and SLC3a2 expression is lower in the SLFN5 KO tumours (Figure 4-4.a). The 22Rv1 KO cells from which the tumours were derived from presented similar pattern of expression, where SLFN5 KO causes reduced expression of the LAT1 components (Figure 4-4.b). In the LNCaP AI KO models, SLC7a5 expression was also decreased (Figure 4-4.c), while SLC3a2 was not detectable (data not shown). In the case of LNCaP OE2 clone, the increased levels of SLFN5 translated in an increase in SLC7a5 protein levels (Figure 4-4.d). Interestingly, that was not the case for the LNCaP OE3 clone, which did not show altered SLC7a5 expression. This might be due to the fact that in the LNCaP OE3 clone SLFN5 does not localise into the nucleus (Figure 3-18), suggesting the need of SLFN5 nuclear localisation in order to drive up expression of LAT1.

Interestingly, this same pattern of expression was found in the wild type PC models. The CRPC variants had increased levels of SLC7a5 in comparison to their hormone naïve counterparts, matching the increased levels of SLFN5 (Figure 4-4.e). This was also true for orthograft tumours derived from those same cell lines (Figure 4-4.f).

As described in the introduction, LAT1 expression has been found to be upregulated in advanced and castration resistant prostate cancer, where LAT1 helps tumour cells to keep up with the increased nutrient demand. Here, the data further established SLFN5 as a protein emerging in CRPC, with its expression repressed by the presence of androgens and androgen signalling. In addition, increased LAT1 expression correlates with SLFN5 presence in multiple prostate cancer cell line derived models, pointing to a regulatory role of SLFN5 over LAT1.

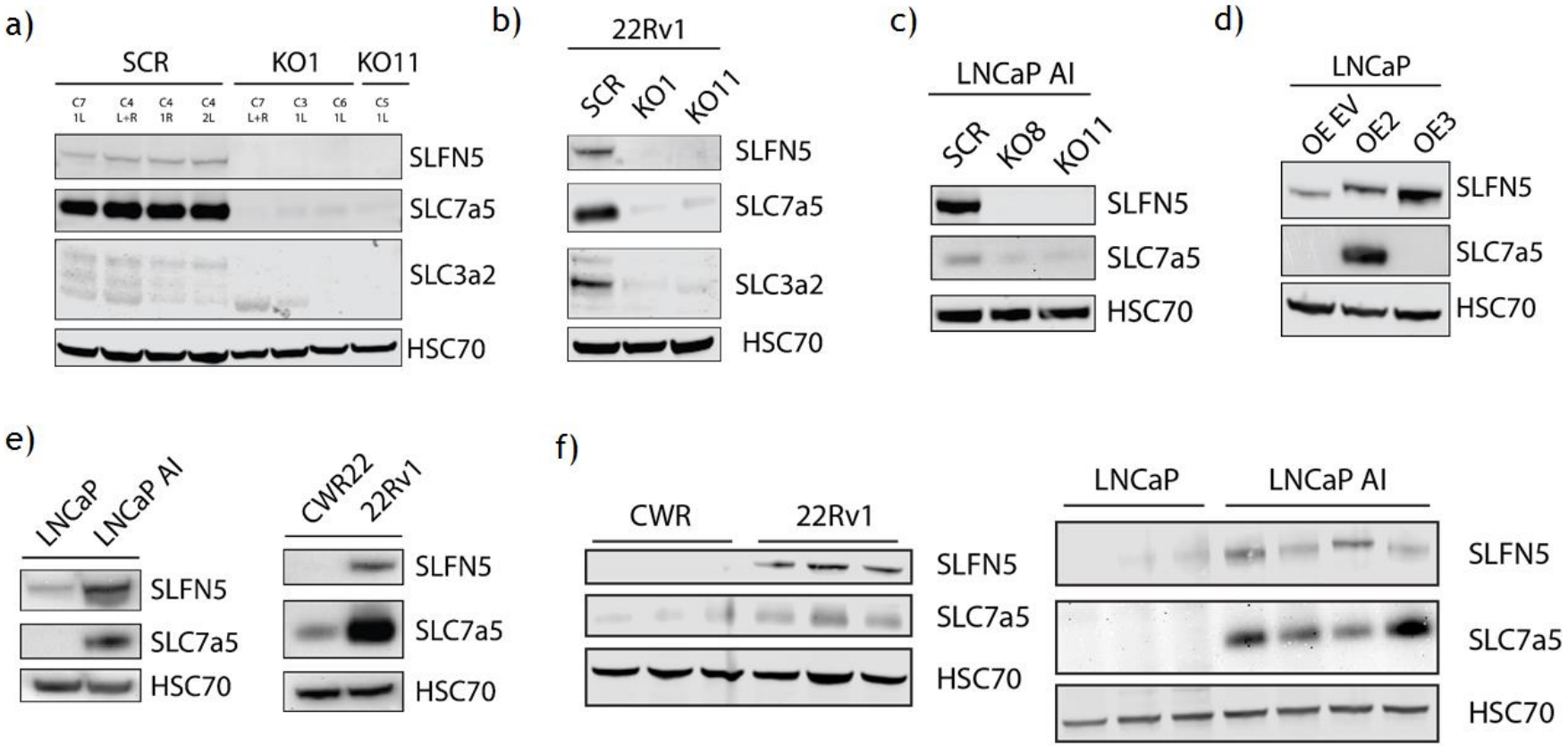

Figure 4-4 – Western Blot expression of LAT1 across several prostate cancer models

For figures b, c, d and e, at least two biological replicates were assessed for SLC7a5 and SLC3a2 expression. Each sample analysed in figures a and f is an independent biological replicate. HSC70 was used as loading control.

Finally, to further probe the regulation of LAT1 by SLFN5, the protein levels of LAT1 were measured in 22Rv1 and LNCaP AI after treatment with siSLFN5 for 72 hours. In both cell lines, silencing SLFN5 caused a decrease in SLC7a5 protein levels (Figure 4-5).

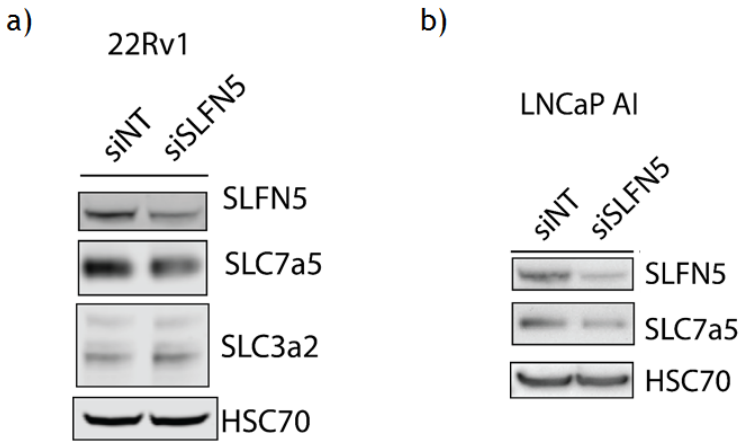

Figure 4-5 – LAT1 protein expression in 22Rv1 and LNCaP AI under siSLFN5 treatment
a) 22Rv1 cells treated during 72h with siRNA for SLFN5, n=3. b) LNCaP AI cells treated during 72h with siRNA for SLFN5, n=2. HSC70 was used as a loading control.

Study of MYC and ATF4 in prostate cancer in relation to SLFN5

The nature of the mechanism by which SLFN5 regulates LAT1 expression is highly relevant to this project, as SLFN5 and LAT1 levels seem to correlate along several models of prostate cancer. SLFN5 is a nuclear protein and has been described to act as a co-repressor by interacting with the STAT1 transcription factor[123]. Not being a transcription factor itself, SLFN5 may however regulate the expression of target genes through its function as a cofactor for other transcription factors. Transcription factors MYC and ATF4 are described as two of the main regulators of LAT1 expression in prostate cancer by the literature, prompting interest in their relationship with SLFN5.

One of the ways MYC acts as a driver for protein synthesis and growth is by increasing amino acid availability. MYC and LAT1 participate in a reciprocal feedback loop, where MYC increases LAT1 expression, only for the increased availability of essential amino acids caused by LAT1 transport to drive MYC

expression further upwards[203]. In prostate cancer specifically, MYC is known to be overexpressed in a significant percentage of clinical cases[204].

The stress response related transcription factor ATF4 has been shown to drive LAT1 expression in prostate cancer in response to reduced levels of androgens, as SLFN5 is suggested to do by the previously shown results. In this reported case, interruption of AR signalling in LNCaP cells results in loss of the LAT3 amino acid transporter, causing metabolic stress due to reduced leucine availability. ATF4 then drives LAT1 expression up to compensate, transforming the model to be LAT1 dependent[185]. At the same time, ATF4 has also been shown to be involved in stress response to MYC driven cancer, putting a brake to uncontrolled protein synthesis and antagonising mTOR growth signalling[205]. ATF4 functions as an element of metabolic balance, thus allowing the cells to cope with the increased demands of an unsuppressed growth process while keeping it under control to avoid undesired side effects.

The described regulation of LAT1 by MYC and ATF4 transcription factors coupled with the apparent need of nuclear localisation of SLFN5 in order to drive LAT1 expression up opens the idea that SLFN5 might be interacting (directly or indirectly) with MYC or ATF4 to regulate the expression of LAT1 and other targets.

To investigate if MYC was capable of regulating the expression of *SLC7a5*, *SLFN5* or any of the selected genes affected by SLFN5 KO, we treated 22Rv1 cells with *MYC* siRNA for 72 hours and measured the mRNA levels of said genes by PCR (Figure 4-6). Interestingly, silencing of *MYC* seemed to be able to increase *SLFN5* expression inconsistently, but did not significantly reduce the levels of any of the studied transcripts.

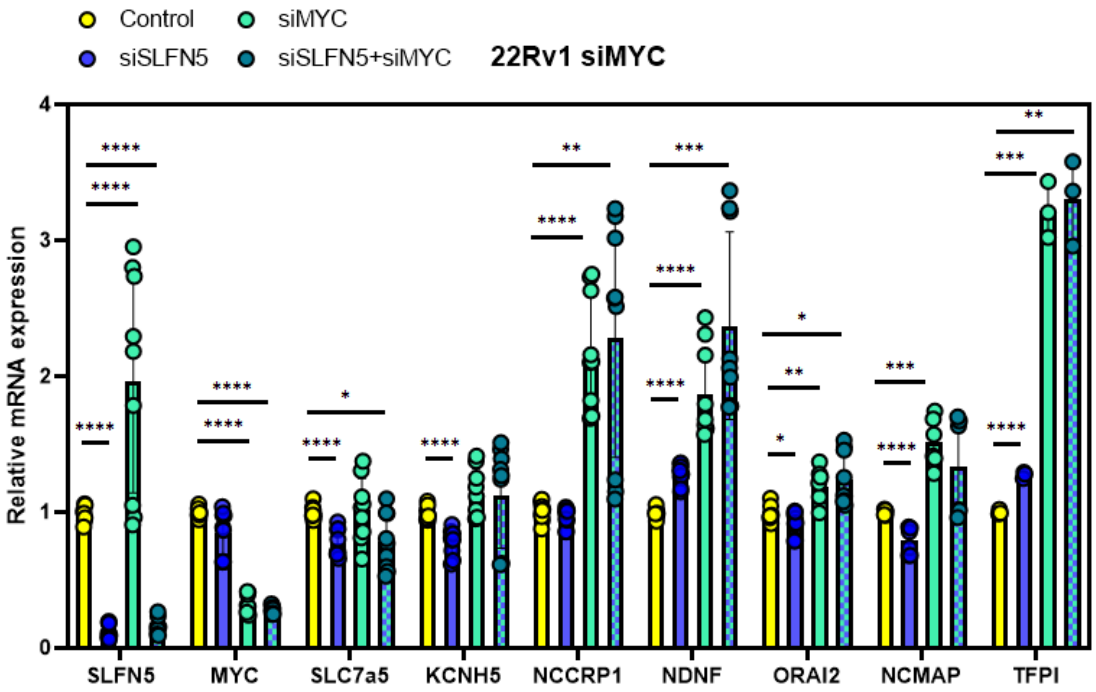

Figure 4-6 – siMYC treatment of 22Rv1 cells

22Rv1 cells were treated with siRNA for *MYC* for 72 hours. The graph shows data from three biological replicates for all genes except for *NCMAP* (n=2) and TFPI (n=1) due to technical problems. *CASC3* was used as a reference gene for normalisation and the fold change compared to average of control is shown. Error bars represent Standard Deviation Figure shows data points from each technical replicate, n=3, three technical replicates per n. (* = p<0.05, ** = p<0.005, *** = p<0.0005, **** = p<0.00005, Holm-Sidak method of multiple t-test comparisons). siSLFN5 data corresponds with (Figure 4-3) and (Figure 4-7), as it was performed as a single experiment.

22Rv1 cells were also treated with siRNA for *ATF4* to examine its effect on the expression of the same selected set of genes (Figure 4-7). Silencing *ATF4* did significantly reduce *SLC7a5* expression, more so than silencing *SLFN5*. The mRNA of *KCNH5*, *NDNF*, *ORAI2*, *NCMAP* and *TFPI* were also significantly reduced by treatment with siATF4. Combination treatment of siATF4 with siSLFN5 decreased *SLC7a5* expression more than siATF4 treatment alone. Although the comparison was not significant using the Bonferroni-corrected p value for the comparison outputted by the Holm-Sidak method, there was a trend (p = 0.0513). The double treatment did significantly reduce the levels of *KCNH5* and *NCCRP1* further than treatment with siATF4 alone.

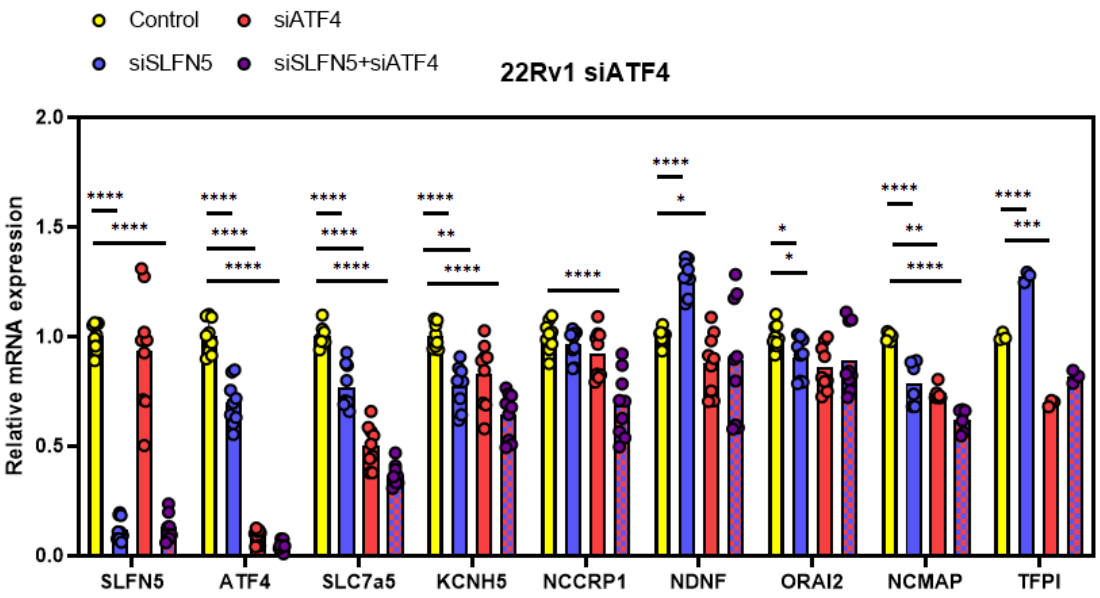

Figure 4-7 – siATF4 treatment of 22Rv1 cells

The graph shows technical replicates from three biological repeats for all genes except for *NCMAP* (n=2) and *TFPI* (n=1) due to technical problems. *CASC3* was used as a reference gene for the ΔΔCt analysis (* = p<0.05, ** = p<0.005, *** = p<0.0005, **** = p<0.00005, Holm-Sidak method of multiple t-test comparisons). Error bars represent Standard Deviation, n=3 save aforementioned exceptions, three technical replicates per n. siSLFN5 data corresponds with (Figure 4-3) and (Figure 4-6), as it was performed as a single experiment.

To further investigate the possible link between SLFN5 and ATF4, table of the top 26 genes affected by SLFN5 KO *in vitro* was provided to by Dr. Paul Peixoto from the University of Franche-Comté to be analysed for known ATF4 binding sites[205,206]. ATF4 positive genes were defined when an ATF4 consensus sequence was detected with a confidence of $p < 0.0001$. 15 out of 26 genes presented at least one site with an ATF4 binding site (Table 4-6). Furthermore, at least one binding site with a confidence of $p < 0.001$ was detected in 24 out of 26 genes (data not shown). These data strongly suggest a relationship between the regulatory programme of SLFN5 and ATF4.

Table 4-6 – ATF4 binding sites in SLFN5 KO affected genes

Analysis was kindly performed by Dr. Paul Peixoto. Shown in the table are the genes where an ATF4 consensus sequence was detected with a confidence of p < 0.0001.

Gene symbol	Localisation (hg38)	Sites (-5000 +1000)	p-value
NDNF	chr4:121070535–121074535	-4108	0.0001
TFPI	chr2:187552435–187556435	-1241	0.0001
KCNH5	chr14:63043427–63047427	-2467	0.0001
LUM	chr12:91109490–91113490	-2181	0.0001
SLC401A	chr2:189578783–189582783	-4427	0.0001
CFAP61	chr20:20050540–20054540	-3843	0.0001
NCCRP1	chr19:39194963–39198963	810	0.0001
PCDH15	chr10:54799202–54803202	-1935	0.0001
ORAI2	chr7:102434201–102438201	623	0.0001
SLC7A5	chr16:87867505–87871505	683 -1616 -4871	0.0001 0.0001 0.0001
FLRT2	chr14:85528143–85532143	-2228 -2659 -2952	0.0001 0.0001 0.0001
STRBP	chr9:123266586–123270586	-4009	0.0001
RGPD2	chr2:87823796–87827796	-4383	0.0001
TFCP2	chr12:51170791–51174791	-2905	0.0001
ENPP1	chr6:131806019–131810019	-3275	0.0001

Finally, a colocalization study was performed by Dr. Paul Peixoto to determine if SLFN5 and ATF4 closely interact. A proximity ligation assay was performed in 22Rv1 cells and interaction between SLFN5 and ATF4 within the nucleus was confirmed (Figure 4-8), strongly suggesting a coregulatory role for SLFN5 for ATF4 function.

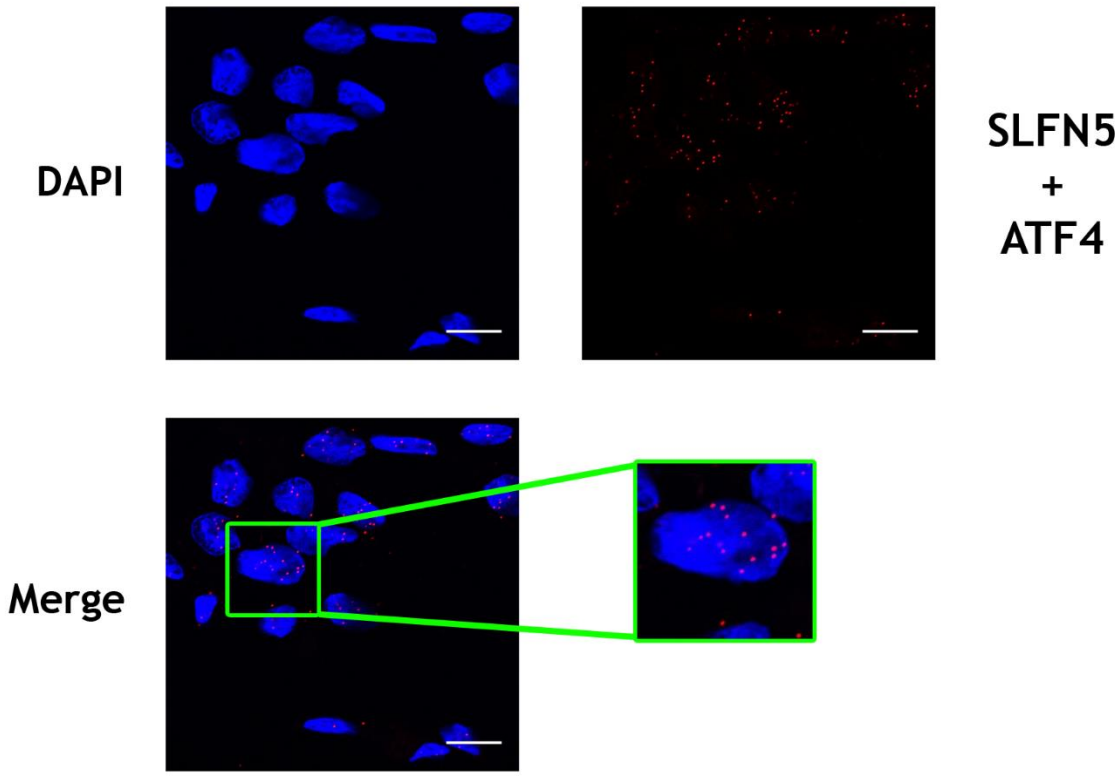

Figure 4-8 – SLFN5 colocalises with ATF4 in the nucleus of 22Rv1 cells

A proximity ligation assay was performed on 22Rv1 cells using antibodies against SLFN5 and ATF4. Co-localisation of both proteins allows for the fluorescent probe to bind to the secondary antibodies and reveals where both proteins are in close proximity.

Chapter 5 - SLFN5 KO Affects mTOR Activation, Autophagy and Intracellular Amino Acid Levels

5.1 SLFN5 KO Affects mTOR Activity in 22Rv1 Cells

Data presented in this thesis have revealed that LAT1 and SLFN5 expression levels correlate in prostate cancer. LAT1 amino acid transporter is an important player in the homeostasis and amino acids availability during prostate carcinogenesis. LAT1 mediated intake of several EAA, especially leucine, regulates activation of the mTOR pathway, which acts as a controller of cellular growth and metabolism by sensing nutrient availability. LAT1 not only modulates the intracellular levels of amino acids that mTOR senses, but also plays a more direct role in mTOR activation by transporting leucine into the lysosomes. There, leucine is sensed by a protein complex, encouraging translocation of mTOR complex 1 to the lysosomal surface. After that, mTORC1 can be activated and growth signaling occurs.

As we have seen, LAT1 expression is deeply affected in the SLFN5 KO models. Activation of the mTOR pathway was measured by phosphorylation of several of its downstream targets and was presented as a western blot in Figure 5-1. 22Rv1 KO cells exhibited reduced levels of phosphorylated P70S6K and its phosphorylation target S6. They also showed increased levels of unphosphorylated 4EBP1, a translation inhibitor that is inactivated as a result of phosphorylation by mTORC1. At the same time, LC3 protein is lipidated in higher amounts in the SLFN5 KO clones. Lipidation of LC3 is a marker of autophagosome formation, a step in the autophagy process prior to the fusion of autophagosome with the lysosome where its internal contents are digested. Autophagy is supressed by the mTOR pathway, as it serves as a backup mechanism to recycle nutrients when they are not available to the cell in its environment. Reduction in AKT phosphorylation is also observed.

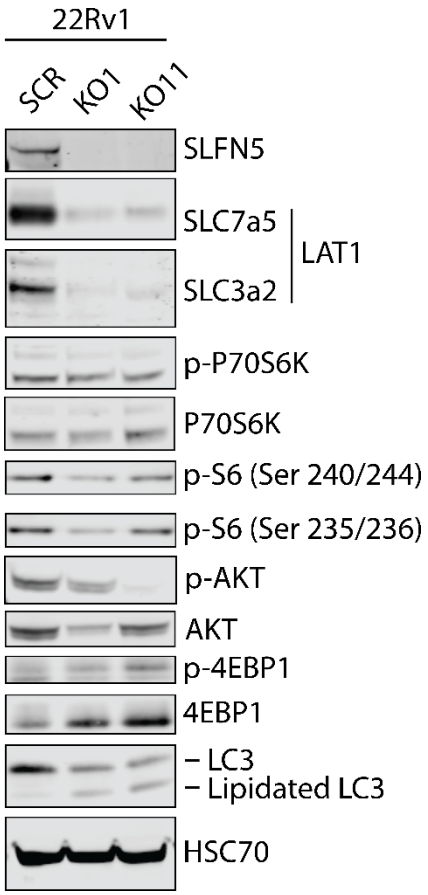

Figure 5-1 – SLFN5 knockout affects mTOR status in 22Rv1 cells

22Rv1 KO cells were grown in 6 well plates and culture media was renewed 72 hours previous to the sampling to keep nutrient availability consistent between all samples. HSC70 was used as loading control. Shown is a representative Western blot of an n=3.

In the 22Rv1 KO derived orthografts, decreased phosphorylation of S6 was detected along with reduced levels of p4EBP1. Added to the elevated lipidation of LC3 protein, these results are consistent with the observed effects of SLFN5 KO in an *in vitro* setting (Figure 5-2). Unfortunately, technical limitations made pP70S6K undetectable in this model by Western blotting.

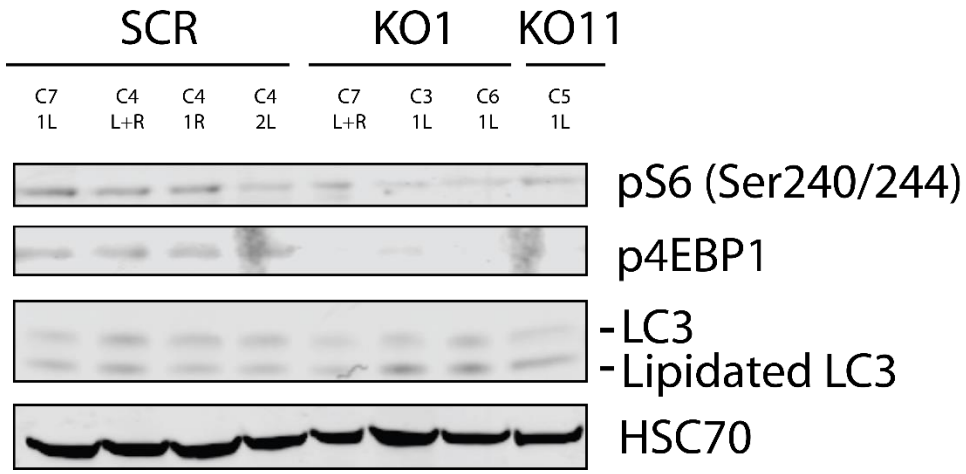

Figure 5-2 – SLFN5 knockout affects mTOR status in 22Rv1 KO derived orthografts

Each sample analysed in the figure is an independent biological replicate. HSC70 was used as loading control. Membrane was shared with Figure 4-4a.

5.2 Metabolomic Analysis of 22Rv1 KO Cells

Diminished LAT1 amino acid transporter levels coupled with the reduced mTOR activation suggest an alteration in amino acid availability can exist in these cells. To observe the amino acid status of the SLFN5 KO cells, metabolomic analysis was performed on the 22Rv1 KO cell lines. After LC-MS analysis 10 metabolites were found to be significantly altered ($p<0.05$) in both 22Rv1 KO clones following the same direction (accumulation or depletion). Of the 7 compounds with reduced levels in the KO cells, 6 of them were proteogenic amino acids: leucine (Leu), isoleucine (Ile), methionine (Met), tyrosine (Tyr), lysine (Lys) and arginine (Arg) (Ornithine is a non-proteogenic amino acid). Among the 6 proteogenic amino acids, 4 of them are EAA and 2 are conditionally essential. It is worth mentioning that 4 of them are known to be transported by LAT1 (Leu, Ile, Met, Tyr).

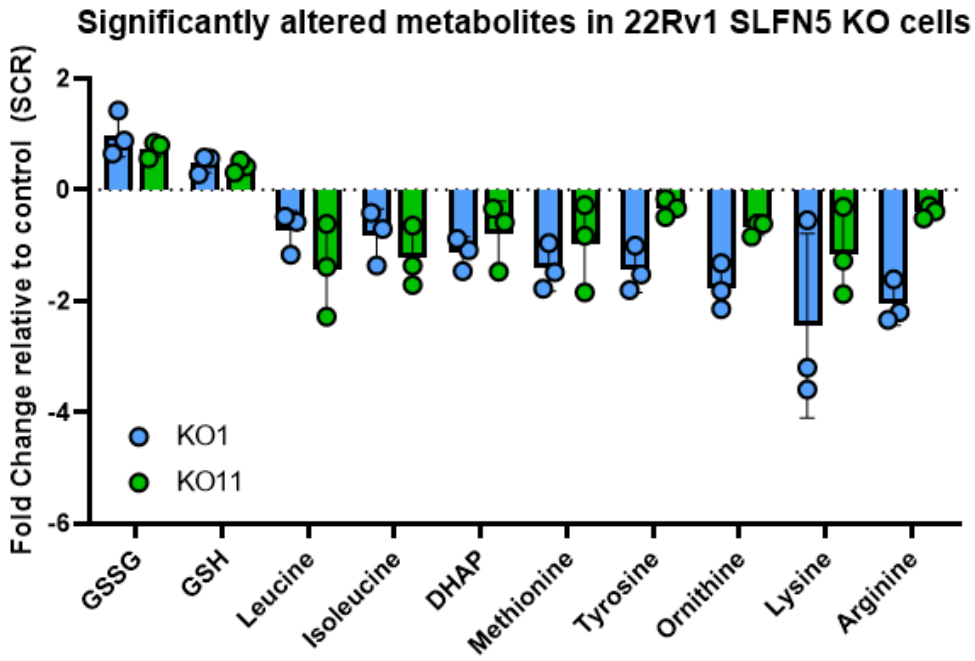

Figure 5-3 – Significantly altered metabolites in 22Rv1 SLFN5 KO cells

Metabolites were extracted from three separate wells and analysed separately. Sampling was performed three times on separate seedings to obtain three biological replicates (n=3). Significance was defined as $p < 0.05$ in a Student's t-test comparison of the fold changes relative to the fold changes of the control sample. Fold changes for each biological replicate were defined over the average normalised intensity for the control sample in each respective replicate. Dots represent the average of each biological replicate, error bars represent Standard Deviation.

These results show that SLFN5 KO deeply affects the uptake of essential amino acid in 22Rv1 cells, reducing the availability of individual EAA for the cell metabolism. This could explain the reduced activation of the mTOR pathway and suggests metabolic struggle as the cause of the reduced tumour growth caused by SLFN5 KO.

5.3 Metabolomic and mTOR Analysis of LNCaP AI KO and LNCaP OE Cells

Following the same method of metabolomics analysis as for 22Rv1 KO cells derived samples, the metabolome of LNCaP AI SLFN5 KO cells was analysed. The only metabolite affected in both LNCaP AI clones was the amino acid valine (Figure 5-4.a), not found to be altered in the 22Rv1 KO model. As an effective counterpart to this model, LNCaP OE metabolites were therefore analysed (Figure 5-4.b). No further alterations in amino acid levels were found in this model. Some altered metabolites in the LNCaP OE can suggest effects to the

pentose phosphate pathway (NADH and pentose phosphate), but overall, the metabolic alterations in these models do not seem to be as wide and defined as the amino acid depletion observed in the 22Rv1 model.

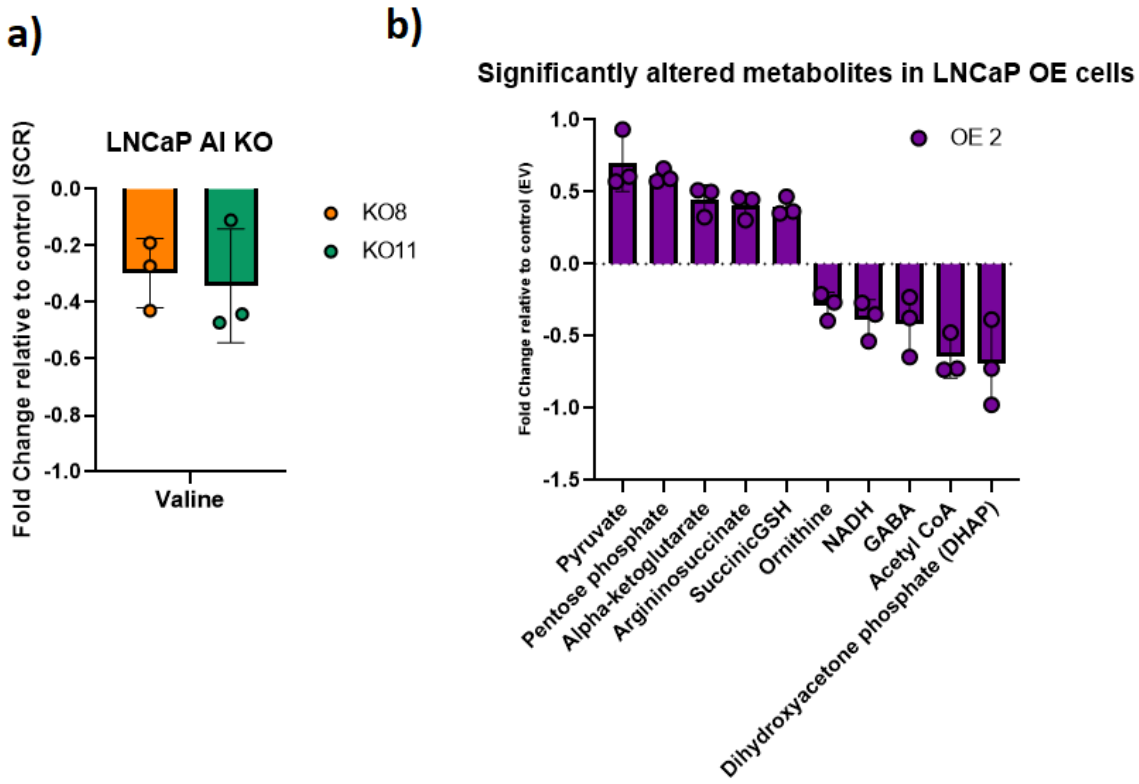

Figure 5-4 - Significantly altered metabolites in LNCaP AI SLFN5 KO and LNCaP OE cells

Metabolites were extracted from three separate wells and analysed separately. Sampling was performed three times on separate seedings to obtain three biological replicates (n=3). Significance was defined as $p < 0.05$ in a Student's t-test comparison of the fold changes relative to the fold changes of the control sample. Fold changes were defined to the average of the normalised intensity for the control sample in each biological replicate. Dots represent the average of each biological replicate, error bars represent Standard Deviation. Figure a) shows significantly altered metabolites in both clones of the LNCaP AI KO model. Figure b) shows significantly altered metabolites in the LNCaP OE2 clone.

Furthermore, when probed for mTOR activity, the LNCaP AI KO model did not present reduced mTOR activation. Contrarily, increased phosphorylation of P70S6K and S6 was observed in the SLFN5 KO LNCaP AI, while total and phosphorylated 4EBP1 remained unaltered. It has been previously characterised that LAT3 is the main LAT transporter in LNCaP, while there is a low basal level of LAT1 expression[185]. Although SLC7a5 expression is higher in LNCaP AI, it might still not be enough to make LNCaP AI a LAT1 dependent model, and therefore

the effects caused by SLFN5 KO in the AI are not comparable to those present on the 22Rv1 model. The data suggest alterations of SLFN5 expression can affect cell metabolism, but its effects are linked with the metabolic characteristics of each particular model. This requires further study into the metabolic needs of the different prostate cancer models as well as in the transcriptional disruptions caused by SLFN5 alteration across several cell lines.

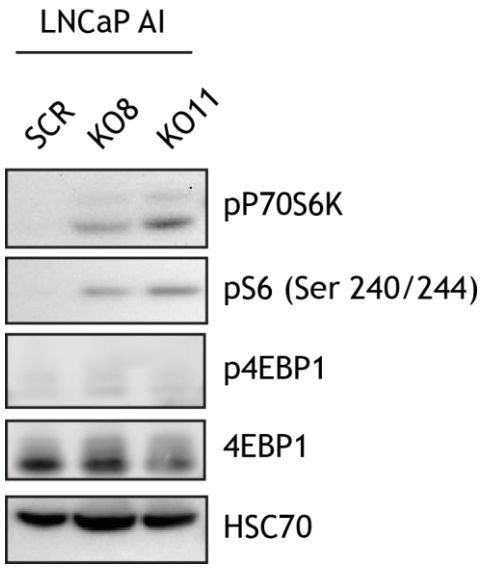

Figure 5-5 – SLFN5 knockout affects mTOR status in LNCaP AI cells

LNCaP AI KO cells were grown in 6 well plates and culture media was renewed 72 hours previous to the sampling to keep nutrient availability consistent between all samples. HSC70 was used as loading control. Shown is a representative Western Blot of an n=3. Re-expression of LAT1 in 22Rv1 SLFN5 KO Cells Rescues mTOR Activation

5.3.1 Re-expression of SLC7a5 increases SLC3a2 levels

Following the observations about the amino acid and mTOR status of the 22Rv1 KO cells along with the intensely reduced expression of LAT1, a rescue model was developed to study the relevance of LAT1 loss in such observations. A plasmid containing the cDNA of MYC-tagged SLC7a5 was introduced into 22Rv1 KO cells to develop stable a stable cell line that lacks SLFN5 expression but expresses LAT1. After monoclonal selection, two distinct clones of MYC-tagged SLC7a5 overexpressing 22Rv1 KO were obtained, named “22Rv1 KO1 7a5” 4B and 252A (Figure 5-6).

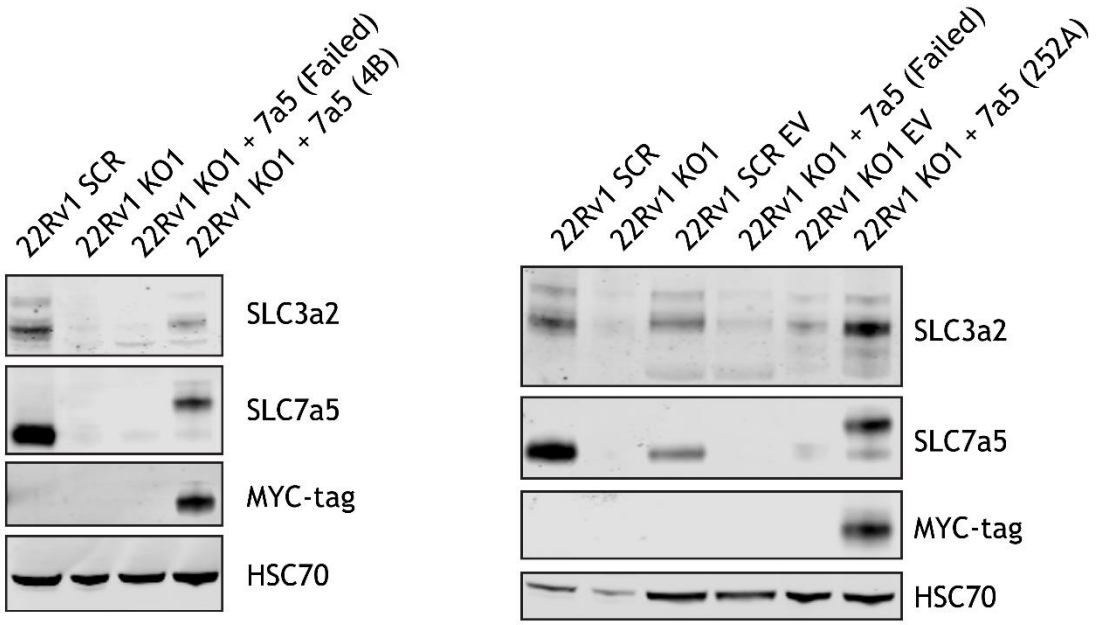

Figure 5-6 – Validation of LAT1 rescued 22Rv1 KO clones

22Rv1 KO1 and 22Rv1 SCR (control) clones were transfected with plasmids containing either an empty vector to serve as control (EV) or MYC-tagged SLC7a5 (7a5) (namely clones 4B and 252A). Failed clone signified the absence of SLC7a5 expression following cell selection. After monoclonal selection and expansion, the clones were surveyed by Western Blot for SLC7a5, SLC3a2 and MYC-tag expression. Clones positive for a successful transfection were defined by MYC-tag expression. HSC70 was used as loading control.

It is interesting to note that reintroduction of SLC7a5 in 22Rv1 KO cells also rescued levels of the SLC3a2 protein. This suggest a direct relation between the expression levels of both components of the LAT1 transporters and supports the rescue of a fully functional LAT1 system.

5.3.2 LAT1 re-expression rescues mTOR activation

Following the successful reintroduction of LAT1 in 22Rv1 KO cells, mTOR status in these cells was probed. As LAT1 is a direct activator of the mTOR system and the 22Rv1 KO cells display functioning LAT1-mTOR signaling, reintroduction of LAT1 could potentially revert the effects SLFN5 KO has on the system. Phosphorylation of mTOR downstream targets P70S6K and S6 showed that mTOR activation was increased following re-expression of LAT1 in 22Rv1 KO cells (Figure 5-7).

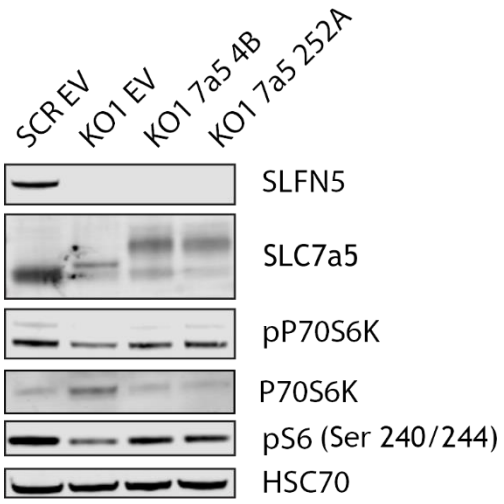

Figure 5-7 – mTORC1 activation is rescued in LAT1 rescued 22Rv1 KO cells

Western Blot shows activation of the mTORC1 pathway as measured by phosphorylation of downstream targets P70S6K and S6. HSC70 was used as loading control, n=2.

5.3.3 Reintroduction of LAT1 does not rescue amino acid levels

As reduced levels of several essential amino acids were shown to occur along with the reduction in mTOR signaling in 22Rv1 KO cells, the rescued mTOR activation that occurs in LAT1 rescued 22Rv1 KO cells could be due to a reestablishment in the intake of those amino acids. Transfected LAT1 could rectify the reduced intracellular availability of amino acids to the cells, which then would result in mTOR activation. Surprisingly, metabolomic analysis of the 22Rv1 KO LAT1 rescued cells showed no restitution of the intracellular amounts of the amino acids of interest (Figure 5-8.a). Furthermore, LAT1 transported amino acids, namely methionine, tyrosine and leucine, were significantly decreased in 22Rv1 KO LAT1 rescued cells in comparison to 22Rv1 KO cells (Figure 5-8.b).

a)

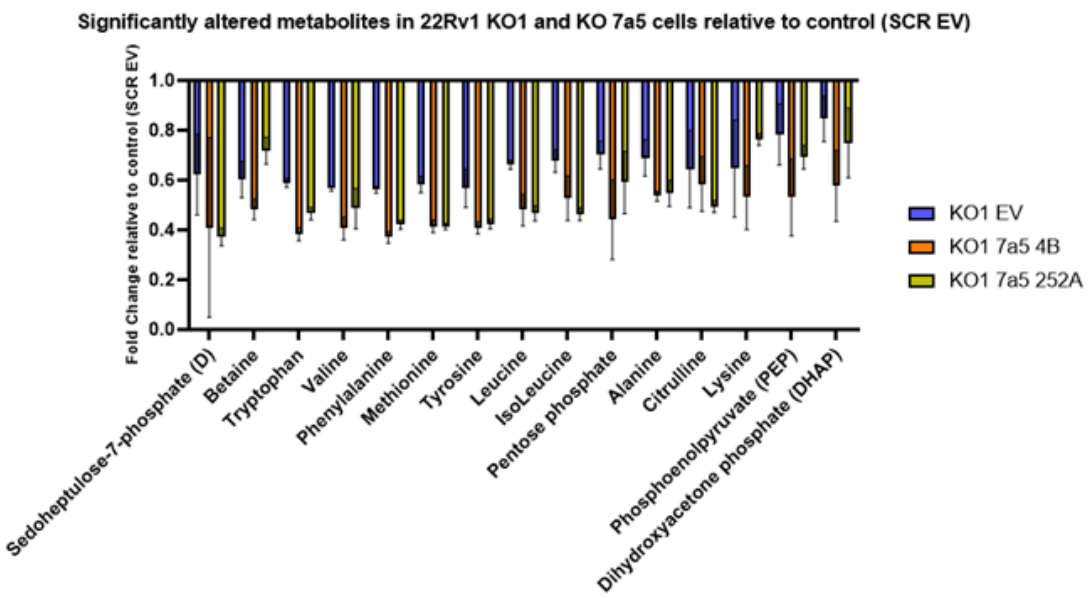

b)

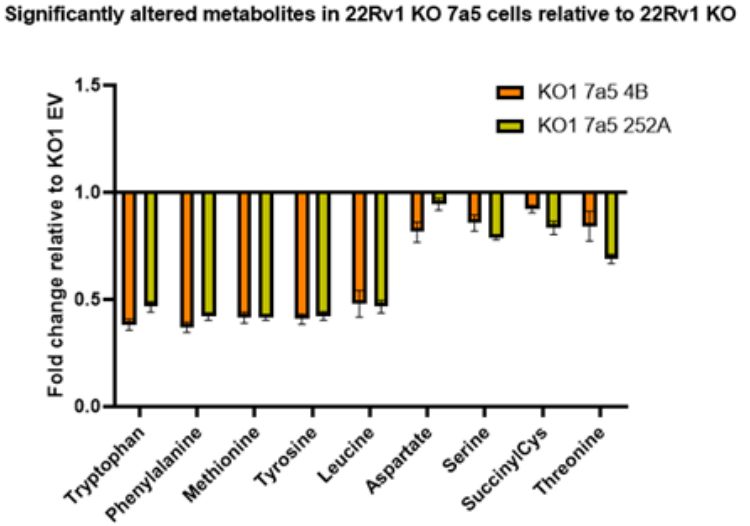

Figure 5-8 – Metabolomic analysis of 22Rv1 KO LAT1 rescued cells

a) Figure shows fold changes for metabolites significantly altered in all samples when compared with the control sample (SCR EV). b) Figure shows fold changes for metabolites significantly altered in 22Rv1 KO LAT1 rescue samples when compared with the SLFN5 KO (KO1 EV). Metabolites were extracted from three separate wells and analysed separately. Sampling was performed three times on separate seedings to obtain three biological replicates (n=3). Significance was defined as $p < 0.05$ in a Student's t-test comparison of the fold changes relative to the control sample. Fold changes were defined to the average of the normalised intensity for the control sample in each biological replicate. Error bars represent Standard Deviation.

Chapter 6 - Discussion

The wide heterogeneity CRPC presents makes adequate management and treatment of the disease currently impossible. For that reason, the identification of biomarkers specifically involved in treatment resistance is essential. Previous work of Dr. Mark Salji focused on identifying the common biochemical characteristics shared by three distinct AR positive CRPC models using proteomics. From his work, the SLFN5 protein was highlighted as commonly upregulated in all three models of CRPC. Until now, this protein had never been studied in the context of prostate cancer. Moreover, the few studies that focused on this protein did not reveal any consistent role for this protein among the cancer types it was studied on.

6.1 SLFN5 expression is affected by perturbations in AR signaling

CRPC is often driven by alterations in AR signalling. The identification of SLFN5 in all three pairs of isogenic hormone naïve and castration resistant orthografts raised the possibility that SLFN5 expression may be modulated by AR function. The initial results of this thesis reveal that the presence or absence of androgens in the culture conditions does affect the expression of SLFN5. Therefore, treatments that aim to reduce circulating levels of androgens (either by stopping the hormonal signalling that leads to endogenous androgen production or by inhibiting key enzymes involved in androgen biosynthesis) will potentially increase SLFN5 levels. In addition, drugs that directly target AR and AR signalling would also cause an increase in tumoural SLFN5 expression, as shown by the treatment of cells with siAR and the higher levels of SLFN5 displayed by LNCaP cells chronically treated with AR inhibitors. Although this regulation of SLFN5 by AR could be expected from the initial observations, these results strengthen the idea of SLFN5 being a key player in the CRPC development process. At the same time, this apparent regulation could be the consequence of processes downstream of AR and not due to direct inhibition of SLFN5 gene expression by the AR. Further studies on short time regulation and confirmation of AR binding to the SLFN5 gene promoter area are needed to clarify the nature of the regulatory relationship.

It is also interesting to discuss why SLFN5 is highly expressed in 22Rv1 cells where the constitutively active AR-V7 variant is present, which suggest that SLFN5 expression should be repressed in these cells. An explanation could be that androgen receptor variants are known to be able to change their regulatory targets resulting in different expression signatures to those of the wild type AR in androgen proficient conditions[80]. This would mean SLFN5 is not a regulation target of the AR-V7 variant in 22Rv1. This is supported by the fact that exogenous DHT is capable of supressing SLFN5 expression, pointing that SLFN5 is susceptible of being repressed by the androgen dependent AR, and the sole presence of the active AR-V7 variant seems not to be enough to supress it.

Finally, to determine the importance of SLFN5 expression in CRPC, its expression was studied in clinical cases of prostate cancer. Using 537 patient samples from the Vancouver Prostate Centre cohort, we determined that an increased expression of SLFN5 correlated with reduced time of disease free survival (as measured by time to PSA recurrence), and cancer aggressiveness (higher Gleason scoring, higher development of metastases, higher mortality). These results provide a strong indication that SLFN5 expression has an actual impact in the severity of prostate cancer and the development of CRPC. Therefore, SLFN5 is confirmed as an important target of study in prostate cancer and CRPC.

6.2 SLFN5 Knockout Models Show SLFN5 drives growth Under Androgen Deprivation

Once the relevance of SLFN5 in CRPC was established, further insight into the biological mechanisms of SLFN5 action was required. Knowing how SLFN5 affects CRPC development is key to ultimately exploit the potential of SLFN5 as a CRPC marker or a therapeutic target. The development of SLFN5 knockout and overexpressing lines provides excellent tools to study the role of this gene in prostate cancer. CRPC cell lines that lack SLFN5 constitute elegant models that allow for easy phenotypic characterisation of the role of SLFN5. In order to generate such models, CRISPR/Cas9 technology was used to delete SLFN5 expression from the CRPC cell lines 22Rv1 and LNCaP AI. Genomic deletion by CRISPR/Cas9 followed by clonal selection allowed for the generation of SLFN5 Knockout (KO) cell lines where SLFN5 protein expression was not detectable. As a counterpart to this model, overexpression of SLFN5 was induced in the

androgen naïve LNCaP using plasmid transfection. Both the KO and overexpressing OE models allowed us to study how prostate cancer cells are affected by the alteration of a single protein.

In vitro characterization studies were then performed the developed models. The growth of SLFN5 KO and OE cells in regular 2D monolayer culture and anchorage independent growth in agar was studied, with LNCaP AI KO cells displaying impaired growth under androgen deprivation and reduced migration capabilities in a trans-well membrane assay. These results showed that SLFN5 can have a phenotypical effect on prostate cancer cells. Interestingly, 22Rv1 KO cells showed similar growth to the control cells *in vitro*, but did not increase in size as *in vivo* orthografts. 22Rv1 KO cells were orthotopically injected into castrated mice, in order to evaluate tumour growth under androgen deprived conditions. Although the 22Rv1 cells that lacked SLFN5 expression were able to establish properly defined tumours, their growth rate severely decreased once they were formed, with KO1 and KO11 tumours averaging 1.04 and 1.08 fold increases respectively at endpoint over their initial volume. Meanwhile, the control 22Rv1 cells were able to double their tumour size during the 7 weeks the experiment was carried for, averaging a 1.91 fold change over their initial size. This meant that SLFN5 knockout affected 22Rv1 cells, but the harsher growth conditions of the *in vivo* orthograft model (when compared to 2D cell culture) were required to notice its impact on cell growth under androgen deprivation.

In the *in vivo* experiment, the average initial and final sizes of the tumours were different between both SLFN5 KO clones (Figure 3-21.b). The size disparity could potentially be the consequence of difficulties in the counting of these cells in preparation for the injection. 22Rv1 cells have a tendency to aggregate when lifted from the surface, which results in inaccurate cell counts. As well, some clones resulted more prone to form clumps of cells, in the end resulting in different number of cells being injected in the same amount of injection volume. For that reason, the initial volume was used to normalise allowing for a consistent measurement over time. After normalisation, the growth trend is consistent and comparable among the clones. Even though control tumours started with an average closer to the KO1 tumours and ended with a similar size to KO11 derived ones, while none of the KO derived tumours significantly

changed size. On top of that, the smaller KO1 tumours showed no significant difference in growth rate to the KO11 tumours ($p = 0.88$, One-way ANOVA).

These *in vivo* results along with the *in vitro* growth experiments indicate that SLFN5 effects on the survival of CRPC are contingent to the growth conditions and the cellular model used. In the case of the LNCaP AI KO, reduced growth could be observed in regular 2D cell culture, while in the 22Rv1 KO cells, the severe conditions of the *in vivo* system were required to observe the effects of SLFN5 depletion. At the same time. the reduced migratory properties of LNCaP AI KO cells also suggest that SLFN5 expression can affect processes beyond cell growth in carcinogenesis. Altogether, eliminating SLFN5 expression in CRPC revealed a role for this protein in prostate cancer cells under androgen deprivation.

6.3 Analysis Of 22Rv1 KO Transcriptome and Proteome Reveals Set of Genes Affected by SLFN5 Knockout

After validating the impact of SLFN5 on cancer growth *in vivo*, it was necessary to investigate the molecular mechanisms underlying SLFN5-driven tumour growth. For that purpose, the 22Rv1 KO model was subjected to unbiased transcriptomic analysis. The transcriptome of 22Rv1 KO cells, both grown *in vitro* as a monolayer and *in vivo* as orthografts was analysed. In order to find which of the genes were consistently affected the by SLFN5 knockout, a list of transcripts that were potentially regulated by SLFN5 in both KO cell lines and across both growth conditions was obtained. A further selection of top targets affected by SLFN5 KO was validated by PCR. To study how the observed transcript alterations reflected into protein expression, proteomic analysis of the 22Rv1 KO derived orthograft was further performed. This added another layer of confidence to the transcriptomic results and narrowed down the targets of interest. When the transcriptomic and proteomic results were compared, a list of 9 potential regulation targets whose transcript and protein levels were significantly altered across all the models studied was defined.

It is notable that 52 out of the 64 genes (81%) included in the final list of affected transcripts had reduced expression in the KO cells (Table 4-2). This

trend was exacerbated when the proteomic analysis was combined the transcriptomic data, where 8 out of the 9 genes that were found to be significantly altered saw their levels reduced (Table 4-5). This data suggest that the regulatory role of SLFN5 in prostate cancer is more likely to positively regulate the expression of other genes rather than act as a repressor as has been described in the literature in other biological contexts[118].

As SLFN5 localises in the nucleus and has a domain predicted to interact with DNA or RNA, there was a possibility of SLFN5 acting as a regulator of gene expression (by affecting gene transcription or through a direct interaction with transcripts). To study the short-term effects of SLFN5 depletion on gene transcription, silencing experiments with siRNA were conducted on wild type 22Rv1 cells, focusing on genes that were highly affected by SLFN5 knockout. Although it was observed that 3 of the studied genes (*SLC7a5*, *KCNH5*, *NCMAP*) saw their transcript levels reduced, the transcript levels of 2 of them (*NDNF* and *TFPI*) were increased after treatment. This discrepancy suggests the regulation of these genes by SLFN5 might involve other factors, require deeper transcriptome changes or a complete depletion of SLFN5. The short term and limited reduction in SLFN5 levels caused by the siRNA treatment seems not enough to mirror the effects of the full depletion caused by the CRISPR knockout.

6.4 Correlation Between SLFN5 and LAT1 Expression is Validated Across Several Models of Prostate Cancer

Interestingly, among the genes affected at both transcript and protein level two proteins whose function is highly intertwined were found; The LAT1 transporter components SLC7a5 and SLC3a2. As described in the introduction chapter, these two proteins dimerize with each other to form the LAT1 amino acid transporter. This transporter has been found to be expressed in several types of cancer, including prostate cancer. LAT1 expression has been found to correlate with faster time to develop CRPC[186] and with high Gleason score[184], similar to what was observed about SLFN5. Furthermore, a study describing LAT1 over-expression following androgen deprivation postulates that LAT1 becomes the main amino acid transporter in CRPC[185], overtaking the related transporter LAT3.

This encouraged us to further study the relation between SLFN5 and LAT1 expression.

To validate the relationship between LAT1 and SLFN5, protein levels of LAT1 were assessed across several SLFN5 KO, OE and wild type prostate cancer models by Western Blot. As expected from the omic analyses, the protein levels of SLC7a5 and SLC3a2 were considerably lower in the 22Rv1 SLFN5 knockout, both when cultured *in vitro* and *in vivo* as orthografts. In the LNCaP AI KO model, SLC7a5 protein was severely reduced as well. Interestingly, exogenous overexpression of SLFN5 also caused increased levels of SLC7a5 in the LNCaP OE model, but only when SLFN5 was shown to localise on the nucleus. This suggests the nuclear localisation of SLFN5 is required for it to perform its regulatory functions. Finally, when wild type prostate cancer cells were probed for SLFN5 and SLC7a5 expression, it was found that SLC7a5 protein was more abundant in the CRPC cell lines and tumours, in correlation with SLFN5 expression. These results validated the induction of LAT1 expression caused by SLFN5 in different models of prostate cancer.

6.5 ATF4 Participates on SLFN5-Mediated LAT1 Regulation

To further inquire in the regulatory mechanism of SLFN5, interaction with transcription factors MYC and ATF4 was considered. This was a possibility, as SLFN5 has been previously reported to act as a corepressor of transcription factor STAT1[123], and its nuclear localisation seems to be a requirement to induce SLC7a5 expression in the LNCaP OE model. At the same time, these transcription factors have both been described previously as drivers of LAT1 expression in a prostate cancer context[185,203]. This suggest the idea of SLFN5 regulating LAT1 expression trough interaction with one of these transcription factors. To assess if ATF4 or MYC were involved in the alterations caused by SLFN5 knockout, 22Rv1 cells were treated with siRNA against both transcription factors and the transcript levels of several top targets were measured.

Interestingly, treatment with MYC siRNA did not decrease the transcript levels of any of the studied genes, but significantly increased *NCCRP1*, *NDNF*, *ORAI2*, *NCMAP* and *TFPI* expression. This suggests a suppressor role for MYC over SLFN5

KO affected genes, which makes it behave in regulatory terms opposite to SLFN5. This is an interesting discovery, as SLFN5 might be part of the ATF4 counterbalance to MYC driven growth[205], or even constitute an entire alternative route for non-MYC driven CRPC. Finally, *SLC7a5* mRNA levels were not affected by *MYC* suppression in the 22Rv1 models, only being significantly altered when *SLFN5* expression was being repressed as well. Overall, these results rule out MYC as a participant in the LAT1 regulation by SLFN5.

On the other hand, results showed that silencing of *ATF4* alone or together with *SLFN5* brings the levels of *SLC7a5* transcript down by 50% or more in that same 72 hours, with 5 other genes affected by SLFN5 KO also being significantly altered by the siATF4 treatment (*KCNH5*, *NDNF*, *ORAI2*, *NCMAP* and *TFPI)*. This meant there was an overlap between the genes affected by SLFN5 depletion and genes affected by transient silencing of ATF4. To further inquire the nature of the SLFN5-ATF4 relationship, a collaborative effort with Dr. Paul Peixoto from Université Bourgogne Franche-Comté was established. Predicted ATF4 binding sites were found with high confidence ($p < 0.0001$) in 15 out of the 26 most affected genes by SLFN5 KO, further reinforcing the involvement of ATF4. Finally, a proximity ligation assay demonstrated that ATF4 and SLFN5 interacted with each other in the nucleus of 22Rv1 cells. These results strongly suggest that SLFN5 is capable of driving expression of SLC7a5 by acting as a coactivator of ATF4. Further ChiP studies will help to demonstrate this hypothesis, evidencing potential interaction sites at the promoter of SLC7a5 and other genes affected by SLFN5 knockout.

6.6 SLFN5 KO Affects the Metabolism of 22Rv1 Cells

The LAT1 transporter is described to have two main roles: intake of amino acids into the cell[207] and sensing intracellular amino acid levels to induce activation of mTORC1[144]. Both roles fundamentally allow the cell to obtain nutrients that cannot be synthesized *de novo* (such as essential amino acids) and engage the growth signalling machinery to stimulate cell growth and division. We therefore thought that SLFN5 knockout could affect mTOR activation in 22Rv1 cells with such depressed levels of this transporter. To investigate the status of mTOR signalling in the 22Rv1 KO cells, the phosphorylation of mTORC1 downstream

targets was measured. Western blot experiments demonstrated the reduced activation of mTOR signalling, as evidenced by the reduced phosphorylation of P70S6Ka, S6 and AKT (T308[208]), and increased levels of unphosphorylated 4EBP1.

It is interesting to discuss the relation between AKT and mTOR. The mTORC1 sits downstream of AKT and continues the phosphorylation chain through P70S6K and then S6. At the same time, a feedback loop downstream of mTORC1 acting through of mTORC2 reduces AKT phosphorylation and activation[209]. As both mTOR and AKT activation seem to be affected by SLFN5 knockout, this opens the possibility that SLFN5 might be promoting AKT activation and mTOR activation as a result. This could expand the promalignant effects of this protein beyond alterations of the mTOR pathway. AKT plays an important role in cell signalling beyond mTORC1 activation. Activated AKT by itself supresses apoptosis by blocking pro-apoptotic elements FOXO and Bad, which could further reinforce the survival capabilities of SLFN5 expressing CRPC cells[210]. Even though LAT1 affects mTORC1 activation, future studies about a directrelation between SLFN5 and AKT could provide insight into novel effects of SLFN5 overexpression.

At the same time, while a reduced mTORC1 activation is observed in downstream proteins, 22Rv1 KO cells do not show any significant proliferation defect when cultured *in vitro*. This could be potentially attributed to the lower activation level that remains being enough to carry the cell growth in *in vitro* conditions, but not enough for *in vivo*. It can be that mTORC1 activation is not a cornerstone for the survival of these cells but rather a system that encourages further growth under unfavourable circumstances, such as the more restrictive environment of the *in vivo* orthograft setting. That could explain why 22Rv1 KO tumours, even though their size increase was marginal, they still were well constituted and alive tumours.

The observed mTOR signalling reduction could be indicative of metabolic issues, particularly in cells with decreased levels of LAT1. In order to study the metabolic status of the 22Rv1 KO cells, metabolomic analysis was performed on these cells. The analysis revealed the 22Rv1 KO present reduced levels of several essential amino acids, including leucine. Leucine is also one of the main amino acids sensed by the mTOR machinery to engage mTORC1 signalling, with LAT1 being a participant of such system[143]. Consequently, both the reduced

intracellular levels of EAA and the inability to amino acid sensing machinery in the lysosome could be the cause of the hindered mTOR activation.

Altogether, these data suggest that the growth arrest observed in the 22Rv1 KO tumours could be the consequence of the metabolic struggle caused by insufficient amino acid uptake and mTOR driven growth signalling. The Effects of SLFN5 Expression are Different from 22Rv1 in The LNCaP and AI Models

When the metabolite levels of the LNCaP AI KO and LNCaP OE models were probed, no alteration was found in the amino acids affected in the 22Rv1 KO model. At the same time, the LNCaP AI KO showed increased mTOR activation, in contradiction to what was observed in the 22Rv1 KO model. This discrepancy could be explained by a reduced reliance in LAT1. While SLC7a5 expression in these models has been shown to correlate with levels of SLFN5, the observed increase in LAT1 could not be enough to transform the LNCaP AI and LNCaP OE into LAT1 dependant models. When compared to the 22Rv1 cells, the observed levels of SLC7a5 in these cells are low, and SLC3a2 is not detectable. Moreover, LNCaP cells have been characterised as reliant in the LAT3 transporter for amino acid intake and mTOR activation[185], while in the same study, LAT1 dependence was observed only in the AR negative PC3 cell line and in hormone ablated tissue. The LNCaP AI on the other hand, were derived from LNCaP by continued in vitro culture in absence of androgens, and express similar levels of AR as LNCaP[105]. While able to grow in androgen deprived conditions, the accuracy with which the AI model can parallel a CRPC phenotype similar to that undergone by tumours might not be entirely accurate. Overall, further phenotypic studies of these models would benefit the characterization of SLFN5 in CRPC, as it can potentially reveal new roles enabled by the molecular context of LNCaP and LNCaP AI.

These results are a reminder that the heterogeneity of CRPC is a complex issue, and even strong shared events such as SLFN5 overexpression do not necessarily result in common alterations. This idea is further reinforced by observations such as the nature of the SLFN5-ATF4 interaction. This is a reminder that the effects produced by one single gene are usually dependant on its interaction, direct or indirect, with a complex network of associated genes. For that reason, divergent results can be obtained depending on the genetic context of the

studied model. Albeit SLFN5 is overexpressed in the CRPC models studied, not all the same downstream mechanisms might be engaged across all models.

6.7 Reintroduction of LAT1 Expression Rescues mTOR Activation

To address which effects observed in the 22Rv1 KO models were caused by the SLFN5-driven LAT1 depletion, SLC7a5 was genetically reintroduced into the KO cells. 22Rv1 cells that lacked SLFN5 expression, but whose LAT1 levels had been rescued were generated and named 22Rv1 KO 7a5. This model allowed us to evaluate the SLFN5 effects that were dependent on LAT1.

Interestingly, the introduction of SLC7a5 caused the cells to rescue their levels of SLC3a2 as well (Figure 5-6). Regarding the nature of the regulation of SLC3a2 by SLC7a5, not much is known to date. From what has been observed in these SLC7a5 rescue models, it is suggested that SLC7a5 can regulate SLC3a2, or at least, that SLC7a5 is required for SLC3a2 to be expressed. One possibility is that SLC3a2 protein is degraded when not complexed with SLC7a5 to form LAT1. At the same time, transcript levels of *SLC3a2* are also profoundly affected along *SLC7a5* transcript levels in the SLFN5 KO models, indicating that it is a possibility that SLC7a5 regulates *SLC3a2* gene expression. Short-term SLC7a5 re-expression in these models could provide further insight on the nature of such regulation.

When activation of the mTOR pathway was measured in the 22Rv1 KO 7a5 cells, it was shown that the reintroduction of LAT1 rescued mTOR activation, as measured by the increased phosphorylation of its downstream targets. On the other hand, metabolomic analysis showed that the amino acid levels of the LAT1 rescued cells were not back to normal, and instead, were even lower in the LAT1 re-expressing cells. To address the apparent disparity of both observations an explanation of how LAT1 affects mTOR activation is required. The way LAT1 participates in mTOR activation is by taking cytoplasmatic leucine and introducing it into the lysosomal lumen, where it is sensed by a compound system of proteins, resulting in mTORC1 translocation to the lysosomal surface and its subsequent activation[140]. Observing the 22Rv1 KO cells, where levels of leucine and other essential amino acids are low and mTOR activation is hindered, it seemed obvious to attribute the latter to the former. But the

observation that mTOR activation can be rescued while intracellular amino acids remain low requires further consideration. As explained before, these results could mean that LAT1 is not the main amino acid importer in these cells, and other uncharacterized accessory systems might be performing the majority of the amino acid uptake. Still, amino acid uptake in 22Rv1 KO cells is impaired and further analysis and characterization is required to determine the cause of the diminished amino acid levels in these cells. A complementary explanation of the reduced amino acid levels on the mTOR active 22Rv1 KO 7a5 could be increased consumption of these amino acids, as one of the main consequences of mTOR signalling activation is increased proteogenesis. If the 22Rv1 KO 7a5 cells reactivate their translation machinery due to LAT1 mediated mTORC1 activation while the amino acid import machinery remains weak, this can lead to further reduced levels of amino acids in the cells. A steady state where amino acid consumption increases more than the intake can cause reduced levels of free amino acids. To determine the validity of this hypothesis, further experiments comparing the protein synthesis rate and free amino acid consumption of these cells should be conducted.

Although SLFN5 has been shown to directly affect mTOR signalling through LAT1 expression, it is necessary to validate the impaired mTOR activation caused by LAT1 loss as the cause of the reduced tumour growth. In order to achieve that, a subsequent *in vivo* orthograft experiment mirroring the one performed with the 22Rv1 KO using the LAT1 rescued 22Rv1 KO model should be undertaken.

6.8 Final Remarks

Going forward, the study of SLFN5 in CRPC should not be confined to the 22Rv1 model. Indeed, SLFN5 is overexpressed in different CRPC models and clinical data indicates SLFN5 is a significant player in castration resistance. The LNCaP OE and LNCaP AI KO models have been observed to behave differently to the 22Rv1 models in some aspects, but still, antioncogenic behaviours such as reduced cell growth and migration have been observed in the LNCaP AI KO. An in-depth characterization of these models, similar to the workflow followed for the 22Rv1 KO should shed light on potential additional roles for SLFN5 beyond mTOR related signalling. A comparison between the transcriptomes of LNCAP AI KO and LNCaP OE should prove interesting and yield reliable targets of study.

Genes whose expression is altered by SLFN5 knockout in both models would potentially be strong SLFN5 regulation targets and provide further insight into the regulome of SLFN5. *In vivo* growth experiments should also be considered, with the added strength of having a "rescue model"; LNCaP OE. This model would be useful to determine if introducing SLFN5 to a hormone naïve cell line can facilitate tumour growth under androgen deprivation, thus supporting the observation that a high SLFN5 expression correlates with reduced time to develop CRPC.

In conclusion, SLFN5 has been characterised as a novel actor in CRPC development and a significant player in prostate cancer progression under androgen deprivation. At the same time, the validation of SLFN5 as an important protein in CRPC strongly demonstrates the potential of multi-model screening studies, particularly in highly heterogeneous pathologies such as castration resistant prostate cancer. SLFN5 is a promising target, and further prostate cancer models should be incorporated to broaden the insight into the roles of this protein and properly define its effects in prostate cancer. This way, detection of SLFN5 driven CRPC could be a helpful tool in the clinic by providing a well characterized subpopulation to manage and treat.

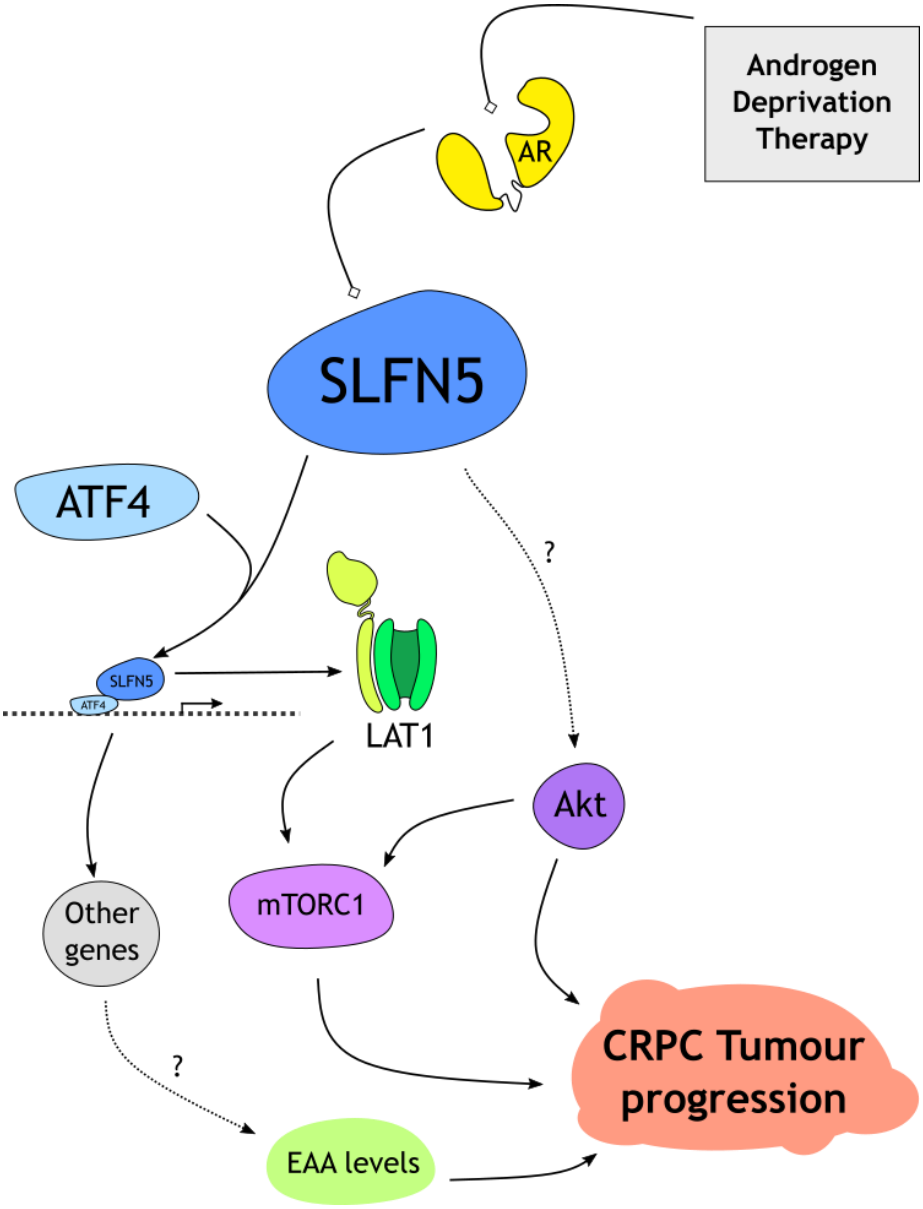

Figure 6-1 – Purposed working model for SLFN5 in CRPC progression.

Chapter 7 - List of References

1. Komura, K. *et al*. Current treatment strategies for advanced prostate cancer. *Int. J. Urol.* **25**, 220–231 (2018).
2. UK, C. R. Prostate cancer statistics. (2017).
3. Grozescu, T. & Popa, F. Prostate cancer between prognosis and adequate/proper therapy. *J. Med. Life* **10**, 5–12 (2017).
4. Goldgar, D. E., Easton, D. F., Cannon-albright, L. A. & Skolnick, M. H. Systematic population-based assessment of cancer risk in first-degree relatives of cancer probands. *J. Natl. Cancer Inst.* **86**, 1600–1608 (1994).
5. Schaid, D. J. The complex genetic epidemiology of prostate cancer. *Hum. Mol. Genet.* **13**, 103R – 121 (2004).
6. Cheng, H. H., Sokolova, A. O., Schaeffer, E. M., Small, E. J. & Higano, C. S. Germline and somatic mutations in prostate cancer for the clinician. *JNCCN J. Natl. Compr. Cancer Netw.* **17**, 515–521 (2019).
7. Rajab, T. K., Bordeianou, L. G., von Keudell, A., Rajab, H. & Zhou, H. Digital Rectal Examination and Anoscopy. *N. Engl. J. Med.* **378**, e30 (2018).
8. Naji, L. *et al*. Digital rectal examination for prostate cancer screening in primary care: A systematic review and meta-analysis. *Ann. Fam. Med.* **16**, 149–154 (2018).
9. Okotie, O. T. *et al*. Characteristics of Prostate Cancer Detected by Digital Rectal Examination Only. *Urology* **70**, 1117–1120 (2007).
10. Rao, A. R., Motiwala, H. G. & Karim, O. M. A. The discovery of prostate-specific antigen. *BJU Int.* **101**, 5–10 (2008).
11. Kim, E. H. & Andriole, G. L. Prostate-specific antigen-based screening: Controversy and guidelines. *BMC Med.* **13**, (2015).
12. Nguyen-Nielsen, M. & Borre, M. Diagnostic and Therapeutic Strategies for Prostate Cancer. *Semin. Nucl. Med.* **46**, 484–490 (2016).
13. Turkbey, B. *et al*. Prostate Imaging Reporting and Data System Version 2.1: 2019 Update of Prostate Imaging Reporting and Data System Version 2. *Eur. Urol.* **76**, 340–351 (2019).
14. Li, R. *et al*. The use of PET/CT in prostate cancer. *Prostate Cancer Prostatic Dis.* **21**, 4–21 (2018).
15. Epstein, J. I. *et al*. The 2014 international society of urological pathology (ISUP) consensus conference on gleason grading of prostatic carcinoma definition of grading patterns and proposal for a new grading system. *Am. J. Surg. Pathol.* **40**, 244–252 (2016).
16. Stark, J. R. *et al*. Gleason score and lethal prostate cancer: Does 3 + 4 = 4 + 3? *J. Clin. Oncol.* **27**, 3459–3464 (2009).
17. Epstein, J. I. *et al*. A Contemporary Prostate Cancer Grading System: A Validated Alternative to the Gleason Score. *Eur. Urol.* **69**, 428–435 (2016).
18. Knudsen, B. S. *et al*. Application of a Clinical Whole-Transcriptome Assay for Staging and Prognosis of Prostate Cancer Diagnosed in Needle Core Biopsy Specimens. *J. Mol. Diagnostics* **18**, 395–406 (2016).
19. Laudicella, R. *et al*. 18 F-Facbc in Prostate Cancer: A Systematic Review and Meta-Analysis. *Cancers (Basel).* **11**, 1348 (2019).
20. Heinlein, C. A. & Chang, C. Androgen receptor in prostate cancer. *Endocr. Rev.* **25**, 276–308 (2004).
21. Deslypere, J. P., Young, M., Wilson, J. D. & McPhaul, M. J. Testosterone and 5α-dihydrotestosterone interact differently with the androgen receptor to enhance transcription of the MMTV-CAT reporter gene. *Mol.*

Cell. Endocrinol. **88**, 15–22 (1992).
22. Dai, C., Heemers, H. & Sharifi, N. Androgen signaling in prostate cancer. *Cold Spring Harb. Perspect. Med.* **7**, (2017).
23. Eisermann, K. & Fraizer, G. The androgen receptor and VEGF: Mechanisms of androgen-regulated angiogenesis in prostate cancer. *Cancers (Basel).* **9**, 1–10 (2017).
24. Jenster, G. *et al.* Domains of the human androgen receptor involved in steroid binding, transcriptional activation, and subcellular localization. *Mol. Endocrinol.* **5**, 1396–1404 (1991).
25. Smith, D. F. & Toft, D. O. The intersection of steroid receptors with molecular chaperones: Observations and questions. *Mol. Endocrinol.* **22**, 2229–2240 (2008).
26. Simental, J. A., Sar, M., Lane, M. V., French, F. S. & Wilson, E. M. Transcriptional activation and nuclear targeting signals of the human androgen receptor. *J. Biol. Chem.* **266**, 510–518 (1991).
27. Choong, C. S. & Wilson, E. M. Trinucleotide repeats in the human androgen receptor: A molecular basis for disease. *J. Mol. Endocrinol.* **21**, 235–257 (1998).
28. Platz, E. A. Racial Variation in Prostate Cancer Incidence and in Hormonal System Markers Among Male Health Professionals. *J. Natl. Cancer Inst.* **92**, 2009–2017 (2000).
29. Hur, E. *et al.* Recognition and accommodation at the androgen receptor coactivator binding interface. *PLoS Biol.* **2**, (2004).
30. Callewaert, L., Van Tilborgh, N. & Claessens, F. Interplay between two hormone-independent activation domains in the androgen receptor. *Cancer Res.* **66**, 543–553 (2006).
31. Roche, P. J., Hoare, S. A. & Parker, M. G. A consensus dna-binding site for the androgen receptor. *Mol. Endocrinol.* **6**, 2229–2235 (1992).
32. Schoenmakers, E. *et al.* Differential DNA binding by the androgen and glucocorticoid receptors involves the second Zn-finger and a C-terminal extension of the DNA-binding domains. *Biochem. J.* **341**, 515–21 (1999).
33. Jenster, G., van der Korput, H. A., Trapman, J. & Brinkmann, A. O. Identification of two transcription activation units in the N-terminal domain of the human androgen receptor. *J. Biol. Chem.* **270**, 7341–7346 (1995).
34. Zhou, Z. X., Sar, M., Simental, J. A., Lane, M. V. & Wilson, E. M. A ligand-dependent bipartite nuclear targeting signal in the human androgen receptor. Requirement for the DNA-binding domain and modulation by NH2-terminal and carboxyl-terminal sequences. *J. Biol. Chem.* **269**, 13115–13123 (1994).
35. Ozanne, D. M. *et al.* Androgen Receptor Nuclear Translocation Is Facilitated by the Protein Filamin. 1618–1626 (2015).
36. Saporita, A. J. *et al.* Identification and Characterization of a Ligand-regulated Nuclear Export Signal in Androgen Receptor. *J. Biol. Chem.* **278**, 41998–42005 (2003).
37. Tan, M. E., Li, J., Xu, H. E., Melcher, K. & Yong, E. L. Androgen receptor: Structure, role in prostate cancer and drug discovery. *Acta Pharmacol. Sin.* **36**, 3–23 (2015).
38. Bennett, N. C., Gardiner, R. A., Hooper, J. D., Johnson, D. W. & Gobe, G. C. Molecular cell biology of androgen receptor signalling. *Int. J. Biochem. Cell Biol.* **42**, 813–827 (2010).
39. Jha, S. K. *et al.* KLK3 / PSA and cathepsin D activate. *Elife* **1**, 1–30 (2019).
40. Cao, X. *et al.* Regulator of G-protein signaling 2 (RGS2) inhibits androgen-

independent activation of androgen receptor in prostate cancer cells. *Oncogene* **25**, 3719–3734 (2006).
41. Gioeli, D. *et al*. Androgen receptor phosphorylation. Regulation and identification of the phosphorylation sites. *J. Biol. Chem.* **277**, 29304–29314 (2002).
42. Rochette-Egly, C. Nuclear receptors: Integration of multiple signalling pathways through phosphorylation. *Cell. Signal.* **15**, 355–366 (2003).
43. Nazareth, L. V. & Weigel, N. L. Activation of the human androgen receptor through a protein kinase A signaling pathway. *J. Biol. Chem.* **271**, 19900–19907 (1996).
44. Klokk, T. I. *et al*. Ligand-Specific Dynamics of the Androgen Receptor at Its Response Element in Living Cells. *Mol. Cell. Biol.* **27**, 1823–1843 (2007).
45. Gritsina, G., Gao, W.-Q. & Yu, J. Transcriptional repression by androgen receptor: roles in castration-resistant prostate cancer. *Asian J. Androl.* **21**, 215–223 (2019).
46. He, B., Kemppainen, J. A., Voegel, J. J., Gronemeyer, H. & Wilson, E. M. Activation function 2 in the human androgen receptor ligand binding domain mediates interdomain communication with the NH2-terminal domain. *J. Biol. Chem.* **274**, 37219–37225 (1999).
47. Gaughan, L., Logan, I. R., Neal, D. E. & Robson, C. N. Regulation of androgen receptor and histone deacetylase 1 by Mdm2-mediated ubiquitylation. *Nucleic Acids Res.* **33**, 13–26 (2005).
48. Bill-Axelson, A. *et al*. Radical prostatectomy or watchful waiting in early prostate cancer. *N. Engl. J. Med.* **370**, 932–942 (2014).
49. Wilt, T. J. *et al*. Radical Prostatectomy versus Observation for Localized Prostate Cancer. *N. Engl. J. Med.* **367**, 203–213 (2012).
50. Filson, C. P., Marks, L. S. & Litwin, M. S. Expectant management for men with early stage prostate cancer. *CA. Cancer J. Clin.* **65**, 264–282 (2015).
51. Dearnaley, D. *et al*. Conventional versus hypofractionated high-dose intensity-modulated radiotherapy for prostate cancer: 5-year outcomes of the randomised, non-inferiority, phase 3 CHHiP trial. *Lancet Oncol.* **17**, 1047–1060 (2016).
52. Gordon, L., Dickinson, A. & Offredy, M. Information in radiotherapy for men with localised prostate cancer: An integrative review. *Eur. J. Cancer Care (Engl).* **28**, 1–21 (2019).
53. Veiby Holm, H., Dahl, A. A., Harald Klepp, O. & Fosså, S. D. Modern treatment of metastatic prostate cancer. *Tidsskr Nor Legeforen nr* **11**, 803–6 (2017).
54. Anheuser, P., Kranz, J., Will, J. & Dieckmann, K. P. Komplikationen bei inguinaler ablatio testis und skrotaler orchiektomie. *Urol. - Ausgabe A* **53**, 676–682 (2014).
55. Schally, A. V., Block, N. L. & Rick, F. G. Discovery of LHRH and development of LHRH analogs for prostate cancer treatment. *Prostate* **77**, 1036–1054 (2017).
56. Kittai, A. S., Blank, J. & Graff, J. N. Gonadotropin-Releasing Hormone Antagonists in Prostate Cancer. *Oncology (Williston Park).* **32**, 599-602,604-606 (2018).
57. Crawford, E. D. & Hou, A. H. The role of LHRH antagonists in the treatment of prostate cancer. *Oncology (Williston Park).* **23**, 626–630 (2009).
58. Attard, G., Belldegrun, A. S. & De Bono, J. S. Selective blockade of androgenic steroid synthesis by novel lyase inhibitors as a therapeutic strategy for treating metastatic prostate cancer. *BJU Int.* **96**, 1241–1246

(2005).
59. Chen, Y., Clegg, N. & Scher, H. Antiandrogens and androgen depleting therapies in prostate cancer: novel agents for an established target. *Lancet Oncol.* **10**, 981–991 (2010).
60. Tran, C. *et al.* Development of a second-generation antiandrogen for treatment of advanced prostate cancer. *Science (80-.).* **324**, 787–790 (2009).
61. Hussain, M. *et al.* Enzalutamide in Men with Nonmetastatic, Castration-Resistant Prostate Cancer. *N. Engl. J. Med.* **378**, 2465–2474 (2018).
62. Nader, R., El Amm, J. & Aragon-Ching, J. B. Role of chemotherapy in prostate cancer. *Asian J. Androl.* **20**, 221–229 (2018).
63. Lohiya, V., Aragon-Ching, J. B. & Sonpavde, G. Role of Chemotherapy and Mechanisms of Resistance to Chemotherapy in Metastatic Castration-Resistant Prostate Cancer. *Clin. Med. Insights Oncol.* **10s1**, 57–66 (2016).
64. Heidenreich, A. *et al.* EAU guidelines on prostate cancer. Part II: Treatment of advanced, relapsing, and castration-resistant prostate cancer. *Eur. Urol.* **65**, 467–479 (2014).
65. Mostaghel, E. A. & Nelson, P. S. Intracrine androgen metabolism in prostate cancer progression: mechanisms of castration resistance and therapeutic implications. *Best Pract. Res. Clin. Endocrinol. Metab.* **22**, 243–258 (2008).
66. Cai, C. & Balk, S. P. Intratumoral androgen biosynthesis in prostate cancer pathogenesis and response to therapy. *Endocr Relat Cancer* **53**, 820–833 (2009).
67. Ceder, Y. *et al.* The Molecular Evolution of Castration-resistant Prostate Cancer. *Eur. Urol. Focus* **2**, 506–513 (2016).
68. Waltering, K. K. *et al.* Increased expression of androgen receptor sensitizes prostate cancer cells to low levels of androgens. *Cancer Res.* **69**, 8141–8149 (2009).
69. Koivisto, P. *et al.* Androgen receptor gene amplification: A possible molecular mechanism for androgen deprivation therapy failure in prostate cancer. *Cancer Res.* **57**, 314–319 (1997).
70. Linja, M. J. *et al.* Amplification and overexpression of androgen receptor gene in hormone-refractory prostate cancer. *Cancer Res.* **61**, 3550–3555 (2001).
71. Visakorpi, T. *et al.* In vivo amplification of the androgen receptor gene and progression of human prostate cancer. *Nat. Genet.* **9**, 401–406 (1995).
72. Kawata, H. *et al.* Prolonged treatment with bicalutamide induces androgen receptor overexpression and androgen hypersensitivity. *Prostate* **70**, 745–754 (2010).
73. Veldscholte, J. *et al.* A mutation in the ligand binding domain of the androgen receptor of human LNCaP cells affects steroid binding characteristics and response to anti-androgens. *Biochem. Biophys. Res. Commun.* **173**, 534–540 (1990).
74. Zhao, X. Y. *et al.* Two mutations identified in the androgen receptor of the new human prostate cancer cell line MDA PCa 2a. *J. Urol.* **162**, 2192–2199 (1999).
75. Zhao, X. Y. *et al.* Glucocorticoids can promote androgen-independent growth of prostate cancer cells through a mutated androgen receptor. *Nat. Med.* **6**, 703–706 (2000).
76. Hara, T. *et al.* Novel mutations of androgen receptor: A possible mechanism of bicalutamide withdrawal syndrome. *Cancer Res.* **63**, 149–153 (2003).

77. Balbas, M. D. *et al*. Overcoming mutation-based resistance to antiandrogens with rational drug design. *Elife* **2013**, 1–21 (2013).
78. Culig, Z. *et al*. Mutant androgen receptor detected in an advanced-stage prostatic carcinoma is activated by adrenal androgens and progesterone. *Mol. Endocrinol.* **7**, 1541–1550 (1993).
79. Dehm, S. M. & Tindall, D. J. Alternatively spliced androgen receptor variants. *Endocr. Relat. Cancer* **18**, 183–196 (2011).
80. Shafi, A. A., Yen, A. E. & Weigel, N. L. Androgen receptors in hormone-dependent and castration-resistant prostate cancer. *Pharmacol. Ther.* **140**, 223–238 (2013).
81. Hu, R. *et al*. Ligand-independent androgen receptor variants derived from splicing of cryptic exons signify hormone-refractory prostate cancer. *Cancer Res.* **69**, 16–22 (2009).
82. Guo, Z. *et al*. A novel androgen receptor splice variant is up-regulated during prostate cancer progression and promotes androgen depletion-resistant growth. *Cancer Res.* **69**, 2305–2313 (2009).
83. Sun, S. *et al*. Castration resistance in human prostate cancer is conferred by a frequently occurring androgen receptor splice variant. *J. Clin. Invest.* **120**, 2715–2730 (2010).
84. Jagla, M. *et al*. A splicing variant of the androgen receptor detected in a metastatic prostate cancer exhibits exclusively cytoplasmic actions. *Endocrinology* **148**, 4334–4343 (2007).
85. Tatarov, O. *et al*. Src family kinase activity is up-regulated in hormone-refractory prostate cancer. *Clin. Cancer Res.* **15**, 3540–3549 (2009).
86. Mahajan, N. P. *et al*. Activated Cdc42-associated kinase Ack1 promotes prostate cancer progression via androgen receptor tyrosine phosphorylation. *Proc. Natl. Acad. Sci. U. S. A.* **104**, 8438–8443 (2007).
87. Debes, J. D., Schmidt, L. J., Huang, H. & Tindall, D. J. P300 Mediates Androgen-Independent Transactivation of the Androgen Receptor By Interleukin 6. *Cancer Res.* **62**, 5632–5636 (2002).
88. Chun, J. Y. *et al*. Interleukin-6 regulates androgen synthesis in prostate cancer cells. *Clin. cancer Res. an Off. J. Am. Assoc. Cancer Res.* **15**, 4815–4822 (2009).
89. Doldi, V. *et al*. Integrated gene and miRNA expression analysis of prostate cancer associated fibroblasts supports a prominent role for interleukin-6 in fibroblast activation. *Oncotarget* **6**, 31441–31460 (2015).
90. Isikbay, M. *et al*. Glucocorticoid Receptor Activity Contributes to Resistance to Androgen-Targeted Therapy in Prostate Cancer. *Horm. Cancer* **5**, 72–89 (2014).
91. Sahu, B. *et al*. FoxA1 specifies unique androgen and glucocorticoid receptor binding events in prostate cancer cells. *Cancer Res.* **73**, 1570–1580 (2013).
92. Arora, V. K. *et al*. Glucocorticoid receptor confers resistance to antiandrogens by bypassing androgen receptor blockade. *Cell* **155**, 1309–1322 (2013).
93. Álvarez-Garcia, V., Tawil, Y., Wise, H. M. & Leslie, N. R. Mechanisms of PTEN loss in cancer: It's all about diversity. *Semin. Cancer Biol.* **59**, 66–79 (2019).
94. Grasso, C. S. *et al*. The mutational landscape of lethal castration-resistant prostate cancer. *Nature* **487**, 239–243 (2012).
95. Jamaspishvili, T. *et al*. Clinical implications of PTEN loss in prostate cancer. *Nat. Rev. Urol.* **15**, 222–234 (2018).
96. Panel, C. & Genome, H. Androgen-independent prostate cancer. **1**, 34–45

(2001).
97. Renner, W., Langsenlehner, U., Krenn-Pilko, S., Eder, P. & Langsenlehner, T. BCL2-Genotypen und Überleben bei Prostatakrebs. *Strahlentherapie und Onkol.* **193**, 466–471 (2017).
98. Takayama, K. ichi, Misawa, A. & Inoue, S. Significance of microRNAs in androgen signaling and prostate cancer progression. *Cancers (Basel).* **9**, 1–16 (2017).
99. Shi, X. B. *et al.* An androgen-regulated miRNA suppresses Bak1 expression and induces androgen-independent growth of prostate cancer cells. *Proc. Natl. Acad. Sci. U. S. A.* **104**, 19983–19988 (2007).
100. Ribas, J. *et al.* miR-21: An androgen receptor-regulated microRNA that promotes hormone-dependent and hormone-independent prostate cancer growth. *Cancer Res.* **69**, 7165–7169 (2009).
101. Zheng, Q. *et al.* Investigation of miR-21, miR-141, and miR-221 expression levels in prostate adenocarcinoma for associated risk of recurrence after radical prostatectomy. *Prostate* **74**, 1655–1662 (2014).
102. Dong, B. *et al.* IL-6 inhibits the targeted modulation of PDCD4 by miR-21 in prostate cancer. *PLoS One* **10**, 1–10 (2015).
103. Östling, P. *et al.* Systematic analysis of microRNAs targeting the androgen receptor in prostate cancer cells. *Cancer Res.* **71**, 1956–1967 (2011).
104. Salji, M. J. Quantitative Proteomics and Metabolomics of Castration Resistant Prostate Cancer. (2018).
105. Lu, S., Tsai, S. Y. & Tsai, M. J. Molecular mechanisms of androgen-independent growth of human prostate cancer LNCaP-AI cells. *Endocrinology* **140**, 5054–5059 (1999).
106. Xu, G. *et al.* Characterization of the small RNA transcriptomes of androgen dependent and independent prostate cancer cell line by deep sequencing. *PLoS One* **5**, (2010).
107. Tepper, C. G. *et al.* Characterization of a novel androgen receptor mutation in a relapsed CWR22 prostate cancer xenograft and cell line. *Cancer Res.* **62**, 6606–6614 (2002).
108. Sramkoski, R. M. *et al.* A new human prostate carcinoma cell line, 22Rv1. *Vitr. Cell. Dev. Biol. - Anim.* **35**, 403–409 (1999).
109. Korenchuk, S. *et al.* VCaP, a cell-based model system of human prostate cancer. *In Vivo* **15**, 163–168 (2001).
110. Schwarz, D. A., Katayama, C. D. & Hedrick, S. M. Schlafen, a New Family of Growth Regulatory Genes that Affect Thymocyte Development. *Immunity* **9**, 657–668 (1998).
111. Geserick, P., Kaiser, F., Klemm, U., Kaufmann, S. H. E. & Zerrahn, J. Modulation of T cell development and activation by novel members of the Schlafen (slfn) gene family harbouring an RNA helicase-like motif. *Int. Immunol.* **16**, 1535–1548 (2004).
112. Bustos, O. *et al.* Evolution of the Schlafen genes, a gene family associated with embryonic lethality, meiotic drive, immune processes and orthopoxvirus virulence. *Gene* **447**, 1–11 (2009).
113. Liu, F., Zhou, P., Wang, Q., Zhang, M. & Li, D. The Schlafen family: complex roles in different cell types and virus replication. *Cell Biol. Int.* **42**, 2–8 (2018).
114. Neumann, B., Zhao, L., Murphy, K. & Gonda, T. J. Subcellular localization of the Schlafen protein family. *Biochem. Biophys. Res. Commun.* **370**, 62–66 (2008).
115. Mavrommatis, E., Fish, E. N. & Platanias, L. C. The Schlafen family of proteins and their regulation by interferons. *J. Interf. Cytokine Res.* **33**,

206–210 (2013).
116. Katsoulidis, E. *et al*. Role of interferon α (IFNα)-inducible Schlafen-5 in regulation of anchorage-independent growth and invasion of malignant melanoma cells. *J. Biol. Chem.* **285**, 40333–40341 (2010).
117. Atala, A. Human Schlafen 5 (SLFN5) is a Regulator of Motility and Invasiveness of Renal Cell Carcinoma Cells. *J. Urol.* **195**, 1169 (2016).
118. Wan, G. *et al*. SLFN5 suppresses cancer cell migration and invasion by inhibiting MT1- MMP expression via AKT / GSK-3 ß / ß -catenin pathway. *Cell. Signal.* **59**, 1–12 (2019).
119. Zhang, S., Zhang, Q., Yin, J. & Wu, X. Overlapped differentially expressed genes between acute lymphoblastic leukemia and chronic lymphocytic leukemia revealed potential key genes and pathways involved in leukemia. *J. Cell. Biochem.* **120**, 15980–15988 (2019).
120. Companioni Nápoles, O. *et al*. SCHLAFEN 5 expression correlates with intestinal metaplasia that progresses to gastric cancer. *J. Gastroenterol.* **52**, 39–49 (2017).
121. Merchant, J. L. & Ding, L. Hedgehog Signaling Links Chronic Inflammation to Gastric Cancer Precursor Lesions. *Cmgh* **3**, 201–210 (2017).
122. Guo, L., Liu, Z. & Tang, X. Overexpression of SLFN5 induced the epithelial-mesenchymal transition in human lung cancer cell line A549 through ß-catenin/Snail/E-cadherin pathway. *Eur. J. Pharmacol.* **862**, 172630 (2019).
123. Arslan, A. D. *et al*. Human SLFN5 is a transcriptional co-repressor of STAT1-mediated interferon responses and promotes the malignant phenotype in glioblastoma. *Oncogene* **36**, 6006–6019 (2017).
124. Wan, G. *et al*. Human Schlafen 5 regulates reversible epithelial and mesenchymal transitions in breast cancer by suppression of ZEB1 transcription. *Br. J. Cancer* (2020) doi:10.1038/s41416-020-0873-z.
125. Sancak, Y. *et al*. PRAS40 Is an Insulin-Regulated Inhibitor of the mTORC1 Protein Kinase. *Mol. Cell* **25**, 903–915 (2007).
126. Peterson, T. R. *et al*. DEPTOR Is an mTOR Inhibitor Frequently Overexpressed in Multiple Myeloma Cells and Required for Their Survival. *Cell* **137**, 873–886 (2009).
127. Jhanwar-Uniyal, M. *et al*. Diverse signaling mechanisms of mTOR complexes: mTORC1 and mTORC2 in forming a formidable relationship. *Adv. Biol. Regul.* **72**, 51–62 (2019).
128. Brunn, G. J. *et al*. Phosphorylation of the translational repressor PHAS-I by the mammalian target of rapamycin. *Science* **277**, 99–101 (1997).
129. Burnett, P. E., Barrow, R. K., Cohen, N. A., Snyder, S. H. & Sabatini, D. M. RAFT1 phosphorylation of the translational regulators p70 S6 kinase and 4E-BP1. *Proc. Natl. Acad. Sci. U. S. A.* **95**, 1432–1437 (1998).
130. Magnuson, B., Ekim, B. & Fingar, D. C. Regulation and function of ribosomal protein S6 kinase (S6K) within mTOR signalling networks. *Biochem. J.* **441**, 1–21 (2012).
131. Biever, A., Valjent, E. & Puighermanal, E. Ribosomal protein S6 phosphorylation in the nervous system: From regulation to function. *Front. Mol. Neurosci.* **8**, 1–14 (2015).
132. Laplante, M. & Sabatini, D. M. Regulation of mTORC1 and its impact on gene expression at a glance. *J. Cell Sci.* **126**, 1713–1719 (2013).
133. Bakan, I. & Laplante, M. Connecting mTORC1 signaling to SREBP-1 activation. *Curr. Opin. Lipidol.* **23**, 226–234 (2012).
134. Dibble, C. C. & Cantley, L. C. Regulation of mTORC1 by PI3K signaling. *Trends Cell Biol.* **25**, 545–555 (2015).
135. Inoki, K., Li, Y., Xu, T. & Guan, K. L. Rheb GTpase is a direct target of

TSC2 GAP activity and regulates mTOR signaling. *Genes Dev.* **17**, 1829–1834 (2003).
136. Manuscript, A. The TSC1-TSC2 complex- a molecular switchboard. *Genetics* **290**, 1717–1721 (2009).
137. Ma, L., Chen, Z., Erdjument-Bromage, H., Tempst, P. & Pandolfi, P. P. Phosphorylation and functional inactivation of TSC2 by Erk: Implications for tuberous sclerosis and cancer pathogenesis. *Cell* **121**, 179–193 (2005).
138. Yao, Y., Jones, E. & Inoki, K. Lysosomal regulation of mTORC1 by amino acids in mammalian cells. *Biomolecules* **7**, 1–18 (2017).
139. Jewell, J. L., Russell, R. C. & Guan, K. L. Amino acid signalling upstream of mTOR. *Nat. Rev. Mol. Cell Biol.* **14**, 133–139 (2013).
140. Panic, B. *et al.* mTORC1 Senses Lysosomal Amino Acids Through an Inside-Out Mechanism That Requires the Vacuolar H(+)-ATPase. *Science (80-.).* **334**, 678–683 (2011).
141. Stransky, L. A. & Forgac, M. Amino acid availability modulates vacuolar H+-ATPase assembly. *J. Biol. Chem.* **290**, 27360–27369 (2015).
142. Atherton, P. J., Smith, K., Etheridge, T., Rankin, D. & Rennie, M. J. Distinct anabolic signalling responses to amino acids in C2C12 skeletal muscle cells. *Amino Acids* **38**, 1533–1539 (2010).
143. Ishizuka, Y., Kakiya, N., Nawa, H. & Takei, N. Leucine induces phosphorylation and activation of p70S6K in cortical neurons via the system L amino acid transporter. *J. Neurochem.* **106**, 934–942 (2008).
144. Milkereit, R. *et al.* LAPTM4b recruits the LAT1-4F2hc Leu transporter to lysosomes and promotes mTORC1 activation. *Nat. Commun.* **6**, 1–9 (2015).
145. Beaumatin, F. *et al.* mTORC1 Activation Requires DRAM-1 by Facilitating Lysosomal Amino Acid Efflux. *Mol. Cell* **76**, 163-176.e8 (2019).
146. Taylor, B. S. *et al.* Integrative Genomic Profiling of Human Prostate Cancer. *Cancer Cell* **18**, 11–22 (2010).
147. Pourmand, G. *et al.* Role of PTEN gene in progression of prostate cancer. *Urol. J.* **4**, 95–100 (2007).
148. Wise, H. M., Hermida, M. A. & Leslie, N. R. Prostate cancer, PI3K, PTEN and prognosis. *Clin. Sci.* **131**, 197–210 (2017).
149. Nardella, C. *et al.* Differential requirement of mTOR in post-mitotic tissues and tumorigenesis. *Sci. Signal.* **2**, 1–18 (2010).
150. Hsieh, A. C. *et al.* The translational landscape of mTOR signalling steers cancer initiation and metastasis. *Nature* **485**, 55–61 (2012).
151. Carver, B. S. *et al.* Reciprocal Feedback Regulation of PI3K and Androgen Receptor Signaling in PTEN-Deficient Prostate Cancer. *Cancer Cell* **19**, 575–586 (2011).
152. Hsieh, A. & Edlind, M. PI3K-AKT-mTOR signaling in prostate cancer progression and androgen deprivation therapy resistance. *Asian J. Androl.* **16**, 378 (2014).
153. Bitting, R. L. & Armstrong, A. J. Targeting the PI3K/Akt/mTOR pathway in castration-resistant prostate cancer. *Endocr. Relat. Cancer* **20**, 83–99 (2013).
154. Statz, C. M., Patterson, S. E. & Mockus, S. M. mTOR Inhibitors in Castration-Resistant Prostate Cancer: A Systematic Review. *Target. Oncol.* **12**, 47–59 (2017).
155. Meijer, A. J., Lorin, S., Blommaart, E. F. & Codogno, P. Regulation of autophagy by amino acids and MTOR-dependent signal transduction. *Amino Acids* **47**, 2037–2063 (2015).
156. Kim, Y. C., Guan, K., Kim, Y. C. & Guan, K. mTOR : a pharmacologic target for autophagy regulation. *J. Clin. Invest.* **125**, 25–32 (2015).

157. Ziparo, E. *et al*. Autophagy in prostate cancer and androgen suppression therapy. *Int. J. Mol. Sci.* **14**, 12090–12106 (2013).
158. Li, M. *et al*. Autophagy protects LNCaP cells under androgen deprivation conditions. *Autophagy* **4**, 54–60 (2008).
159. Nguyen, H. G. *et al*. Targeting autophagy overcomes Enzalutamide resistance in castration-resistant prostate cancer cells and improves therapeutic response in a xenograft model. *Oncogene* **33**, 4521–4530 (2014).
160. Blessing, A. M. *et al*. Transcriptional regulation of core autophagy and lysosomal genes by the androgen receptor promotes prostate cancer progression. *Autophagy* **13**, 506–521 (2017).
161. Farrow, J. M., Yang, J. C. & Evans, C. P. Autophagy as a modulator and target in prostate cancer. *Nat. Rev. Urol.* **11**, 508–516 (2014).
162. Oxender, D. L. & Christensen, H. N. Evidence for two types of mediation of neutral amino-acid transport in Ehrlich cells. *Nature* **197**, 765–767 (1963).
163. Napolitano, L. *et al*. Novel insights into the transport mechanism of the human amino acid transporter LAT1 (SLC7A5). Probing critical residues for substrate translocation. *Biochim. Biophys. Acta - Gen. Subj.* **1861**, 727–736 (2017).
164. Uchino, H. *et al*. Transport of amino acid-related compounds mediated by L-type amino acid transporter 1 (LAT1): Insights into the mechanisms of substrate recognition. *Mol. Pharmacol.* **61**, 729–737 (2002).
165. Kanai, Y. *et al*. Expression cloning and characterization of a transporter for large neutral amino acids activated by the heavy chain of 4F2 antigen (CD98). *J. Biol. Chem.* **273**, 23629–23632 (1998).
166. Yan, R., Zhao, X., Lei, J. & Zhou, Q. Structure of the human LAT1–4F2hc heteromeric amino acid transporter complex. *Nature* **568**, 127–130 (2019).
167. Napolitano, L. *et al*. LAT1 is the transport competent unit of the LAT1/CD98 heterodimeric amino acid transporter. *Int. J. Biochem. Cell Biol.* **67**, 25–33 (2015).
168. Fotiadis, D., Kanai, Y. & Palacín, M. The SLC3 and SLC7 families of amino acid transporters. *Mol. Aspects Med.* **34**, 139–158 (2013).
169. El Ansari, R. *et al*. The multifunctional solute carrier 3A2 (SLC3A2) confers a poor prognosis in the highly proliferative breast cancer subtypes. *Br. J. Cancer* **118**, 1115–1122 (2018).
170. Ikeda, K. *et al*. Slc3a2 Mediates Branched-Chain Amino-Acid-Dependent Maintenance of Regulatory T Cells. *Cell Rep.* **21**, 1824–1838 (2017).
171. Fuchs, B. C. & Bode, B. P. Amino acid transporters ASCT2 and LAT1 in cancer: Partners in crime? *Semin. Cancer Biol.* **15**, 254–266 (2005).
172. Hosios, A. M. *et al*. Amino Acids Rather than Glucose Account for the Majority of Cell Mass in Proliferating Mammalian Cells. *Dev. Cell* **36**, 540–549 (2016).
173. Dolgodilina, E. *et al*. Brain interstitial fluid glutamine homeostasis is controlled by blood-brain barrier SLC7A5/LAT1 amino acid transporter. *J. Cereb. Blood Flow Metab.* **36**, 1929–1941 (2016).
174. Ritchie, J. W. A. & Taylor, P. M. Role of the System L permease LAT1 in amino acid and iodothyronine transport in placenta. *Biochem. J.* **356**, 719–725 (2001).
175. Liao, Z. & Cantor, J. M. Endothelial Cells Require CD98 for Efficient Angiogenesis - Brief Report. *Arterioscler. Thromb. Vasc. Biol.* **36**, 2163–2166 (2016).
176. Baumer, Y. *et al*. CD98 regulates vascular smooth muscle cell proliferation in atherosclerosis. *Atherosclerosis* **256**, 105–114 (2017).

177. Hayashi, K., Jutabha, P., Maeda, S. & Supak, Y. LAT1 acts as a crucial transporter of amino acids in human thymic carcinoma cells. *J. Pharmacol. Sci.* **132**, 201–204 (2016).
178. Nawashiro, H. *et al.* L-type amino acid transporter 1 as a potential molecular target in human astrocytic tumors. *Int. J. Cancer* **119**, 484–492 (2006).
179. Ichinoe, M. *et al.* L-type amino acid transporter 1 (LAT1) expression in lymph node metastasis of gastric carcinoma: Its correlation with size of metastatic lesion and Ki-67 labeling. *Pathol. Res. Pract.* **211**, 533–538 (2015).
180. Yanagisawa, N. *et al.* High expression of L-type amino acid transporter 1 (LAT1) predicts poor prognosis in pancreatic ductal adenocarcinomas. *J. Clin. Pathol.* **65**, 1019–1023 (2012).
181. Altan, B. *et al.* Relationship between LAT1 expression and resistance to chemotherapy in pancreatic ductal adenocarcinoma. *Cancer Chemother. Pharmacol.* **81**, 141–153 (2018).
182. Kaira, K. *et al.* Prognostic significance of L-type amino acid transporter 1 expression in resectable stage I-III nonsmall cell lung cancer. *Br. J. Cancer* **98**, 742–748 (2008).
183. Sakata, T. *et al.* L-type amino-acid transporter 1 as a novel biomarker for high-grade malignancy in prostate cancer. *Pathol. Int.* **59**, 7–18 (2009).
184. Segawa, A. L-type amino acid transporter 1 expression is highly correlated with Gleason score in prostate cancer. *Mol. Clin. Oncol.* 274–280 (2012) doi:10.3892/mco.2012.54.
185. Wang, Q. *et al.* Androgen receptor and nutrient signaling pathways coordinate the demand for increased amino acid transport during prostate cancer progression. *Cancer Res.* **71**, 7525–7536 (2011).
186. Xu, M. *et al.* Up-Regulation of LAT1 during antiandrogen therapy contributes to progression in prostate cancer cells. *J. Urol.* **195**, 1588–1597 (2016).
187. Greiner, M., Kreutzer, B., Unteregger, G., Wullich, B. & Zimmermann, R. Real-time analysis of LNCaP cell growth in different media. *Biochemica* **1**, 14–15 (2010).
188. Corcoran, N. M. *et al.* Salvage prostatectomy post-definitive radiation therapy: The Vancouver experience. *Can. Urol. Assoc. J.* **7**, 87–92 (2013).
189. Horibata, S., Vo, T. V., Subramanian, V., Thompson, P. R. & Coonrod, S. A. Utilization of the soft agar colony formation assay to identify inhibitors of tumorigenicity in breast cancer cells. *J. Vis. Exp.* **2015**, 1–7 (2015).
190. Fisher, S. *et al.* A scalable, fully automated process for construction of sequence-ready human exome targeted capture libraries. *Genome Biol.* **12**, 1–15 (2011).
191. Blomme, A. *et al.* 2,4-dienoyl-CoA reductase regulates lipid homeostasis in treatment-resistant prostate cancer. *Nat. Commun.* **11**, 2508 (2020).
192. Rappsilber, J., Mann, M. & Ishihama, Y. Protocol for micro-purification, enrichment, pre-fractionation and storage of peptides for proteomics using StageTips. *Nat. Protoc.* **2**, 1896–1906 (2007).
193. Cox, J. & Mann, M. MaxQuant enables high peptide identification rates, individualized p.p.b.-range mass accuracies and proteome-wide protein quantification. *Nat. Biotechnol.* **26**, 1367–1372 (2008).
194. Cox, J. *et al.* Andromeda: A peptide search engine integrated into the MaxQuant environment. *J. Proteome Res.* **10**, 1794–1805 (2011).
195. The Universal Protein Resource (UniProt) in 2010. *Nucleic Acids Res.* **38**, D142-8 (2010).

196. Tyanova, S. *et al.* The Perseus computational platform for comprehensive analysis of (prote)omics data. *Nat. Methods* **13**, 731–740 (2016).
197. Cox, J. *et al.* Accurate proteome-wide label-free quantification by delayed normalization and maximal peptide ratio extraction, termed MaxLFQ. *Mol. Cell. Proteomics* **13**, 2513–2526 (2014).
198. Mackay, G. M., Zheng, L., van den Broek, N. J. F. & Gottlieb, E. Analysis of Cell Metabolism Using LC-MS and Isotope Tracers. *Methods Enzymol.* **561**, 171–196 (2015).
199. Gauthier, T., Claude-Taupin, A., Delage-Mourroux, R., Boyer-Guittaut, M. & Hervouet, E. Proximity ligation in situ assay is a powerful tool to monitor specific ATG protein interactions following autophagy induction. *PLoS One* **10**, 1–16 (2015).
200. Sikora, M. J., Johnson, M. D., Lee, A. V. & Oesterreich, S. Endocrine response phenotypes are altered by charcoal-stripped serum variability. *Endocrinology* **157**, 3760–3766 (2016).
201. Tu, C. *et al.* Proteomic Analysis of Charcoal-Stripped Fetal Bovine Serum Reveals Changes in the Insulin-like Growth Factor Signaling Pathway. *J. Proteome Res.* **17**, 2963–2977 (2018).
202. Heise, R. *et al.* Interferon alpha signalling and its relevance for the upregulatory effect of transporter proteins associated with antigen processing (TAP) in patients with malignant melanoma. *PLoS One* **11**, 1–19 (2016).
203. Yue, M., Jiang, J., Gao, P., Liu, H. & Qing, G. Oncogenic MYC Activates a Feedforward Regulatory Loop Promoting Essential Amino Acid Metabolism and Tumorigenesis. *Cell Rep.* **21**, 3819–3832 (2017).
204. Hawksworth, D. *et al.* Overexpression of C-MYC oncogene in prostate cancer predicts biochemical recurrence. *Prostate Cancer Prostatic Dis.* **13**, 311–315 (2010).
205. Tameire, F. *et al.* ATF4 couples MYC-dependent translational activity to bioenergetic demands during tumour progression. *Nat. Cell Biol.* **21**, 889–899 (2019).
206. Han, J. *et al.* ER-stress-induced transcriptional regulation increases protein synthesis leading to cell death. *Nat. Cell Biol.* **15**, 481–490 (2013).
207. Scalise, M., Galluccio, M., Console, L., Pochini, L. & Indiveri, C. The human SLC7A5 (LAT1): The intriguing histidine/large neutral amino acid transporter and its relevance to human health. *Front. Chem.* **6**, 1–12 (2018).
208. Vincent, E. E. *et al.* Akt phosphorylation on Thr308 but not on Ser473 correlates with Akt protein kinase activity in human non-small cell lung cancer. *Br. J. Cancer* **104**, 1755–1761 (2011).
209. Julien, L.-A., Carriere, A., Moreau, J. & Roux, P. P. mTORC1-Activated S6K1 Phosphorylates Rictor on Threonine 1135 and Regulates mTORC2 Signaling. *Mol. Cell. Biol.* **30**, 908–921 (2010).
210. Nitulescu, G. M. *et al.* The Akt pathway in oncology therapy and beyond (Review). *Int. J. Oncol.* **53**, 2319–2331 (2018).